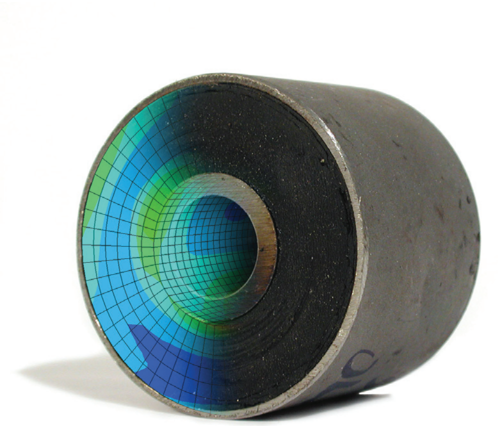

FINITE ELEMENT PROCEDURES IN MODELLING THE DYNAMIC PROPERTIES OF RUBBER

ANDERS K. OLSSON

Structural
Mechanics

Doctoral Thesis

Department of Construction Sciences
Structural Mechanics

ISRN LUTVDG/TVSM--07/1021--SE (1-116)
ISBN 978-91-628-7130-7 ISSN 0281-6679

FINITE ELEMENT PROCEDURES IN MODELLING THE DYNAMIC PROPERTIES OF RUBBER

Doctoral Thesis by

ANDERS K. OLSSON

Copyright © Anders K. Olsson, 2007.
Printed by KFS i Lund AB, Lund, Sweden, March 2007.

For information, address:
Division of Structural Mechanics, LTH, Lund University, Box 118, SE-221 00 Lund, Sweden.
Homepage: http://www.byggmek.lth.se

Preface

The work presented in this doctoral thesis was carried out at the Division of Structural Mechanics, Lund University, Sweden. The partial financial support from the National Graduate School of Scientific Computing is gratefully acknowledged.

I would like to express my gratitude to my supervisor Per-Erik Austrell for his great knowledge within this field and for the guidance and encouragement he has given me. To Volvo Car Corporation, especially Lars Janerstål and Anders Wirje, for funding and carrying out the tests in Paper III and IV. To Kent Lindgren and Leif Kari at the Royal Institute of Technology (KTH) for all the tests in Paper II and valuable discussions.

I would also like to thank all my friends and colleagues at the Division of Structural Mechanics, for all their support and for making the time at work enjoyable.

Last but not least, I wish to thank family and friends for their support throughout the course of my work and for spurring me on by continuously asking about the ever so distant dissertation date.

Lund, March 2007

Anders Olsson

Abstract

Rubber is not only a non-linear elastic material, it is also dependent on strain rate, temperature and strain amplitude. The non-linear elastic property and the strain amplitude dependence give a non-linear dynamic behavior that is covered by the models suggested in this thesis. The focus is on a finite element procedure for modelling these dynamic properties of rubber in a way that is easy to adopt by the engineering community.

The thesis consists of a summary and five appended papers.

The first paper presents a method to model the rate and amplitude dependent behavior of rubber components subjected to dynamic loading. Using a standard finite element code, it is shown how a model can be obtained through an overlay of viscoelastic and elastoplastic finite element models.

The model presented in the first paper contains a large number of material parameters that have to be identified. The second paper suggests a method to identify the material parameters of this model in a structured way. Experimental data for thirteen different materials were obtained from harmonic shear tests. Using a minimization approach it is shown how the viscoelastic-elastoplastic model can be fitted to the experimental data.

Using the methods presented in the first two papers, a radially loaded rubber bushing was modelled in the third paper. The material properties of the finite element model were based on dynamic shear tests. The dynamic response of the finite element model of the bushing was then compared to measurements of a real bushing. Thus, verifying the entire procedure from material test to finite element model.

Steady state loading is a very common load case for many rubber components. Although it is possible to analyze this load with the earlier discussed viscoplastic model, the regularity of this load lends it self to described in a more efficient way. For this load case a simplified viscoelastic method is adopted. The basic idea of this model is to create a new viscoelastic model for each amplitude. In paper IV this method is compared to the previous viscoplastic model as well as verifying measurements.

In paper V both the viscoelastoplastic model and the modified viscoelastic model are used to analyze rubber coated rollers. Different aspects of the two models are highlighted and the models are used to analyze how the non-linear dynamic characteristics of the rubber material influences the rolling contact.

Together the five papers present a set of tools for analyzing the dynamic behavior of rubber components, from material testing to finite element modelling.

Contents

I Introduction 1

1 Background and Purpose 3

2 Overview 5

3 Material Properties 7
- 3.1 Brief History 7
- 3.2 Molecular Structure 7
- 3.3 Damping and Dynamic Modulus 8
- 3.4 Elasticity 9
- 3.5 Rate Dependence 9
- 3.6 The Fletcher-Gent effect 10
- 3.7 Mullins effect 11
- 3.8 Other Properties 11

4 Modelling General Dynamic Loads 13
- 4.1 Elasticity 13
- 4.2 Rate Dependence 14
- 4.3 Amplitude Dependence 15
- 4.4 The Overlay Method 16
- 4.5 Parameter Identification 17
  - 4.5.1 Minimization of the Relative Error 17
  - 4.5.2 Implementation 18

5 Modelling Stationary Dynamic Loads 21
- 5.1 Equivalent Viscoelasticity 21

5.2 Rolling Dynamics 22

6 Future Research 23

II Appended Papers 27

Paper I – Modelling Amplitude Dependent Dynamics of Rubber by Standard FE-codes 29

Paper II – Parameter Identification for a Viscoelastic-Elastoplastic Material Model 51

Paper III – Finite Element Analysis of a Rubber Bushing Considering Rate and Amplitude Dependent Effects 75

Paper IV – Considering Amplitude Dependent Effects During Cyclic Loads by an Equivalent Viscoelastic Model 91

Paper V – Modelling the Dynamic Properties of Rubber in Rolling Contact 107

III Appendix 123

A1 Notation A-1

Part I

Introduction

Chapter 1

Background and Purpose

Dynamically loaded rubber components, such as flexible joints, vibration isolators and shock absorbers, can be found in many mechanical systems and are often of crucial importance. Moreover,demands for better performing products at lower costs within shorter development cycles are a constant challenge to modern industry. As a response to this challenge, traditional physical prototyping and testing are gradually being replaced by virtual prototyping and simulations. Until recently, rubber components have been more or less overlooked in this context, partly because of the difficulty of modelling the complex characteristics of rubber, but also due to a limited understanding of the mechanical properties of rubber materials. The traditional way to develop new rubber products is through physical prototyping and testing [11], which is a highly time-consuming and expensive process.

The aim of this thesis has been to develop new and improved methods for virtual prototyping, in order to predict the dynamic behavior of rubber components. This includes new finite element models as well as methods to fit these models to experimental data. The focus has been on developing finite element procedures that can easily be adopted by practicing engineers. To limit the task, only non-linear elasticity, rate and amplitude dependence have been addressed in the proposed methods.

Chapter 2

Overview

This thesis presents two fundamentally different approaches to model the rate and amplitude dependent properties of rubber: The overlay method and the equivalent viscoelastic method. Both models are based on using commercially available finite elements codes.

The overlay method models the amplitude and frequency dependence in two parallel constitutive branches. This is done by superimposing a viscoelastic and an elastoplastic finite element model by an overlay of element meshes. This approach makes it possible to use commercially available finite element codes, using only the constitutive models that have already been implemented. One of the difficulties with this model is the large number of material parameters that need to be determined. This is done using a minimization procedure which focuses on good fit to dynamic modulus and damping.

The equivalent viscoelastic method is restricted to model stationary dynamic loads. The basic idea is to create an individual viscoelastic model for each amplitude. For each amplitude, the frequency behavior is addressed by a standard viscoelastic model. This provides a model that is easier to fit to material tests and is computationally more efficient.

Both models uses harmonic shear tests to characterize the dynamic properties of the rubber material. Based on the expected working condition of the component, the tests are carried out for a range of different frequencies and amplitudes. An advantage with the simple shear test, is that the elastic part of the rubber behavior is rather linear. This makes it easier to observe the rate and amplitude dependence.

Together the different methods provide a useful toolbox from an engineering point of view. The methods are briefly described in Chapters 4 and 5 and more details are provided in the appended papers. In Chapter 3 a short introduction to the mechanical properties of rubber is given.

Chapter 3

Material Properties

This chapter is a brief introduction to various aspects of the mechanical properties of rubber. It should be noted that rubber is not *one* material, but is a widely used term including a great variety of very unique materials, all with highly individual properties. Hence, the properties described certainly do not apply to all rubbers. It is estimated that there are as many as 50,000 rubber compounds on the market today. Although the focus of this section is on traditional vulcanized rubber, other rubber-like materials such as the thermoplastic elastomers show similar mechanical behavior, although the chemical composition is quite different.

3.1 Brief History

Produced from the sap of rubber trees, rubber was first discovered by ancient native tribes in South and Central America. The word "caoutchouc" comes from the Indian word "cahuchu", meaning "weeping wood". Rubber was discovered and brought back to Europe by Columbus. As more rubber found its way to Europe, early scientists began to take an interest. The poor mechanical properties of unvulcanized rubber meant that it had little value as an engineering material. This was all to change in 1839, when Charles Goodyear heated sulphur-coated rubber by accident, thus discovering the process of vulcanization. Producing a firm and stable rubber material, this discovery was the start of the modern rubber industry [5]. Ever since, new and improved rubber formulas and manufacturing processes have kept on adding to the variety of rubber products available today.

3.2 Molecular Structure

Vulcanized rubber consists of long cross-linked polymer molecules making up a highly elastic matrix. For nearly all engineering applications, reinforcing filler, usually carbon-black, is added to the rubber compound (see Figure 3.1). The fine filler particles form a structure within the material. During vulcanization the filler structure forms both physical and chemical bonds with the polymer chains. Depending on the application, there can be several reasons for introducing fillers, such as increasing stiffness, damping, abrasion resistance and tear strength. In other cases, filler is simply introduced to reduce material costs.

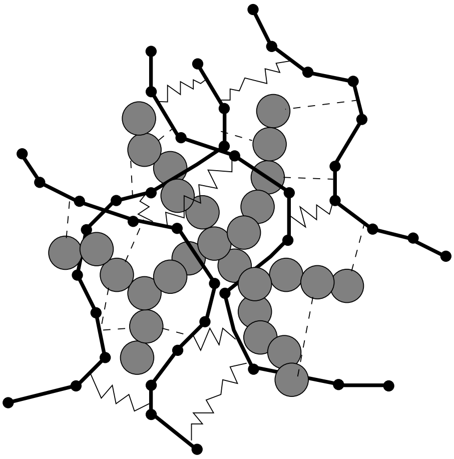

Figure 3.1: Microstructure for a carbon-black-filled rubber vulcanizate. Grey circles: carbon particles. Solid lines: polymer chains. Zigzag and dashed lines: crosslinks.

3.3 Damping and Dynamic Modulus

In the literature, several different ways to characterize damping and dynamic modulus can be found. A common way to describe the characteristics of linear viscoelastic materials is in terms of a complex modulus [8]. The complex modulus consists of a real part (storage modulus) and an imaginary part (loss modulus). Another way to describe the complex modulus is in terms of the absolute value (dynamic modulus) and phase angle.

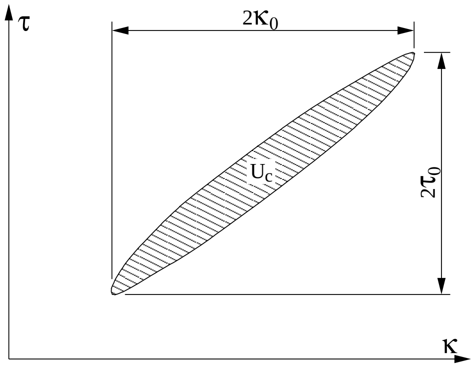

Figure 3.2: A typical hysteresis loop in harmonic shear.

Since the dynamic properties of rubber are more or less non-linear, it is not entirely appropriate to describe the characteristics in terms of a complex modulus. Based on the hysteresis loop in Figure 3.2, the following two definitions of dynamic shear modulus, G_{dyn}, and damping, d, have been used throughout the thesis. The dynamic shear modulus

$$G_{dyn} = \frac{\tau_0}{\kappa_0} \tag{3.1}$$

corresponds to the tilting angle of the hysteresis loop. As seen in Figure 3.2, τ_0 is the shear stress amplitude, κ_0 is the shear strain amplitude and U_c is the energy loss per unit volume for one cycle. For a linear viscoelastic material definition 2 equals the absolute value of the complex shear modulus.

The damping

$$d = \frac{U_c}{\pi \kappa_0 \tau_0} \tag{3.2}$$

can be interpreted as a relative measure of the thickness of the hysteresis loop. Applied to a linear dynamic material, this definition is the sine of the phase angle δ, i.e. $d = sin(\delta)$. For small phase angles it is noted that $sin(\delta) \approx \ delta \approx tan(\delta)$ which often seen in the literature when damping is discussed.

3.4 Elasticity

Although rubber is usually thought of as an elastic, incompressible material, in real life there is no such thing as a purely elastic rubber. Nevertheless, treating rubber as elastic can in some cases be a good approximation. Examples of this are dynamically loaded unfilled rubber and filled rubber subjected to quasi-static loads. For many unfilled rubbers, the hysteretic loss is often very small and can thus be neglected. However, these rubbers are of limited use in practice.

Another example where it can be useful to use an elastic model is for statically loaded rubber components. In this case a good approximation can often be achieved by fitting an elastic model to an experimental loading curve, ignoring the unloading curve. Such a model will yield fairly accurate results during loading.

3.5 Rate Dependence

It is a well-known fact that the response of rubber components is influenced by the load rate. In the case of a harmonic load, rate dependence or frequency dependence is shown as an increase in modulus with increasing frequency, as seen in Figure 3.3. For an increasing frequency the loss factor will increase at low frequencies, reach a maximum and then decrease at very high frequencies [8]. Since the emphasis in this thesis is on low frequency behavior (beneath about 200Hz) of rubber, the measurements presented does not show a decrease in the loss factor. Nevertheless, the models presented are capable of modelling this behavior as well.

The rate dependent loss is usually attributed to the resistance in reorganizing the polymeric chains during loading. Since this reorganization cannot occur instantaneously, the loss of energy will be rate dependent.

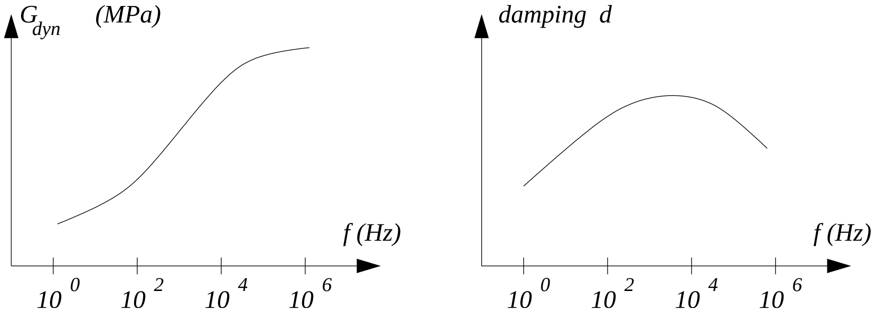

Figure 3.3: General frequency dependence of dynamic shear modulus and damping for a filled rubber.

3.6 The Fletcher-Gent effect

The amplitude dependence, also known as the Fletcher-Gent or Payne effect [9], is usually not as well-known as the rate dependence, although in many cases the amplitude dependence is by far the most prominent of the two. The effect of the amplitude dependence for a harmonically loaded rubber is illustrated in Figure 3.4. As can be seen, an increase in amplitude will lead to a decrease in modulus. The loss factor, on the other hand, will reach a maximum at moderate strain amplitudes.

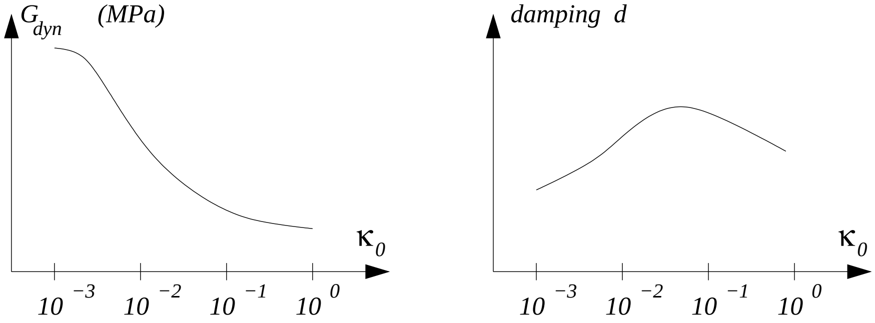

Figure 3.4: General strain amplitude dependence of dynamic shear modulus and damping for a filled natural rubber.

From a micro-mechanical point of view, the amplitude dependence is traditionally attributed to the breakdown and reforming of the filler structure. However, more recent research suggests that the amplitude dependence is caused by changes in the weak bonds between the filler structure and the polymeric chains. As the rubber is deformed, these bonds will move along the surface of the filler, resulting in a rate-independent energy loss.

3.7 Mullins effect

Mullins effect can in some way also be considered an amplitude dependence. In the case of a cyclic load, the Mullins effect [7] is observed as a decrease in stiffness during the first few load cycles. This is often referred to as “mechanical conditioning” or “scragging” of the rubber. Considering an unconditioned virgin material, further increasing the strain amplitude will lead to an decreasing modulus partly due to Mullins effect and partly due to the previously mentioned Fletcher-Gent effect. Contrary to the Fletcher-Gent effect, Mullins effect is not fully reversible. However, if let alone for a couple of hours or more, the material will heal and the stiffness of the virgin material will be at least partly restored.

3.8 Other Properties

Besides the rate and amplitude dependence and the non-linear elasticity accounted for in this thesis, there are a number of other properties worth mentioning.

One property that was encountered during the experimental testing in this work is the temperature dependence. During tests with a large harmonic load the rubber specimen will heat up due to material damping. The resulting increase in temperature will have a similar effect on the dynamic properties of rubber as that of a decrease in frequency described by the WLF-shift model [1]. This effect can also be important for rubber components subjected to changes in external temperature.

The working environment also poses other concerns such as aging and swelling. Oxidation and ozone cracking, often in combination with thermal aging, may drastically shorten the life span of a rubber component. This is especially true for thin components, since the aging process is initiated at the surface. Also, many chemicals such as oil are known to destroy the crosslinks, thereby reverting the rubber to the gum state, and also causing swelling. Depending on the specific rubber material, application and environment, different properties have to be considered during the design phase of a rubber component.

Chapter 4

Modelling General Dynamic Loads

As mentioned earlier, the main object of this thesis is to model the rate and amplitude dependent effects of rubber materials, using the finite element method. For simple shear, the amplitude and rate dependence can be modelled with simple one-dimensional models. These one-dimensional models do not only form the basis of the overlay method presented later, but they also provide a valuable tool for understanding the fundamental behavior of rubber dynamics. Since the one-dimensional models are based on the same principles as the finite element models, it is possible to transfer the parameters between the two models.

The finite element analyzes in this thesis have been carried out in $Abaqus$ [2]. The choice of using a commercial finite element code makes it easier to focus on the engineering problem rather than a detailed description of complex finite element models. It will also result in methods that can be put directly to use in industry. On the downside is the lack of control of how the models are implemented in $Abaqus$. Although $Abaqus$ provides a very good manual there will always be details that are left out of the manual.

4.1 Elasticity

For finite element analysis, rubber is often modelled as a hyperelastic material [4]. Stress-strain relationships are derived from a strain energy function usually based on the first, and sometimes also second, strain invariant. Due to incompressibility it can be argued that the third invariant is constant and thus will not influence the strain energy. However, when analyzing highly confined rubber components, the incompressibility properties cannot be neglected and are usually included by an extra term in the strain energy function based on the volumetric change.

In this thesis only the Yeoh and Neo-Hookean models have been used. These models are only dependent on the first strain invariant. This single invariant dependence gives the advantage of more robust models than for instance the Mooney-Rivlin model, which is also dependent on the second strain invariant. A Mooney-Rivlin model fitted to a uniaxial test might behave very nonphysically when loaded in a different direction. In contrast, the Neo-Hookean and Yeoh models will always yield a physically correct behavior in all directions, as long as they are correctly fitted for one direction. The strain energy density function of the Yeoh model is given by:

$$W = C_{10}(I_1 - 3) + C_{20}(I_1 - 3)^2 + C_{30}(I_1 - 3)^3 \tag{4.1}$$

Putting C_{20} and C_{30} at zero yields the simpler Neo-Hooke model. The main difference between the two models is the inability of the Neo-Hooke model to capture the increase in stiffness of rubber during large tensile strains. The Neo-Hooke model is also incapable of modelling the modest non-linear behavior during shear.

4.2 Rate Dependence

The rate dependence is modelled using a viscoelastic model. The most simple one-dimensional viscoelastic model to yield a physically correct behavior is the so called standard linear solid (SLS) model. The SLS model consists of a single Maxwell element coupled in parallel with an elastic spring. This model will yield good results for a small range of frequencies. In order to achieve a better fit to a larger range of frequencies, the SLS model can be expanded with several Maxwell elements coupled in parallel, resulting in the generalized Maxwell model shown in Figure 4.1.

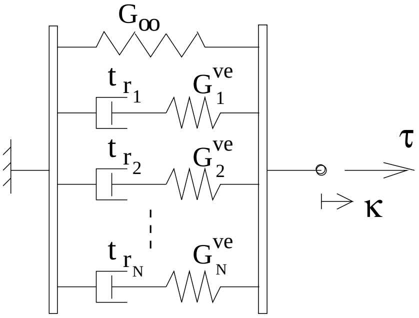

Figure 4.1: The generalized Maxwell model.

The stress response of the generalized Maxwell model is the sum of all the parallel element stresses. The viscoelastic stress response is given by a hereditary integral according to

$$\tau_i^{ve}(t) = \int_{-\infty}^{t} G_{R_i}(t - t')d\kappa(t') \tag{4.2}$$

where the relaxation modulus G_{R_i} for a Maxwell element i is given by

$$G_{R_i} = G_i^{ve} exp\left(\frac{-t}{t_{r_i}}\right) \tag{4.3}$$

Combining Equations (4.2) and (4.3), and approximating according to the trapezoidal rule, the viscoelastic stress for Maxwell element i can be expressed in an incremental form as

$$\Delta\tau_i^{ve} \approx \tau_i^{ve}\left(exp\left(\frac{-\Delta t}{t_{r_i}}\right) - 1\right) + \frac{G_i^{ve}\Delta\kappa}{2}\left(1 + exp\left(\frac{-\Delta t}{t_{r_i}}\right)\right) \tag{4.4}$$

where τ_i^{ve} is the stress at the previous step [10]. Thus, for transient analysis, only the previous step has to be taken into consideration. The total viscoelastic stress increment for the whole model is then obtained by adding all incremental stress contributions from all elements.

In the finite element software $Abaqus$, the generalized Maxwell (or Prony series) model has been implemented based on a hyperelastic model suitable for elastomers.

Another approach to modelling the rate dependence is to use fractional derivatives to describe it [3]. The advantage of the fractional model is its ability to model a wide range of frequencies and time resolutions using only a few material parameters, as compared to the many parameters needed for the generalized Maxwell model. This approach is very powerful for frequency analysis. For transient analysis, however, fractional derivatives tend to be more time-consuming, since the entire strain history has to be taken into account at each time step. Another drawback of this approach is that it is not yet implemented in commercial finite element codes.

4.3 Amplitude Dependence

In one dimension, the amplitude dependent dynamic stiffness and loss angle can be modelled with simple Coulomb frictional elements. When coupled together with elastic springs, as shown in Figure 4.2, it is possible to obtain a rather smooth response as well as a good fit to a large range of amplitudes. The elastoplastic behavior of this model will be piece-wise kinematic hardening.

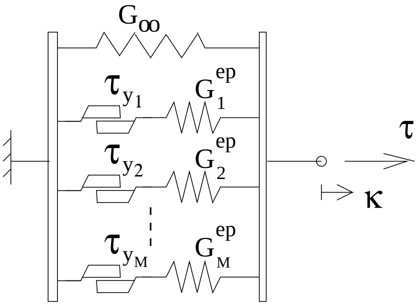

Figure 4.2: The generalized one-dimensional elastoplastic model.

A frictional element coupled in series with an elastic spring yields the most simple non-hardening elastoplastic model. The stress response for such an elastoplastic element j can be expressed in the following incremental form:

$$\Delta\tau_j^{ep} = \begin{cases} G_j^{ep}\Delta\kappa & \text{if elastic} \\ 0 & \text{otherwise} \end{cases} \tag{4.5}$$

The total incremental elastoplastic stress response for the one-dimensional model is then given as the sum of all parallel elastoplastic elements.

In three dimensions, amplitude dependence is modelled by an elastoplastic model. The preferred model would be a kinematic hardening model based on the same hyperelastic model as the viscoelastic and elastic models. However, in $Abaqus$ such a model is yet to be implemented.

Instead, an elastoplastic model based on a hypoelastic description has been used. Another problem has been the lack of a kinematic hardening model in $Abaqus/Explicit$. This was solved by overlaying several non-hardening von Mises models, resulting in a piece-wise linear hardening model. In $Abaqus/Standard$ a similar model can be obtained with the use of a single kinematic hardening model.

4.4 The Overlay Method

Experimental findings show that the amplitude dependence and rate dependence can be considered as two independent types of behavior, i.e. the frequency response is the same for all strain amplitudes and vice versa. Although not entirely true, this assumption holds rather well for the materials investigated in this thesis. On the basis of this assumption it can be concluded that the rate dependent model and the amplitude dependent model can be coupled together in parallel, greatly simplifying the modelling task. For the one-dimensional case, this is exemplified in Figure 4.3.

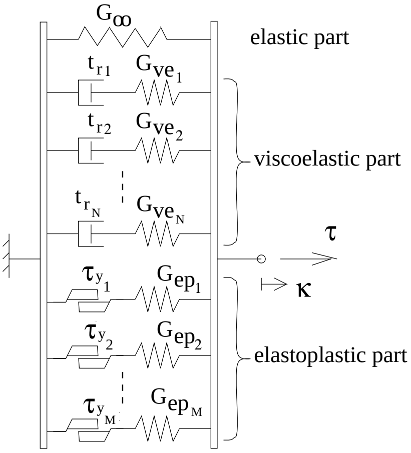

Figure 4.3: One-dimensional equivalence of the viscoelastic-elastoplastic model.

Figure 4.3 clearly shows that the total stress can be obtained as a summation of the stress contributions from all parallel contributions. The same approach is used for the three-dimensional model. Hence, the total stress tensor is obtained as a summation of the stress tensors from all parallel contributions.

$$\boldsymbol{\tau} = \boldsymbol{\tau}^{e} + \boldsymbol{\tau}^{ve} + \boldsymbol{\tau}^{ep} = \boldsymbol{\tau}^{e} + \sum_{i=1}^{M} \boldsymbol{\tau}_{i}^{ve} + \sum_{j=1}^{N} \boldsymbol{\tau}_{j}^{ep} \tag{4.6}$$

For the finite element model, the above summation of stress tensors is achieved by an overlay of finite element meshes, according to Figure 4.4. The general idea of this so called overlay method is to obtain each stress tensor from a separate finite element model. In some finite element codes, such as $Abaqus/Standard$ it is possible to model the first two terms of Equation 4.6 in one model and the third term in a second model. The finite element models are all created with the same topology. The stress summation is then achieved by assembling each layer of elements into one set of nodes. This approach yields a model able to represent the combined rate and amplitude dependence without having to implement any new finite element models.

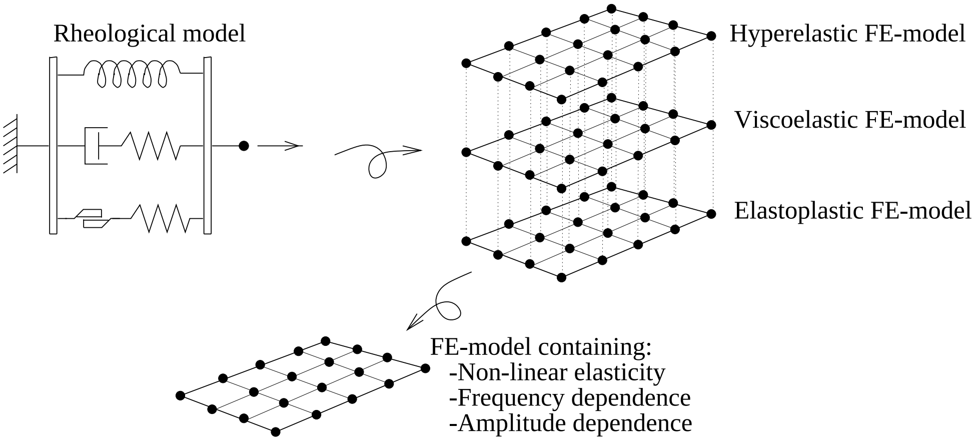

Figure 4.4: Principle of the overlay method.

4.5 Parameter Identification

As previously mentioned, the major drawback of the material model presented was the number of material parameters that have to be identified. In order to remove this obstacle, a structured procedure to determine the material parameters was developed.

Using a harmonic shear test, the rubber is characterized at different frequencies and strain amplitudes. For simple shear, the rubber can be modelled with a one-dimensional model, as presented in Figure 4.3. Since the parameters of the one-dimensional model are directly transferable to the finite element model, it is sufficient to fit the one-dimensional model to experimental data. The material parameters are then simply shifted to the finite element model.

4.5.1 Minimization of the Relative Error

The basis of the parameter identification is a minimization of the relative error between the model and the experimental data. For this purpose an error function ψ, in the least square sense, was defined according to

$$\psi = (1-\alpha)\sum_{i=1}^{m}\left(\frac{d_{dyn,i} - d_{exp,i}}{d_{exp,i}}\right)^2 + \alpha\sum_{i=1}^{m}\left(\frac{G_{dyn,i} - G_{exp,i}}{G_{exp,i}}\right)^2. \tag{4.7}$$

Minimization of ψ gives a good fit to measured damping d_{exp} and dynamic shear modulus G_{exp}. The weight factor α is used to put emphasis either on a good fit to dynamic modulus or on damping. In order to evaluate the error function, the dynamic shear modulus G_{dyn} and the damping d of the model have to be calculated at all the m points of measurement. This can be very time-consuming if the error function has to be evaluated repeatedly during the numerical minimization.

4.5.2 Implementation

The fit of the resulting model will depend on the choice of the weight factor α and the number N of viscoelastic and number M of elastoplastic contributions.

To provide a good understanding of how these three parameters influence the resulting model, it is important that the user gets direct feedback on the chosen material model and weight factor. In order to achieve this user-interactivity, the computational time for the parameter identification has to be short.

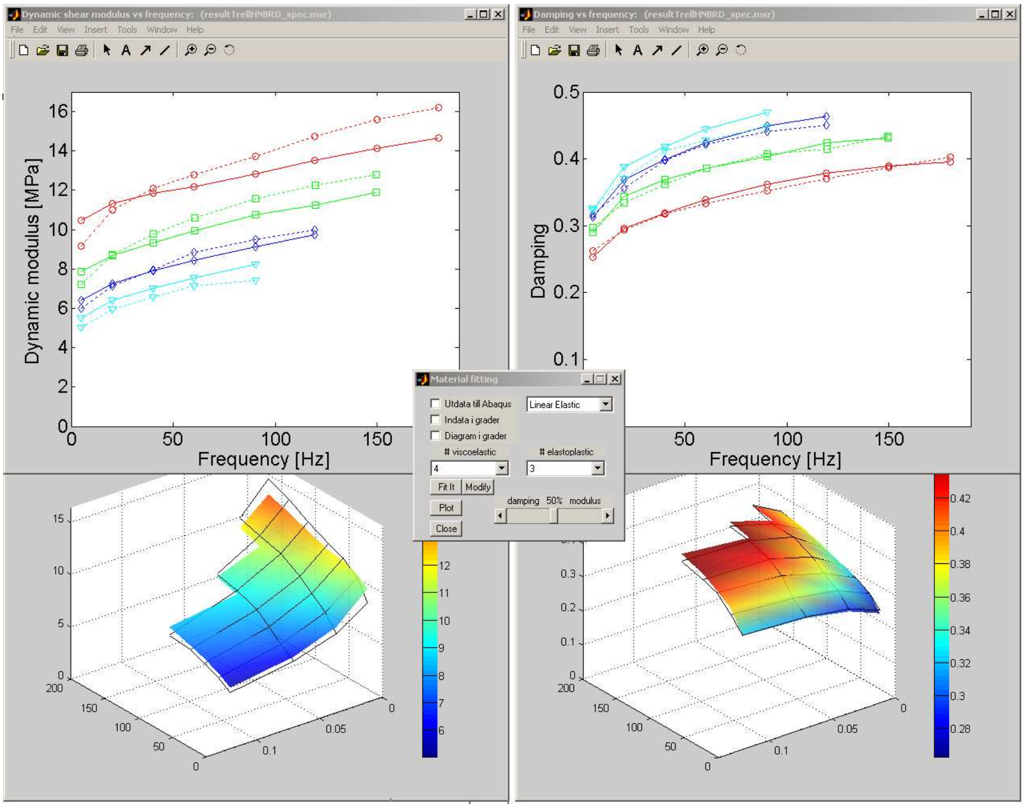
Dynamic shear modulus vs frequency: (resultTrellHNBRD_spec.msr)
File Edit View Insert Tools Window Help
Dynamic modulus [MPa]
Frequency [Hz]
0
2
4
6
8
10
12
14
16
0
50
100
150
Damping vs frequency: (resultTrellHNBRD_spec.msr)
File Edit View Insert Tools Window Help
Damping
0.1
0.2
0.3
0.4
0.5
Material fitting
Fit It
Modify
Plot
Close
15
10
5
0
200
150
100
50
0
0.1
0.05
0
12
11
10
9
8
7
6
0.3
0.2
0.1
0
0.42
0.4
0.38
0.36
0.34
0.32
0.3
0.28

☐ Utdata till Abaqus

☐ Indata i grader

☐ Diagram i grader

Linear Elastic

viscoelastic: 4

elastoplastic: 3

damping 50% modulus

Figure 4.5: Screen capture of the graphical user interface.

Using a combination of analytical approximations and numerical time stepping to calculate the model response, an effective method to minimize the error function was developed. The analytical approximations are used to speed up the costly repeated evaluations of the error function, while the more time-consuming numerical time stepping is used to guarantee the accuracy.

To simplify the process of finding the material parameters, the fitting procedure was implemented in a graphical user interface, using $Matlab$ [6]. The graphical user interface shown in Figure 4.3 makes it easy to try different numbers of viscoelastic and elastoplastic contributions and to test different weight factors in order to obtain the best possible fit.

Chapter 5

Modelling Stationary Dynamic Loads

The case of stationary dynamic loading is found in many industrial applications. Compared to a general dynamic load, the regularity of a stationary dynamic load lends itself to be described in a simplified and also more efficient manner. It should be noted that stationary dynamics also include general periodic loads and is not restricted to only harmonic loads.

5.1 Equivalent Viscoelasticity

The viscoelastic procedures available in commercial finite element codes are in their original form unable to account for the Fletcher-Gent effect.

The basic idea for the equivalent viscoelastic approach is that due to the repetitive character of stationary loading it is possible to foresee the largest amplitude during a load cycle. Based on knowledge of amplitudes in different material points it is possible to create a viscoelastic model that will give a correct estimate of damping and dynamic modulus with respect to frequency for a predicted amplitude.

Compared to the viscoelastoplastic approach of the previously discussed overlay method the equivalent viscoelastic model make no assumptions of the mechanics behind the amplitude dependence. Nor does it require the amplitude and frequency dependence to be independent of each other. This lack of restrictions allows the equivalent viscoelastic model to be fitted more closely to the experimental data. It also means that any amplitude dependence present in the measurement will be included in the model no matter if it is caused by Mullins effect or the Fletcher-Gent effect.

Even if the equivalent viscoelastic model can be made to behave in a correct manner in terms of damping and modulus it should be noted that the time response will be slightly different. Considering the shape of the hysteretic loop during one load cycle the equivalent viscoelastic model will have an almost perfect elliptic shape whereas the hysteretic loop of a typical amplitude dependent rubber material will have sharper corners and a more asymmetric shape, particulary for low frequency loading and quasi-static loading.

The analysis is carried out in two steps. First an initial analysis is carried out. Based on the result of the initial analysis an approximate amplitude for each element is determined. In the second step each element is given an equivalent viscoelastic model based on the amplitude of the previous step.

The viscoelastic model can be either a frequency domain or a time-domain viscoelastic model. The frequency domain model is restricted to harmonic loads.

5.2 Rolling Dynamics

Rolling contact is an important application for rubber. Apart from the obvious application of tires, rubber coated rollers are central to many industrial processes. For rubber coated rollers, it is common with large loads and high speeds. This make it important to include both amplitude and frequency dependence in the model.

It is easy to see that the dynamic modulus is the single most important material property to control the contact pressure and contact width. However, the influence of material damping is not as straight forward. To understand the influence of material damping in rolling, it is noted that damping is a result of a difference between the loading and unloading part of the load cycle. During the initial part of the contact the rubber contact will resist the increasing load and the pressure will increase fast. In the second and unloading part of the load cycle the inherent damping will reduce the force by which the rubber regains its undeformed shape. Thus the contact pressure during rolling will be asymmetric. This is true independent of the damping is caused by plastic or viscous effects.

In general rolling is a transient load case and need to be modelled through a transient time stepping analysis. This general approach is needed when the rolling speed is not constant or when rolling over non-smooth surfaces. As the contact simulation works best with small time steps, an explicit time stepping scheme is usually preferred.

Although not a harmonic load case, steady state rolling over a flat surface is an example of a stationary dynamic load case and is thus suited for the equivalent viscoelastic model. Compared to a transient analysis the equivalent viscoelastic model performs computationally much more efficient for this load case.

Chapter 6

Future Research

As often with research projects, more questions have been raised than answered in the course of this work. By using the present thesis as a basis, it is possible to continue in many directions.

There are other important rubber characteristics that might be incorporated in the model presented, depending on the application and choice of material. Factors such as temperature dependence and a more thorough approach to Mullins effect can be taken into consideration.

Considering the complexity of dynamic harmonic testing, other potentially simpler and less time consuming methods might be interesting to investigate. With a relaxation test it might be possible to characterize the entire rate dependence in a single test. With several relaxation tests of different step sizes it could be possible to cover the amplitude dependence as well. Another approach might be to use different impact tests as a simple way to characterize the dynamic properties of rubber. Viewing the finite element model as an advanced extrapolation of material test data, it can be argued that the test method should be chosen to reflect the load of the intended application. I.e. when modelling a shock absorber it would make good sense to obtain the material parameters from an impact test, whereas a harmonic test method is more suitable when modelling a vibration damper.

Multi-body dynamics (MBD) simulations are another important area for models of rubber dynamics. Bushings incorporated into existing MBD codes such as $ADAMS$ and $DADS$ are greatly simplified and are a source of uncertainty when analyzing system dynamics. A low degree of freedom model for rubber bushings can be based on the same principles as the material models presented in this thesis.

Bibliography

[1] Ferry J.D. 1970,
Viscoelastic Properties of Polymers. J. Wiley and Sons Inc., New York

[2] Hibbit, Karlsson, Sorensen 2003,
Abaqus Theory Manual, Version 6.3, HKS inc., Pawtucket, RI

[3] Sjöberg M., Kari L. 2002,
Nonliear behavior of a rubber isolator system using fractional derivatives. Vehicle System Dynamics 37(3), 217-236

[4] Holzapfel G.A. 2000,
Nonlinear Solid Mechanics. J. Wiley and Sons Inc., New York

[5] The International Rubber Research and Development Board, 2003,
History of Natural Rubber
http://www.irrdb.com/IRRDB/NaturalRubber/History/History1.htm

[6] MATLAB 2003,
"High performance numerical computation and visualization software" Version 6.5, The Math Works Inc.

[7] Mullins L. 1969,
Softening of Rubber by Deformation., Rubber Chemistry and Technology, Vol. 42, pp. 339-362

[8] Nashif A. 1985,
Vibration Damping. Wiley, New York

[9] Payne A.R. 1965,
in *Reinforcement of Elastomers.* Kraus G., Ed., Interscience, Chap. 3, New York

[10] Thelandersson S. 1987,
Notes on linear viscoelasticity. Report TVSM-3009, Division of Structural Mechanics, Lund, Sweden

[11] Werke M. 1999,
Kartläggning av arbetsmetodik vid konstruktion av gummikomponenter. [Survey in working methodology in designing rubber components.], IVF report 98008, The Swedish Institute of Production Engineering Research

Part II

Appended Papers

Paper I

Modelling amplitude dependent dynamics of rubber by standard FE-codes

Presented in abbreviated form at ECCMR Hannover 2001

Modelling amplitude dependent dynamics of rubber by standard FE-codes

Per-Erik Austrell, Anders K Olsson
Division of Structural Mechanics, Lund University, Sweden

ABSTRACT: For most engineering rubbers, material damping is caused by two different mechanisms, resulting in rate dependent and amplitude dependent behavior respectively. This paper presents a simple engineering approach to model the elastic-viscoelastic-elastoplastic characteristics of rubber materials, providing a finite element model suitable for analyzing rubber components subjected to cyclic as well as transient loads. Although constitutive models with the above characteristics exist, they have yet to be implemented in commercial finite element codes. The advantage of the suggested method is the ability to use already existing FE-codes for the purpose of analyzing the amplitude and rate dependent behavior of rubber components. This is done by a simple overlay of finite element meshes, each utilizing a standard hyperelastic, viscoelastic and elastoplastic material model respectively. Hence, no implementation of new material models is required. To demonstrate the ability of the method, an axi-symmetric rubber bushing subjected to a stationary cyclic load has been analyzed, with material properties measured using a sinusoidal shear test.

1 Introduction

Rubber components such as shock absorbers, vibration dampers, flexible joints etc, are often used as coupling elements between less flexible or rigid structures. Knowledge of how these elastomeric components affect the dynamic characteristics of the complete system, are often of crucial importance. In industries, such as the vehicle industry, where rapid development of new products or models is of essence, virtual prototyping and simulations are increasingly important. In most of these simulations, the non-linear dynamic behavior of rubber components are usually completely overlooked or, at best, greatly simplified.

The stiffness and damping properties of dynamically loaded rubber components are usually dependent on both frequency and amplitude. For most engineering rubbers, damping is caused by two different mechanisms at the material level, resulting in viscous (rate dependent) and frictional (amplitude dependent) damping respectively. Constitutive models for rubber used in standard large strain FE-codes are usually either hyperelastic or viscoelastic. Elastoplastic models, needed to model the frictional damping, are also normally supplied in order to model the plastic behavior of metal. Based on these commonly available models, a novel FE-procedure able to model the dynamic behavior of rubber materials including both rate and amplitude dependence as well as nonlinear elastic behavior, is proposed. The model handles both harmonic and transient loads. The advantage of the proposed method is that no advanced constitutive modelling or programming skills are required, since it only utilizes already available and implemented constitutive models.

This paper is a development of a conference proceeding by Austrell & Olsson (2001).

Apart from this introductory section, the paper consists of four major sections, outlining the basic ideas of the overlay method and a final section where the method is applied to a rubber bushing. In section 2 a brief discussion of different material properties for rubber is given and the three constitutive branches used in the presented overlay method is discussed. Section 3 discusses the the double shear test and important properties such as damping and dynamic modulus. It is argued that the elastic response of rubber in simple shear is almost linear, which enables the shear tests to be modelled using one-dimensional symbolic models. Hence, in section 4 different one-dimensional models are examined. For the one-dimensional models the total stress is given as a summation of the shear stresses. In section 5 it is argued, that for a general load case, the one-dimensional models may be generalized into three dimensions by adding stress components instead of only shear stresses. Thus allowing for the material parameters for the one-dimensional model to be copied to the FE-model. This last step is done using the novel approach of overlay of finite element meshes. To demonstrate the ability of the proposed method an axi-symmetric rubber bushing, subjected to a stationary cyclic load, has been analyzed in section 6. It is shown how the presented method can be used to model the non-linear dynamic behavior of a rubber bushing.

2 Constitutive Branches

Rubber has a very complex material behavior. Besides the non-linear elastic behavior, most engineering rubber materials also show a considerable material damping, which give rise to hysteretic response in cyclic loading. Apart from the strain level, the dynamic response of rubber is dependent on the present strain rate and the strain history. For a harmonic load this behavior can be observed through the dependence on frequency and amplitude respectively. Dynamic modulus and damping of a typical engineering rubber can vary with several hundred percents due to variations in frequency and amplitude. Several authors have successfully modelled the frequency and amplitude dependencies as two approximately independent material behaviors (Austrell 1997; Kaliske & Rothert 1998; Miehe 2000 and Sjöberg 2000). The ability to model the rate dependence separately from the amplitude dependence is a useful property, greatly simplifying the material modelling. The treatment of rate and amplitude dependent properties by two independent branches is also used in the presented model. It should however be noted that this theory has mostly been used to model highly filled rubbers which are very common in engineering applications. A study by Chazeau et al (2000) on the amplitude dependence on low-filled rubbers suggests that the observed amplitude effects also contain time dependence.

The mechanical behavior can be divided into three principle branches. The first and most dominant branch in terms of stress magnitude being the non-linear elastic branch. The proposed model does not favor any specific hyperelastic model. Instead the user is free to use whatever hyperelastic model available in the FE-code.

The rate dependent second branch, is modelled using a viscoelastic material model based on a Prony series approach. Other authors, such as Enelund et al. (1996), have proposed the use of fractional derivatives in order to model the rate dependence of rubber. The advantage of fractional derivatives is the ability to model a wide frequency range with only a few material parameters. Prony series on the other hand offer a numerically more effective method to model the response to a general strain history, since only the previous step has to be considered, as compared to the fractional approach were the entire previous strain history has to be considered for each step. Another advantage of the Prony series is that it is already implemented in many commercial FE-codes.

For the rate-independent third branch, only the Payne effect (Payne 1965) is included in the proposed model. For a harmonic load, the Payne effect is observed as a decrease in dynamic modulus for increasing amplitudes. The decrease in modulus is modelled using an elastoplastic material model similar to Kaliske & Rothert (1998) and Miehe (2000). The used elastoplastic model results in a piecewise linear kinematic hardening law after applying the overlay method.

Apart from these three fundamental branches, discussed above, rubber also shows other important material behaviors, such as Mullins effect (Mullins 1969), temperature dependence, swelling and ageing, to name only a few. These effects are however not accounted for in the presented model. The model presented in this paper is applicable for general dynamic loads and for elastomers without pronounced damage behavior. Depending on the type of analysis, the application and elastomer in question, other material behaviors might have to be included in the model. If required, it is possible to include both Mullins effect as well as temperature dependence without any major changes to the model described in this paper. Temperature effects can be added using a WLF-shift function according to (Ferry 1970). The WLF-shift can be viewed as a scaling of the time for the viscoelastic part. Kari & Sjöberg (2003) uses the WLF-shift in conjunction with a fractional viscoelastic model. Mullins effect is usually modelled with a damage model, which basically reduces the elastic strain energy function with a scalar factor dependent on the maximum deformation, see for example Simo (1987) and Miehe (1995). Considering a cyclic load with constant amplitude, Mullins effect is seen to disappear during the first few load cycles.

3 Harmonic Shear Test

Since the elastic part of the material is almost linear during shear, most of the testing is done using a double shear test specimen. The linear elasticity obtained during simple shear makes it easier to observe the nonlinear dynamic properties. The experimental data presented in this article was obtained from a double shear specimen according to Fig. 1. The double shear specimen consists of three steel cylinders connected by two rubber discs.

When subjecting the test specimen to a stationary cyclic load a hysteretic loop according to Fig. 2 is obtained. A correct material model should exhibit the same dynamic shear modulus G_{dyn} and damping d as obtained in the test.

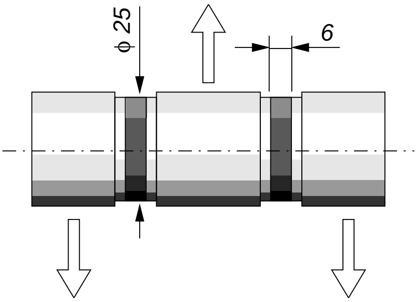

Figure 1: The double shear specimen.

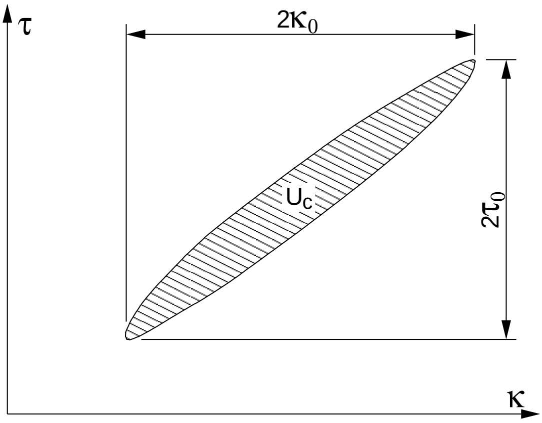
τ
2κ0
Uc
2τ0
κ

Figure 2: Typical hysteretic loop for a rubber material subjected to a stationary cyclic load.

For cyclic loads, the dynamic shear modulus is defined by

$$G_{dyn} = \frac{\tau_0}{\kappa_0}, \tag{1}$$

where τ_0 is the amplitude of the shear stress and κ_0 is the amplitude of the shear strain, as defined in Fig. 2. A correct description of the dynamic modulus, obtained from the material model, is vital in order to achieve a finite element model with a correct dynamic stiffness.

For viscoelastic materials, the damping is attributed the phase angle δ as $d = sin(\delta)$. However, for a material with elastoplastic properties, the phase angle is not well defined. In this paper, the damping d is defined by

$$d = sin(\delta) = \frac{U_c}{\pi \kappa_0 \tau_0} \tag{2}$$

where U_c is the hysteric work, corresponding to the area of the hysteretic loop in Fig. 2. I.e., damping could be viewed as a normalization of the hysteretic work. A large damping yields a large difference between the loading and unloading curves in the hysteric response. For a linear viscoelastic material, definition (2) will yield the same result as the argument of the complex modulus. I.e. the definition is not in conflict with linear viscoelastic theory. Instead it could be viewed as extension of the concept of damping into elastoplasticity.

In Fig. 3 a typical hysteresis loop from the dynamic shear tests is shown. Using the definitions in Eq. (1) and (2) it is easy to calculate the obtained dynamic shear modulus and damping. The deviation from viscoelastic behavior is clearly observed in the sharp corners of the hysteretic loop. A purely viscoelastic material would had exhibited elliptic shaped loops, with rounded corners.

In the following section it is discussed how the dynamic simple shear behavior may be modelled with one-dimensional models.

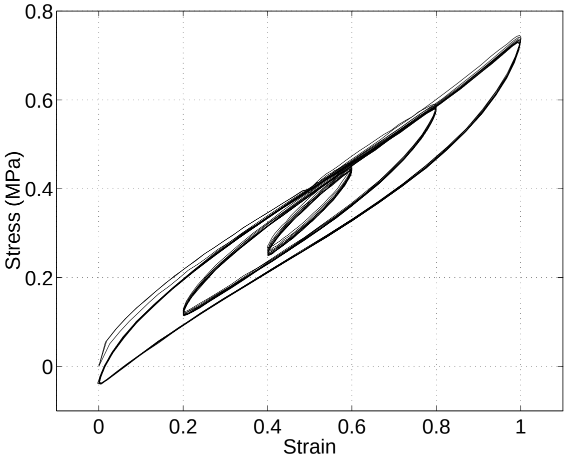

Figure 3: Hysteretic response, obtained from a double shear specimen subjected to a sinusoidal load at $f = 0.05 Hz$.

4 One-Dimensional Models

When subjected to simple shear, the elastic branch of the model behaves almost linear. For simple shear, this observation makes it possible to reduce the material model to a linear one-dimensional elastic-viscoelastic-plastoelastic model. Thus, the behavior of the rubber material, subjected to simple shear, can be discussed using one-dimensional symbolic models.

Using mechanical analogy, one-dimensional models consisting of linear spring and damping elements is used to describe and interpret the dynamic behavior of filled elastomers for simple shear. Models like this can also be used to model rubber components subjected to one-dimensional loads, for instance in vehicle-dynamic simulations. They also provide a useful and illustrative general understanding of the material characteristics.

Next a viscoelastic and an elastoplastic model are discussed. These models are then combined in parallel forming a viscoelastic-elastoplastic model with both frequency and amplitude dependent properties. The viscoplastic model exhibits the same principle behavior as found in the experimentally obtained data. Finally a five-parameter viscoplastic model is used to illustrate the rate and amplitude dependence of the dynamic modulus.

4.1 Viscoelastic model

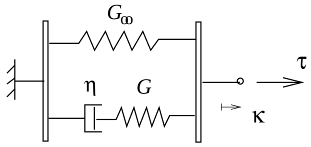

Figure 4: Mechanical anology illustrating a viscoelastic model, the so called standard linear solid model.

The simplest viscoelastic model that exhibits a physically reasonable behavior is a spring combined in parallel with a Maxwell element according to Fig. 4. This is the so called "Standard Linear Solid" model, abbreviated the "SLS-model". The SLS-model is made up of two spring elements with the elastic shear modulus G and G_∞ and a dashpot element with the viscosity coefficient η. This model is able to reproduce the frequency dependent damping of rubber material. It provides a qualitative correct behavior of the dynamic modulus and damping. The dynamic modulus increases with increasing frequency and the damping reaches a maximum where the increase in dynamic modulus is at its maximum. Since the model is purely viscoelastic it does not reflect the amplitude dependence. Therefore the dynamic modulus and the damping is only dependent on the frequency.

In Fig. 5 the dynamic behavior of the SLS-model is shown at three different frequencies. The frequency is increased from 1) representing a low frequency to 3) representing a high frequency. It can be seen that a very low or high frequency results in an almost elastic shear modulus. That is, the damping is almost zero, which is illustrated by the very narrow hysteretic response with the loading and unloading curves being nearly identical. When the frequency is close to zero the elastic shear modulus is given by $G_{dyn} \approx G_\infty$. (Where G_∞ denotes the relaxation modulus at

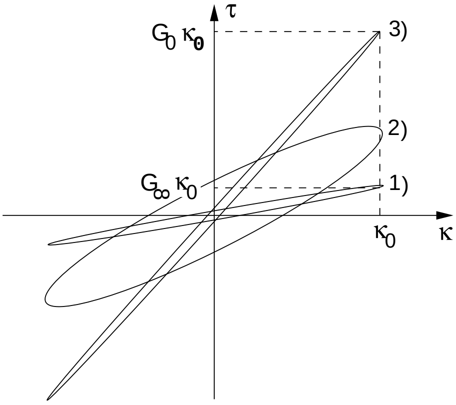

Figure 5: Harmonic excitation of a viscoelastic model and the hysteretic response at increasing frequencies 1) to 3).

time $t = \infty$, corresponding to zero frequency.) The elastic shear modulus corresponding to a high frequency is given by $G_{dyn} = G_0 = G_\infty + G$.

The dynamic shear modulus increases from G_∞ to G_0 with increasing frequency. The maximum damping is found at frequency 2) for which the distance between the loading and unloading curve reaches its maximum.

4.2 Elastoplastic model

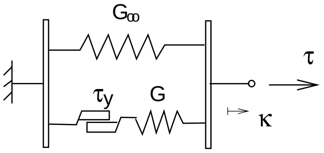

Figure 6: Mechanical analogy illustrating a simple elastoplastic material model, which is able to represent an amplitude dependent dynamic shear modulus.

Besides the viscous type of damping described earlier there is also a rate independent damping in filled rubber materials. A simple model describing rate independent damping is obtained by replacing the dashpot in the SLS-model with a frictional element according to Fig. 6. During slip between the element surfaces, symbolically illustrated in the figure, the frictional element stress is limited to $\pm\tau_y$. The stress is thus limited to the prescribed stress independent of the relative velocity of the contacting surfaces.

The model in Fig. 6, with two parallel springs with the elastic shear modulus G and G_∞, is the mechanical analogy for an elastoplastic material with linear kinematic hardening. The stress in the model is in this case independent of the strain rate.

When the model is subjected to cyclic loading, the frictional element causes a difference between the loading and unloading curves and the hysteretic response is given the shape of a

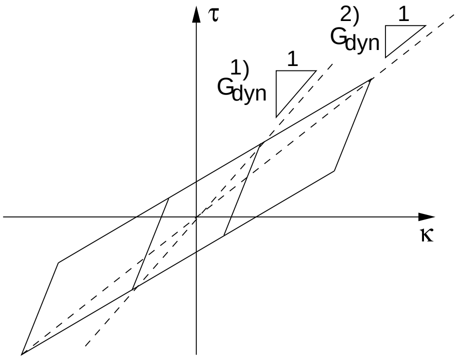

Figure 7: Periodic excitation of an elastoplastic model and the hysteretic response at two different amplitudes. Depending on the amplitude two different dynamic shear modulus are obtained.

parallelogram according to Fig. 7, provided that the limiting stress is reached in the frictional element. All type of periodic loading with a certain amplitude ϵ_0 provides the same results in the stress-strain graph, independent of load shape and load rate.

The frictional element provides a non-linearity that may be observed from the parallelogram shaped hysteretic response. This also results in an amplitude dependent dynamic shear modulus. As can be seen in Fig. 7, it is obvious that the dynamic shear modulus decreases with increasing amplitude.

4.3 Viscoelastic-elastoplastic model

For filled elastomers damping is caused by two different mechanisms at the material level, resulting in viscous and frictional damping respectively. Reorganization of the rubber network during periodic loading results in a viscous type of resistance. A common view is that the Payne effect is caused by frictional damping attributed to the filler structure and the breaking and reforming of the structure which take place during loading and unloading. The stresses obtained in a filled rubber material can thus be divided into a dominant elastic part, but also a viscous and a frictional part.

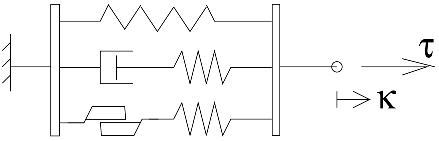

Figure 8: Mechanical analogy illustrating a simple five parameter viscoplastic material model resulting in a frequency and amplitude dependent dynamic shear modulus and damping.

Combining the viscoelastic and the elastoplastic model in parallel yields a material model which sums the elastic, viscous and frictional stresses. A simple model of this viscoplastic type is shown in Fig. 8. The model simulates the frequency and amplitude dependence in a physically correct manner.

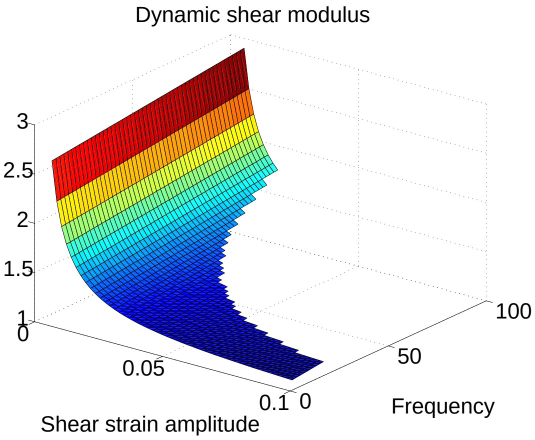

Figure 9: Amplitude and frequency dependence of the dynamic shear modulus (See Eq. (1).) for the simple five parameter model.

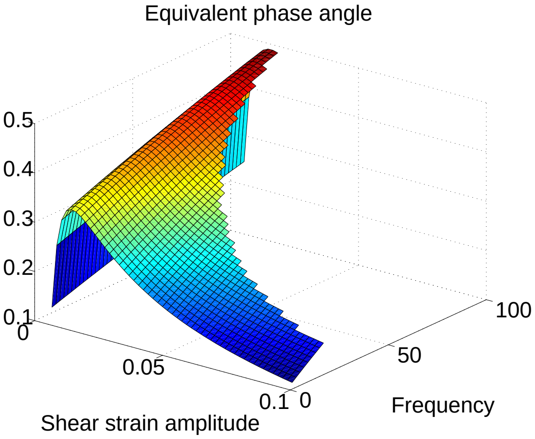

Figure 10: Amplitude and frequency dependence of the phase angle (See Eq. (2).) for the simple five parameter model.

The combined frequency and amplitude dependence of the dynamic shear modulus and phase angle according to the material model in Fig. 8 is illustrated in Fig. 9 and 10. The phase angle is directly proportional to the damping and thus also proportional to the hysteresis. That is, a large phase angle yields a large difference between the loading and unloading curve. Values of the dynamic shear modulus and phase angle for which the amplitude and frequency result in a power output which exceeds a certain limit have been removed from the figure. The separable amplitude and frequency dependence of the model is in agreement with experimental findings according to (Austrell 1997).

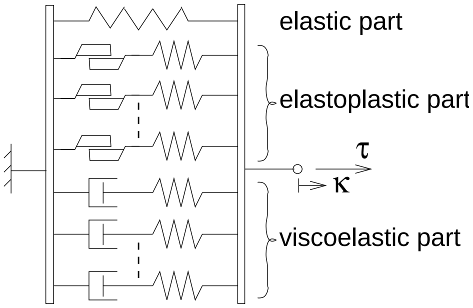

Figure 11: The generalized one-dimensional viscoelastic-elastoplastic model.

The one-dimensional model shown in Fig. 8 can be generalized by adding more viscous and frictional elements in parallel, according to Fig. 1. The model can then be given a quantitative better fit to experimental data. In section 5 this enhanced model is generalized into three dimensions for the purpose of finite element calculations. Since the one-dimensional model is equivalent to simple shear of the the three-dimensional model, the material parameters are the same for the one-dimensional model and the three-dimensional model. Hence, once the one-dimensional model is fitted to the simple shear test, the material parameters can by shifted to the three-dimensional model FE-model.

5 The Overlay Method

According to the one-dimensional viscoplastic model shown in Fig. 1, the total stress is obtained by adding the elastic stress, the viscous stress, and the plastic stress. A direct generalization of the one-dimensional stress to a three dimensional state of stress is to add elastic, plastic and viscous stress tensors. The total stress tensor $\boldsymbol{\tau}$ is then given by

$$\boldsymbol{\tau} = \boldsymbol{\tau}^{e} + \boldsymbol{\tau}^{ep} + \boldsymbol{\tau}^{ve} \tag{3}$$

where the different stress tensors are obtained from a hyperelastic, an elastoplastic and a viscoelastic material model. For consistency, all these models should be based on the same hyperelastic model.

The elastoplastic part of the stress tensor is given by a summation

$$\boldsymbol{\tau}^{ep} = \sum_{j=1}^{M} \boldsymbol{\tau}_j^{ep} \tag{4}$$

where the terms are obtained from a non-hardening plasticity model, according to von Mises, implemented for large strains. The model used in section 6 uses three terms in the summation above.

The viscoelastic stress contribution is also given by a summation according to

$$\boldsymbol{\tau}^{ve} = \sum_{k=1}^{N} \boldsymbol{\tau}_k^{ve} \tag{5}$$

where the terms are obtained from a visco-hyperelastic model, suitable for large strains.

5.1 Implementation of the Overlay Method

Since the commercial FE-codes do not contain any suitable constitutive model, this paper proposes a novel engineering approach. Using only standard FE-codes, a three-dimensional model is obtained through an overlay of FE-meshes. With this approach, the implementation of a new constitutive model is avoided. The basic approach using the overlay method, is to create one hyperelastic, one viscoelastic and one elastoplastic FE-model, all with identical element meshes. Assembling the nodes of these models according to Fig. 12, yields a finite element model that corresponds to the five-parameter model discussed earlier. In order to create a model corresponding to the generalized mechanical analogy in Fig. 1, a suitable number of viscoelastic or elastoplastic FE-models are simply connected in parallel by assembling different layers of elements to the same nodes.

In *Abaqus* both the hyperelastic and the viscoelastic parts can be modelled with a single FE-model based on a viscoelastic Prony series. The elastoplastic part can be modelled with several parallel elastoplastic FE-models based on a non-hardening elastoplastic material model. In Abaqus/Standard there is also a possibility to define a piecewise kinematic hardening elastoplastic model. Unfortunately, neither Abaqus nor Marc contain any elastoplastic models based on hyperelasticity. Hence, in the following section the plastic part is based on a hypoelastic material model.

Preliminary investigations indicate that the material parameters needed for the finite element models can simply be copied from the one-dimensional model which has been fitted to experimental data in simple shear. A fitting procedure for the one-dimensional model is further discussed in (Olsson & Austrell 2001).

The reason why the one-dimensional mechanical analogy seems to be easily generalized into three-dimensions has not been thoroughly investigated. However, one reasonable explanation for this behaviour is that the isotropic and incompressible characteristics of rubber provides a constraint that reduces the degrees of freedom in the three-dimensional model.

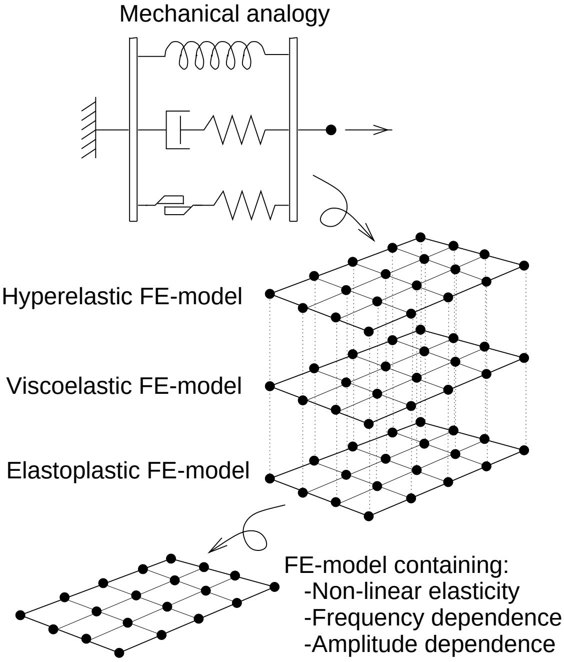
Mechanical analogy
Hyperelastic FE-model
Viscoelastic FE-model
Elastoplastic FE-model
FE-model containing:
-Non-linear elasticity
-Frequency dependence
-Amplitude dependence

Figure 12: Basic idea of the overlay model.

6 Cylindric Rubber Bushing

A cylindric component according to Fig. 13 has been studied when subjected to a stationary cyclic load. The bushing consists of one outer and one inner steel tube, with rubber in between. The component is subjected to large amplitudes at low frequencies. A finite element analysis of the component, using a material model that combines non-linear elastic properties with rate independent damping, has been performed. The dimensions used in the computations are $r = 20$mm, R=40mm and $H = 50$mm.

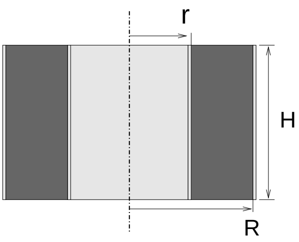

Figure 13: The analyzed cylindric component.

The model was fitted to the hysteretic response presented in Fig. 3. The experimental data were obtained using a double shear test specimen according to Fig. 1. Fig. 14 shows the response of the one-dimensional material model subjected to the same load as the test specimen.

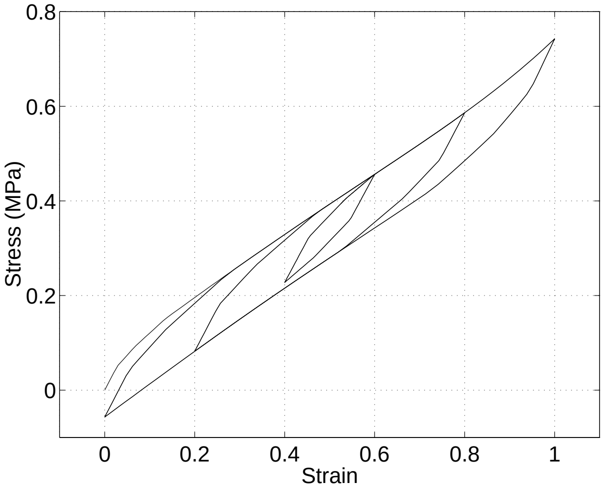

Figure 14: The one-dimensional material model subjected to a sinusoidal shear load at $f = 0.05Hz$.

The rubber bushing was modelled in *Abaqus* combining a hyperelastic material model and three elastoplastic models. The elastoplastic models were based on hypoelasticity with isotropic von Mises plasticity without hardening. An inconsistency with the used model is that the elastoplastic part is hypoelastic while the elastic part is hyperelastic. It would be preferable if the same hyperelastic base was used for the entire model, but as stated previously *Abaqus* does not contain any hyperelastic plastic materials models at the present date.

6.1 Axial Shear Load

Fig. 15 shows the cylindric component during axial cyclic shear loading. The load case is a displacement controlled cyclic loading with gradually increasing amplitude. The state of stress is very close to simple shear.

The shear stress τ shown in the graph is the mean stress computed as the axial load, obtained from the finite element analysis, divided by a cylindric surface area with the radius $(r + R)/2$, resulting in $\tau = P/(\pi(r + R)H)$. As can be seen in the graph, the dynamic modulus decreases with increasing strain amplitude. Another interesting observation made from the graph is that the shape of the hysteretic response is in good agreement with the experimental result, according to Fig. 3, used to obtain the one-dimensional material model.

6.2 Axial Tension

Fig. 16 shows the cylindric component subjected to a homogeneous stress. This load is not in agreement with the present component design, with one inner and one outer metal pipe vulcanized to cylindrical surfaces of the rubber part. However, this load case is of great interest since it shows the behavior of the material model during pure tensile and compressive loading. The load

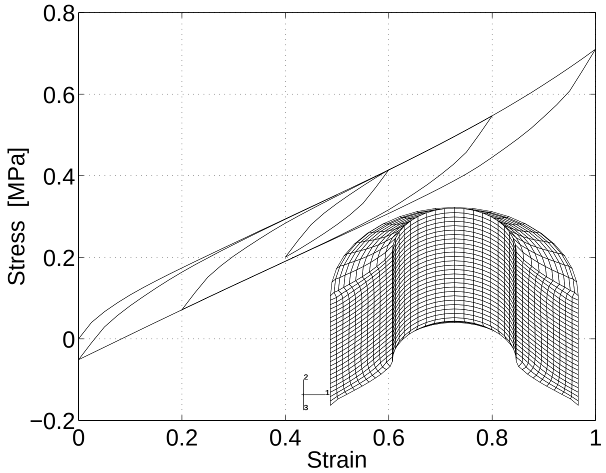

Figure 15: Amplitude dependent dynamic stiffness. Finite element analysis of the cylindric component subjected to an axial cyclic shear loading.

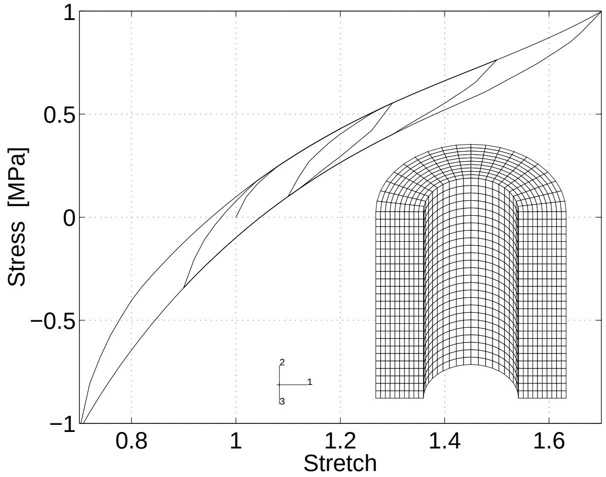

Figure 16: Amplitude dependent dynamic stiffness. Analysis of a cylindric component subjected to axial cyclic tensile/compressive load.

case is a displacement controlled cyclic loading with gradually increasing amplitude. The stress (same in all elements) shown in the graph is calculated as the axial force P, obtained from the finite element analysis, divided by the original cross-sectional area $A = \pi(R^2 - r^2)$. The graph illustrates the influence of the non-linear elastic stress contribution on the hysteretic response at different amplitudes.

6.3 Radial Load

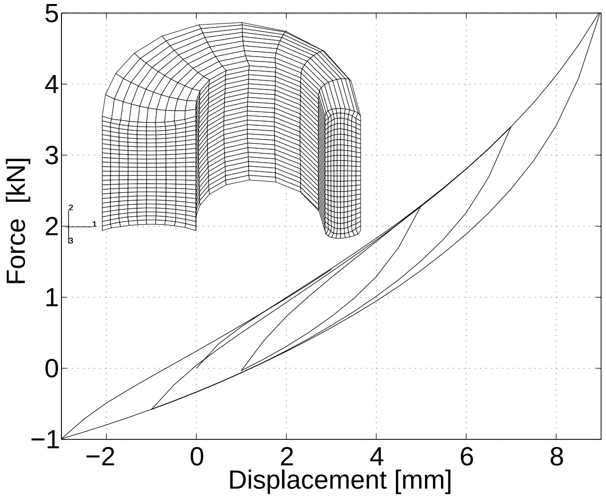

Figure 17: Amplitude dependent dynamic stiffness. Analysis of the cylindric component subjected to a radial cyclic load.

Fig. 17 shows the cylindric component subjected to a radial load. The load case is displacement controlled and cyclic, with gradually increasing amplitude. Since there is no sense in presenting a specific stress in this highly inhomogeneous stress state, the graph shows the relation between the radial force P, obtained from the finite element analysis, and the radial displacement. Similar to the previous load case, the graph also shows the influence of the non-linear elastic stress contribution on the hysteretic response.

6.4 Torsional Load

Fig. 18 shows the cylindric component subjected to a torsional load. The load case is displacement controlled and cyclic, with gradually increasing torsion. The graph shows the relation between the torsional moment M_t, obtained from the finite element analysis, and the torsion presented in radians. As expected the hysteretic response shows in principle the same behavior as for the axial shear load in Fig. 15, since torsion in principle is a state of shear.

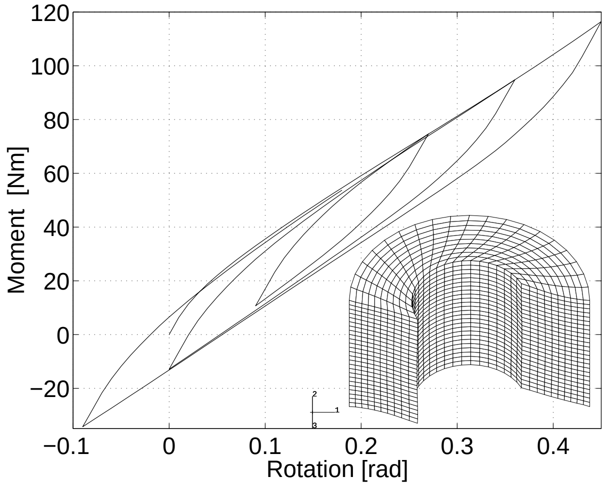

Figure 18: Amplitude dependent dynamic stiffness. Analysis of the cylindric component subjected to a torsional cyclic load.

7 Conclusions

Using a novel engineering approach, it is shown how already existing FE-codes can be used to model the dynamic behavior of rubber components. The use of existing FE-codes makes it easy to create a highly advanced model without implementing a new constitutive model. The presented method is able to represent the non-linear elastic behavior, as well as the rate dependent and amplitude dependent inelastic properties of rubber material. The model discussed works equally well for a general dynamic load as well as for creep and relaxation analysis and other cases of transient dynamic loads.

Finally, a cylindric rubber bushing, subjected to different low frequency cyclic load cases, was analyzed using the proposed method. A harmonic simple shear test was used to obtain the material parameters. The component characteristics were then calculated for different load directions, giving a physically reasonable behavior.

Notation

The following symbols are used in this paper:

G = shear modulus
G_{dyn} = dynamic shear modulus
G_∞ = long term shear modulus
G_0 = instant shear modulus
τ = shear stress
τ_0 = shear stress amplitude
τ_y = yielding shear stress
$\boldsymbol{\tau}$ = stress tensor
κ = shear strain
κ_0 = shear strain amplitude
d = damping
δ = phase angle
U_c = dissipated energy for a closed hysteresis loop
η = viscosity coefficient
M = number of elastoplastic components
N = number of viscoelastic components

Superscripts

e = elastic
ep = elastoplastic
ve = viscoelastic

References

Austrell, P-E. (1997). *Modeling of Elasticity and Damping for Filled Elastomers* Thesis, Lund University, Division of Structural Mechanics, Report TVSM-1009, Sweden

Austrell, P-E., Olsson, A.K., and Jönsson, M. (2001). "A method to analyze the non-linear dynamic behaviour of carbon-black-filled rubber components using standard finite element codes" *Proceedings of the Second European Conference on Constitutive Models for Rubber*, Germany

Chazeau, L., Brown, J., Yanyo, L., and Sternstein, S. (2000). "Modulus recovery kinematics and other insights into the Payne effect for filled elastomers" *Polymer Composites*, 21, No. 2, pp. 202-222

Enelund, M., Mähler, L., Runesson, K., and Josefsson, B.L. (1996). "Unified Formulation and Integration of the Standard Viscoelastic Solid with Integer and Fractional Order Rate Laws" *19th International Congress of Theoretical and Applied Mechanics (ICTAM)*, Kyoto, Japan

Ferry, J.D. (1970). *Viscoelastic properties of polymers* second edition, J Wiley and Sons Inc., Chap. 11, New York

Kaliske, M., and Rothert, H. (1998). "Constitutive Approach to Rate Independent Properties of Filled Elastomers" *Int. J. Solids Structures*, Vol. 35, No. 17, pp. 2057-2071

Kari, L., and Sjöberg M. (2003). "Temperature dependent stiffness of a precompressed rubber isolator in the audible frequency range" Manuscript submitted to *International Journal of Solids and Structures.*

Miehe, C. (1995). "Discontinuous and continuous damage evolution in Ogden-type large-strain elastic materials" *Eur. J. Mech., A/Solids*, 14, pp. 697-720.

Miehe, C., and Keck, J. (2000). "Superimposed finite elastic-viscoelastic-plastoelastic stress response with damage in filed rubbery polymers. Experiments, modelling and algorithmic implementations" *J. Mech. Phys. Solids*, 48, 323-365

Mullins, L. (1969). "Softening of Rubber by Deformation" *Rubber Chemistry and Technology*, Vol. 42, pp. 339-362

Olsson, A.K., and Austrell, P-E. (2001). "A Fitting Procedure for Viscoelastic-Elastoplastic Material Models" *Proceedings of the Second European Conference on Constitutive Models for Rubber*, Germany

Payne, A.R. (1965). *Reinforcement of Elastomers* G. Kraus, Ed., Interscience, Chap. 3, New York

Simo, J.C. (1987). "On a Fully Three-Dimensional Finite-Strain Viscoelastic Damage Model: Formulation and Computational Aspects." *Computer Methods in Applied Mechanics and Engineering*, Vol. 60, pp. 153-173

Sjöberg, M. (2000). "Measurements and modelling using fractional derivatives and friction" *Society of Automotive Engineers*, paper No 2000-013518

Yeoh, O. H. (1993). "Characterization of Elastic Properties of Carbon-black-filled Rubber Vulcanizates" *Rubber Chemistry and Technology*, Vol. 66,pp. 754-772

Paper II

Parameter identification for a Viscoelastic-Elastoplastic Material Model

Presented in abbreviated form at ECCMR Hannover 2001

Parameter identification for a Viscoelastic-Elastoplastic Material Model

Anders K Olsson, Per-Erik Austrell
Division of Structural Mechanics, Lund University, Sweden

ABSTRACT: A fitting procedure for a viscoelastic-elastoplastic material model capable of representing amplitude and rate dependent properties of filled elastomers is presented. The material model contains a lot of parameters that have to be fitted to experimental data. A method to fit such a viscoelastic-elastoplastic material model to data obtained from a stationary dynamic shear test is suggested. Using this method, the material model was fitted to experimental data for thirteen different elastomers. Simulated dynamic modulus and damping are compared to experimental data and presented for a wide range of frequencies and strain amplitudes.

1 Introduction

Filled rubber is a two-phase material consisting of long polymer chains in a structure of microscopical carbon-black particles. Reorganization of the rubber network during dynamic loading gives rise to a viscous damping. When subjected to a dynamic load, breaking and reforming of the carbon-black structure results in a frictional elastoplastic damping.

Experimental results have shown that the viscoelastic behavior is almost independent of the elastoplastic behavior (Warnaka 1962). This observation of independence between the viscoelastic and elastoplastic behavior is the foundation of several models for modelling the dynamic behavior of rubber (Kaliske & Rothert 1998), (Miehe & Keck 2000) and (Sjöberg & Kari 2002).

The model addressed in this paper has previously been described in (Austrell & Olsson 2001). A one-dimensional mechanical analog in simple shear, where the elastic properties of rubber are rather linear, is shown in figure 1. This makes it possible to represent the material model as a one-dimensional model according to the figure, where the elastoplastic elements are coupled in parallel with the viscoelastic elements. The reason for having more than one viscoelastic and more than one elastoplastic stress component, is to get an improved fit to a wider range of frequencies

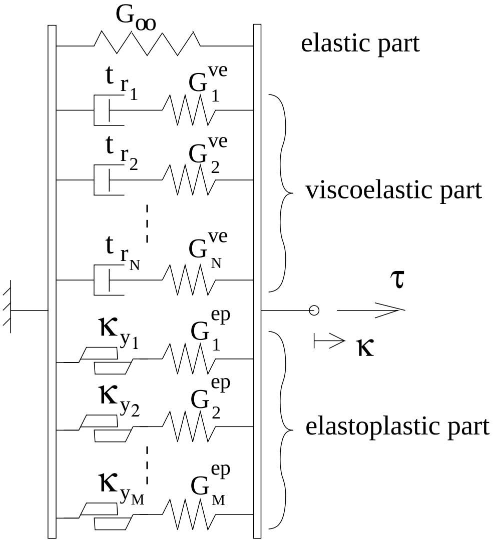

Figure 1: The one-dimensional mechanical analog representation of the material model.

and strain amplitudes.

In (Austrell & Olsson 2001) it is shown how this model is easily generalized into three dimensions by an overlay principle, by merging several viscoelastic and elastoplastic FE-meshes. The advantage of this approach is that it does not require any implementation of new constitutive laws, since it only uses already implemented models. Another advantage of this approach is the ability to use the parameters already obtained for the one-dimensional model in figure 1. Hence, it is sufficient to fit the one-dimensional model to the experimental data. The material parameters can then simply be shifted to the finite element model.

The drawback with the above model is the large number of material parameters that are needed. Because of the number of material parameters, it is almost impossible to fit the material model by hand. This obstacle is removed by the method presented here. A structured fitting procedure makes it easy to obtain the material model from experimental data.

Viscoelastic models using fractional derivatives such as (Enelund et al 1996), (Sjöberg & Kari 2002) generally do not need as many parameters to describe the viscoelastic part of the material and are thus easier to fit to experimental data. Models like these are usually better suited for evaluation in the frequency domain than in the time domain, where they tend to be rather time-consuming. This is due to the fact that the entire load history has to be taken into account at every time increment. In the presented method it is only needed to store the previous stress state in the time stepping. Another obstacle with the fractional derivative model is the absence of commercially available FE-codes.

The elastoplastic part of this model consists of an overlay of ideally (non-hardening) elastoplastic models. When connected together their behavior will be piece-wise kinematic hardening. A continuous kinematic hardening model could replace this elastoplastic part. However, since kinematic hardening still is rare in commercial finite element codes, a simple overlay of ideally elastoplastic models was chosen.

2 Test method

A test batch of 13 different elastomers has been evaluated by dynamic simple shear tests. Experiments were carried out at the Marcus Wallenberg Laboratory in Stockholm (Kari & Lindgren). The test object used is the so called double shear test specimen according to figure 2.

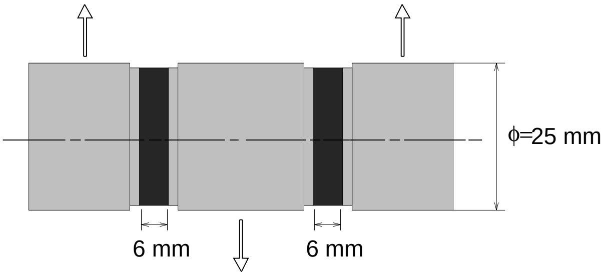

Figure 2: Double shear specimen, used for testing at simple shear.

The test specimens have been subjected to a sinusoidal load, for a wide range of different frequencies and amplitudes, with shear strain amplitudes up to 12% and frequencies up to 180 Hz. To prevent hysteretic heat build-up from ruining the result, the measurements were performed during a very brief time period, but still long enough to obtain a stationary reading. For each strain amplitude and frequency, about 20 load-cycles have been performed, out of which five were evaluated. A typical hysteresis loop from a load cycle is shown in figure 3. For a given frequency, measurements were conducted at four different amplitudes, starting with the smallest amplitude. Thus, also damage effects were included in the measurement. However, the investigated material model does not include any damage effects. This conflict between model and measurement is further discussed in section 6.

The dynamic behavior of rubber materials can be characterized by the dynamic shear modulus and the phase angle, i.e. the aim of the fitting procedure is a material model with the same stiffness and damping properties as the tested rubbers. The dynamic shear modulus G_{dyn} and the corresponding damping parameter d, are defined according to

$$G_{dyn} = \frac{\tau_0}{\kappa_0}, \qquad d = \frac{U_c}{\pi \kappa_0 \tau_0} \tag{1}$$

with variables U_c, τ_0 and κ_0 defined in figure 3. The hysteretic work per unit volume U_c is obtained through numerical integration of the experimentally recorded time history data. It can be noted that the damping parameter d is identical to $sin(\delta)$ for a purely linear viscoelastic model, where δ is the phase angle. Assuming simple shear, the shear stress τ and shear strain κ are calculated according to

$$\tau = \frac{P}{2A}, \qquad \kappa = \frac{u}{H} \tag{2}$$

where P is the shear force, $2A$ is the two shearing areas, u is the displacement and H is the thickness of the shear specimen. This is, however, only true for a pure state of simple shear. Finite element analysis indicates that this approach leads to an underestimate of the shear modulus with approximately 6%. Thus the obtained shear modulus should be increased by 6%.

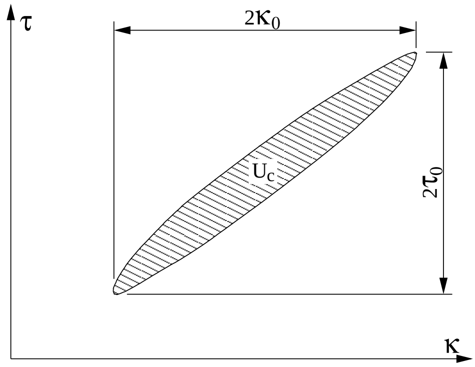

Figure 3: Typical hysteretic loop for a filled rubber.

3 Fitting procedure

Although the one-dimensional material model is rather simple in its appearance, the number of material parameters to be determined makes the fitting procedure difficult. The dynamic behavior of rubber components is mainly attributed the dynamic stiffness and the damping properties. Thus the aim is to obtain a material model that exhibits the same stiffness and damping as the rubber material, for a given range of frequencies and strain amplitudes.

3.1 An optimization approach

The fitting procedure can be viewed as a least square minimization of the relative error of the material model compared to the experimental data. For this purpose an error function ψ is established:

$$\psi = (1-\alpha)\sum_{i=1}^{m}\left(\frac{d_{dyn,i}-d_{exp,\,i}}{d_{exp,\,i}}\right)^2 + \alpha\sum_{i=1}^{m}\left(\frac{G_{dyn,i}-G_{exp,\,i}}{G_{exp,\,i}}\right)^2 \tag{3}$$

The damping d_i and shear modulus $G_{dyn,i}$ are calculated from the material model at the specified frequencies and amplitudes, where m is the total number of measurements. Thus the error function is a function of the material parameters (see fig. 1): $\psi = \psi(G_\infty, G_1^{ve}, t_{r1}, ..., G_1^{ep}, \kappa_{y1}, ...)$. By choosing the scale factor α, it is possible to decide whether to emphasize a correct modelling of the dynamic modulus or a correct modelling of the damping.

In a similar manner it is also possible to chose individual weight factors for each measurement i. This might be useful if the measurements are not evenly distributed or if extra emphasize is to be given for certain frequencies and amplitudes.

Evaluation of theoretical damping and dynamic stiffness can be done in two different ways. The most correct way to obtain the behaviour of the material model is to use a time-stepping algorithm. This is however, a time-consuming procedure, especially if the optimization algorithm is such that the error function needs to be evaluated repeatedly. For a large amount of measurements and an increasing number of material parameters this approach will be very slow. A more efficient approach is to use an analytical approximation. However, the poor accuracy of this approach yields a model with poor fit to experimental data. A way to work around this problem is to use the analytical approach for repeated evaluations and to use the time stepping algorithm to calibrate the analytical expression with certain intervals. The fitting procedure was developed using this basic idea.

3.2 Analytical approximation of damping and modulus

The one-dimensional model consists of three different types of elements, namely the elastic element, the viscoelastic Maxwell element and the elastoplastic element (fig. 1). In order to calculate the total damping d^{tot} and dynamic shear modulus G^{tot}_{dyn} for the entire model, damping and modulus are calculated for each of the elements.

Starting with the single Maxwell element, it can be shown (Austrell 1997) that the viscoelastic damping is given by

$$d_i = sin(\delta_i) = \frac{1}{\sqrt{1+\omega^2 t^2_{r_i}}} \tag{4}$$

and that the dynamic shear modulus is given by

$$G^{ve}_{dyn_i} = \frac{G^{ve}_i \omega^2 t^2_{r_i}}{1+\omega^2 t^2_{r_i}}. \tag{5}$$

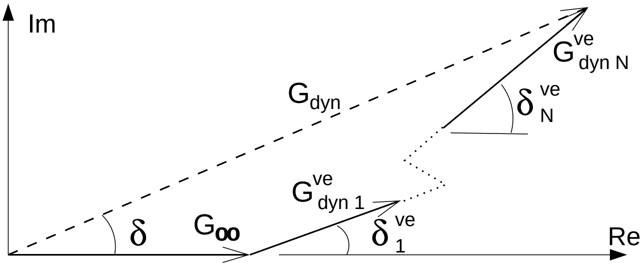

Figure 4: The complex modulus of the viscoelastic Maxwell components (solid lines) and the resulting viscoelastic modulus plotted in the complex plane

In figure 4 the viscoelastic branch is plotted in the complex plane. Summing up the total dynamic contribution from all the N Maxwell elements and the purely elastic element results in the following expression

$$G^{ve}_{dyn} = \sqrt{\left(G_\infty + \sum_{i=1}^{N} G^{ve}_{dyn_i} cos(\delta_i)\right)^2 + \left(\sum_{i=1}^{N} G^{ve}_{dyn_i} sin(\delta_i)\right)^2} \tag{6}$$

where δ_i is the phase angle according to equation (4). In a similar manner the total viscous damping can be expressed as:

$$d^{ve} = \frac{1}{G^{ve}_{dyn}} \sum_{i=1}^{N} \frac{G^{ve}_i \omega^2 t^2_{r_i}}{(1+\omega^2 t^2_{r_i})^{3/2}} \tag{7}$$

Thus, the viscoelastic part of damping and dynamic shear modulus is calculated with the analytical expressions (6) and (7).

The behavior of the elastoplastic element j depends on whether it is plastic or not, i.e. whether the shear strain amplitude κ_0 is larger than the yield strain κ_y or not.

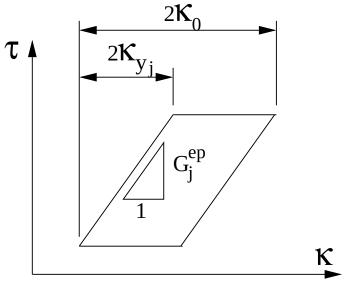

Figure 5: The hysteretic loop of one elastoplastic element.

From the elastoplastic response of a single element, shown in figure 5, it can be seen that the shear stress amplitude $\tau_{0_j}^{ep}$ for an elastoplastic element is given by

$$\tau_{0_j}^{ep} = \begin{cases} G_j^{ep}\kappa_{y_j} & \text{if } \kappa_0 > \kappa_{y_j} \\ G_j^{ep}\kappa_0 & \text{otherwise} \end{cases} \tag{8}$$

Using the definition of equation (1) and by looking at figure 5, it can be seen that the dynamic modulus for an elastoplastic element j is given by:

$$G_{dyn_j}^{ep} = \begin{cases} \frac{G_j^{ep}\kappa_{y_j}}{\kappa_0} & \text{if } \kappa_0 > \kappa_{y_j} \\ G_j^{ep} & \text{otherwise} \end{cases} \tag{9}$$

For the maximal strain $\kappa = \kappa_0$, all the elastoplastic elements will have reached their maximal stress level $\tau_j^{ep} = \tau_{0_j}^{ep}$. Hence, the elastoplastic stress amplitude is obtained as the sum of the stress amplitudes from all of the elastoplastic elements. From the definition of dynamic shear modulus according to equation (1) the total dynamic shear modulus for the elastoplastic part G_{dyn}^{ep} is then given by

$$G_{dyn}^{ep} = \sum_{j=1}^{M} G_{dyn_j}^{ep}. \tag{10}$$

The hysteretic work U_{c_j} is given by the inclosed area in the hysteretic loop, seen in figure 5. Simple geometry yield

$$U_{c_j}^{ep} = \begin{cases} 4\kappa_{s_j}G_j^{ep}(\kappa_0 - \kappa_{y_j}) & \text{if } \kappa_0 > \kappa_{y_j} \\ 0 & \text{otherwise.} \end{cases} \tag{11}$$

Adding up the hysteretic work done in each element, the total plastic damping, as defined in equation (1), is found to be

$$d^{ep} = \frac{\sum_{j=1}^{M} U_{c_j}^{ep}}{\pi \kappa_0 \sum_{j=1}^{M} \tau_{0_j}^{ep}}. \tag{12}$$

Thus, the elastoplastic part of damping and dynamic shear modulus is calculated with the analytical expressions (10) and (12).

Since the largest stress for the total elastoplastic contribution does not occur at the same time as for the viscoelastic contribution, adding the contributions from all elements in the model becomes rather complicated and numerically time consuming. The elastoplastic response can be approximated with its basic Fourier component (Harris & Stevenson 1986). This approximation makes it possible to represent both the elastoplastic response and the viscoelastic response in a complex plane, as seen in figure 6.

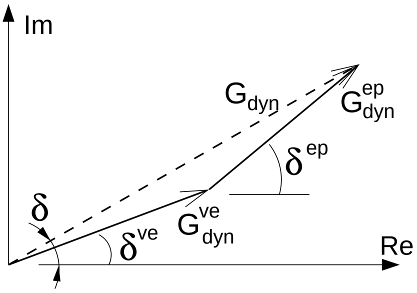

Figure 6: Approximative representation of the viscoelastic and elastoplastic response in the complex plane.

Based on this complex representation and using the approximation $cos(\delta) \approx cos(\delta^{ep}) \approx cos(\delta^{ve})$, the total dynamic shear modulus is obtained from the following expression

$$G_{dyn} \approx G_{dyn}^{ep} + G_{dyn}^{ve} \tag{13}$$

noting that G_{dyn}^{ve} also contains the elastic contribution G_{∞}. Another way to reach expression (13) would be to approximate the viscoelastic part with an elastoplastic part. As explained for equation (10), the total dynamic modulus for elastoplastic models can be derived through a simple summation. Hence, using this elastoplastic approximation will also result in equation (13).

From the representation of figure 6 and some trigonometry, using $d = sin(\delta)$, the total damping is calculated similar to a generalized Maxwell model.

$$d \approx \frac{G_{dyn}^{ep} d^{ep} + G_{dyn}^{ve} d^{ve}}{G_{dyn}} \tag{14}$$

With equation (13) and (14) it is possible to calculate the error function (3) analytically. Due to the approximations introduced, this expression has to be calibrated using a more time consuming time stepping approach. The calibration is done by multiplying equation (13) and (14) with a scalar correction factor. This correction factor will be dependent on both frequency and strain amplitude, as well as the material parameters.

3.3 Numerical evaluation of damping and modulus

A more accurate way to calculate damping and modulus is by a numerical time stepping algorithm. The elastoplastic stress for an element j can be expressed in the following incremental form.

$$\Delta\tau_j^{ep} = \begin{cases} G_j^{ep}\Delta\kappa & \text{if elastic} \\ 0 & \text{otherwise} \end{cases} \tag{15}$$

The viscoelastic stress response is given by a hereditary integral according to

$$\tau_i^{ve}(t) = \int_{-\infty}^{t} G_{R_i}(t-t')d\kappa(t') \tag{16}$$

where the relaxation modulus G_{R_i} for a Maxwell element i is given by

$$G_{R_i} = G_i^{ve} exp\left(\frac{-t}{t_{r_i}}\right) \tag{17}$$

Combining equation (16) and (17), and approximating according to the trapezoidal rule, the viscoelastic stress for element i can be expressed in an incremental form

$$\begin{aligned}\Delta\tau_i^{ve} \approx \tau_i^{ve}\left(exp\left(\frac{-\Delta t}{t_{r_i}}\right)-1\right)+ \\ \frac{G_i^{ve}\Delta\kappa}{2}\left(1+exp\left(\frac{-\Delta t}{t_{r_i}}\right)\right)\end{aligned} \tag{18}$$

where τ_i is the stress at the previous step.

The total stress increment for the whole model is then obtained by adding all incremental stress contributions from all elements. In doing so for each step in strain history, the stress history is derived. From the stress history, the dynamic modulus and damping is obtained using the definitions in equation (1).

3.4 Implementation

The multi-dimensional line search algorithm *fmincon* provided by the optimization tool-box in *Matlab* (MathWorks Inc.) has been used to find the minimum of the error function in equation (3). To do this, the error function has to be calculated at all strains and frequencies where measurements have been made, i.e., damping and dynamic modulus have to be calculated at all experimental points.

To reduce the search area, the following constraints are imposed.

$$\begin{array}{l} t_{r_1} > t_{r_2} > ... > t_{r_N} \\ \kappa_{y_1} > \kappa_{y_2} > ... > \kappa_{y_M} \\ \kappa_{y_1} < max\left(\kappa_0\right) \end{array} \tag{19}$$

To further reduce the search area and to avoid nonphysical material parameters, each parameter is given an upper and a lower bound, besides the bounds in equation (19). This upper and lower bound can also be used to avoid extremely high modulus which will ruin the computational performance when an explicit finite element method is used. The bound is also useful in order to prevent the creation of elastoplastic or viscoelastic contributions that will always behave elastic for the given strain amplitudes and frequencies.

Since the material model may contain a large number of parameters it is often difficult to find a true global optimum. To stabilize the optimization algorithm it is important to use a structured approach. The fitting is done in four steps:

- At first a rough guess of the material parameters is made. Both yield strains and relaxation times are given a logarithmic distribution over the measured amplitudes and frequencies respectively.
- Secondly, the shear moduli of the elastic and the elastoplastic elements are fitted to only the lowest frequency for which the influence of the viscoelastic elements may be neglected. The yield strains for the elastoplastic contributions are unchanged at this stage.
- The third step is to fit all of the shear moduli to all test data. After this step the model should be fairly accurate.
- The final step is then to fit all material parameters to all test data, resulting in a minor adjustment of the material model.

For the last three steps the error-function ψ according to equation (3) is minimized using an iterative method for which the error-function has to be evaluated repeatedly. As already mentioned, the analytical solution by itself is not accurate enough to provide a good fit for the material model and the numerical solution is too time-consuming to be evaluated more than a few times during the fitting algorithm. The solution to this problem, is to use the analytic expression when minimizing. When the minimization has converged, the analytical and numerical damping and modulus are then compared and a correction factor is calculated. The analytical expressions for damping and modulus are then adjusted with the correction factor, in order to give accurate result. The minimization algorithm is repeated using the adjusted analytical expression. This procedure is repeated for the last three steps above. The correction factor will depend on frequency and strain amplitude as well as material parameters.

It should be noted that although the described method has been shown to work well in finding a minimum for the error function, it does not guarantee that the obtained minimum is truly global. Nor is it certain that the true minimum would provide the best material model from an engineering point of view. Once a material model is obtained it therefore has to be compared to the experimental data, as is done in section 5. If the obtained material parameters does not provide a good enough fit, a change in weight factor or number of viscoelastic and elastoplastic contributions are made, and the fitting procedure is restarted with the new error function. Each fitting procedure takes about one minute on a regular $1000MHz$ PC, depending of the number of elements and the number of measurements.

To enhance the interactivity the fitting procedure was implemented using a graphical user-interface in $Matlab$. Weight factor, number of elastoplastic and viscoelastic contributions can be easily set in the user-interface, and the resulting model plotted in comparison with the experimental data.

4 Materials and experimental findings

The dynamic shear modulus and damping have been measured for 13 different rubber materials. The materials and their hardness are presented in table 1. The hardness for the rubber materials has been measured for sample plates from the same batch as the test specimen were manufactured from. Compared to most other rubber the tested materials are relatively hard and with a high degree of damping.

Material	Hardness
NR60, Svedala Skega	$\sim$60
NR80, Svedala Skega	$\sim$80
ECO 3575s, Ahauser	56-59
HGSD 78, Scapa Rolls	76-77
HGSD 85, Scapa Rolls	83-85
HNBR 78 Shore A, Trelleborg	78-82
Hypalon 72 Shore A, Trelleborg	72
EPDM 0591, Ahauser	94-95
PUR 9180h, Ahauser	82-86
PUR 9190h, Ahauser	94-95
PUR 9290h, Ahauser	86-87
Adilithe III, Sami	87
Silicon 80 Shore A, Trelleborg	80-84

Table 1: The tested materials and their measured hardness [Shore A].

- The two NR materials, provided by Svedala Skega, are EV-vulcanized and carbon-black filled natural rubber. The main difference between the two is much higher modulus of the 80 Shore NR compared to the 60 Shore NR. They both clearly exhibit Mullins effect. The natural rubbers show high amplitude dependence, though some of it is clearly accredited to Mullins effect and not to the Payne effect. If previously conditioned, the amplitude dependence would not be as high. The frequency dependent damping behavior of the NR rubber deviates from all the other materials except the EPDM. For all other materials damping increases with an increase in frequency. Comparing hardness and modulus it is noticed that there is no good correlation between the two as reported by (Lindley 1974) for natural rubbers.
- The ECO material from Ahauser is an epichlorohydrine rubber. The ECO, like the two natural rubbers also show a pronounced amplitude dependence.
- The two HGSD materials from Scapa Rolls are different grades of hypalon rubber, as is the hypalon from Trelleborg. The characteristics of the three hypalons are a low modulus in combination with a large frequency dependence and a very small amplitude dependence.
- HNBR is a hydrogenated acrylonitrile butadiene rubber. HNBR is interesting in the sense that it combines high amplitude dependence with a high frequency dependence.
- The EPDM material from Ahauser is an ethylene propylene diene rubber. The material has a higher modulus than the natural rubbers but otherwise very similar in its behavior.

- The PUR materials from Ahauser as well as the Adilithe material from Sami are four different grades of polyurethanes. The four polyurethanes are highly elastic low-damped materials, with a relatively high modulus.

- Finally the last material is a silicon material from Trelleborg. With a high amplitude dependence and a low frequency dependence.

5 Fit to experimental data

In this section the fit of the material model to experimental data from 13 different rubber materials is described. All the tested rubbers exhibit more or less amplitude and frequency dependent modulus and damping.

Using the previously presented method to fit the material model to experimental data, a set of material parameters was obtained for each material. (See table A1 in the appendix.) Different numbers of elastoplastic and viscoelastic contributions, as well as different choices of weight-factors α according to equation (3) were tried. The aim was to find a good fit to both damping and modulus and at the same time keep the needed number of material parameters to a minimum. The number of material parameters is of course dependent on the sought accuracy of the model as well as the range of frequencies and amplitudes in the experimental data.

Since the elastoplastic models in most finite element codes need a yield stress τ_y instead of a yield strain κ_y, only the yield stress is provided in the tables. The relation between yield stress and yield strain is $\tau_y = G\kappa_y$.

In figure 7 to 19 the obtained material models are compared to experimental data. Presented damping and dynamic shear-modulus are defined according to equation (1). The theoretical values, shown in the graphs, are calculated at the same amplitude and frequency as the measured values. Due to difficulties to obtain a specified strain amplitude during the measurements, the amplitude might fluctuate slightly from the specified strain amplitude. This is seen in the model curve as a deviation from the expected smooth curve.

For both the NR materials, there is a clear conflict between appropriate fit to dynamic modulus and fit to damping. This is due to the fact that all tests were carried out on unconditioned rubber and the fact that the filled NR exhibited a lot of damage effects. This effect is further discussed in the next section.

For many of the materials it can be seen that the assumption of independence between amplitude and frequency behavior is not entirely true. For the dynamic shear modulus this is observed as a change in curvature, with respect to frequency, at different amplitudes. If the assumption was completely true, the frequency response of the dynamic shear modulus would have the same shape for all amplitudes. Thus, it is impossible to get a perfect fit to the dynamic shear modulus with the existing model.

The EPDM material and the two NR materials all behave similar with respect to damping. (See figure 14, 7 and 8.) In contrast to the other materials, damping does not increase monotonically with increasing frequency. The frequency response of the damping seem to be highly dependent on the strain amplitude. As seem in the figures this type of behavior is hard to simulate with the material model at hand. It is however possible to model a roughly correct damping.

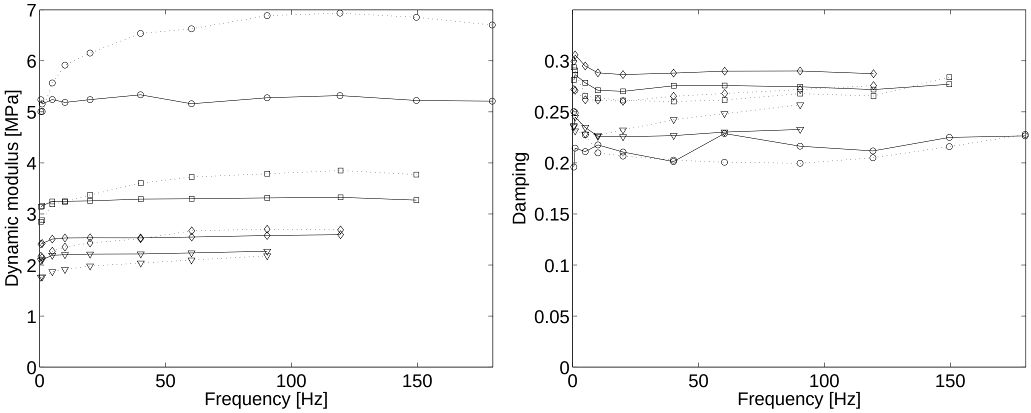

Figure 7: Dynamic shear modulus (left) and damping (right) of NR60. Solid line: material model. Dotted line: experimental data. $\bigcirc$ *:* $\kappa_0 = 1\%$*;* $\bigtriangledown$ *:* $\kappa_0 = 3\%$*;* $\Box$ *:* $\kappa_0 = 7\%$*;* $\bigtriangleup$ *:* $\kappa_0 = 12\%$*.*

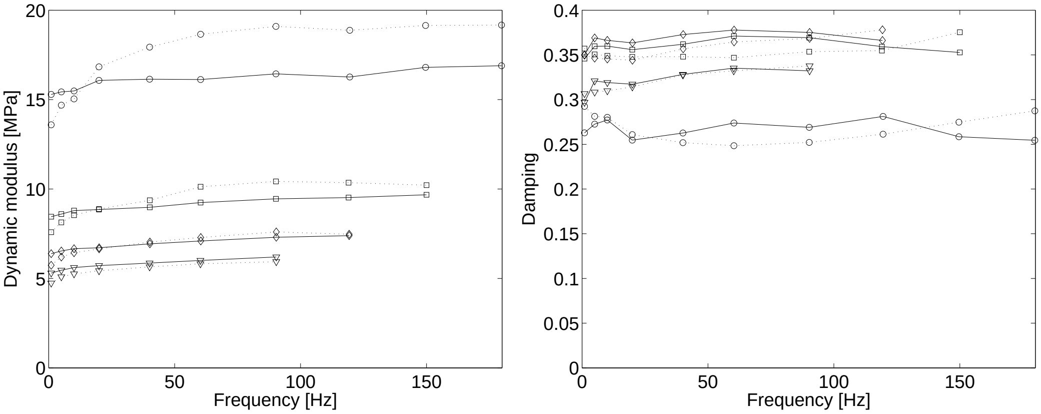

Figure 8: Dynamic shear modulus (left) and damping (right) of NR80. Solid line: material model. Dotted line: experimental data. $\bigcirc$ *:* $\kappa_0 = 1\%$*;* $\bigtriangledown$ *:* $\kappa_0 = 3\%$*;* $\Box$ *:* $\kappa_0 = 7\%$*;* $\bigtriangleup$ *:* $\kappa_0 = 12\%$*.*

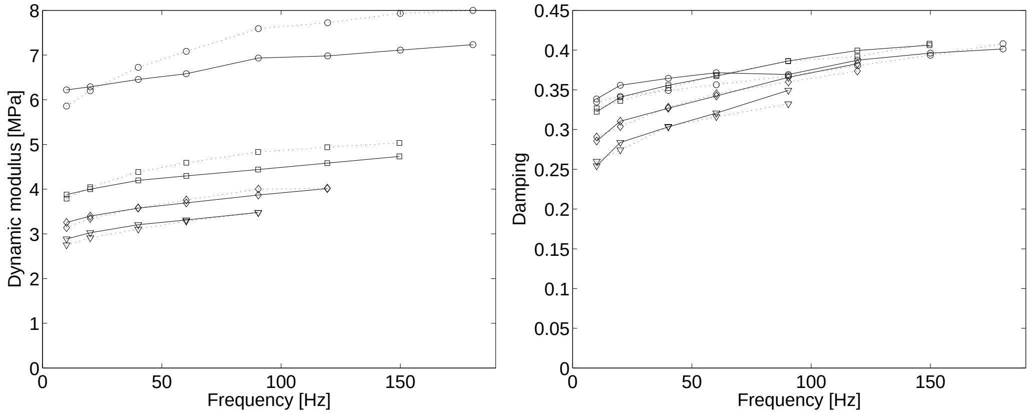

Figure 9: Dynamic shear modulus (left) and damping (right) of Eco3575. Solid line: material model. Dotted line: experimental data. ○ : $\kappa_0 = 1\%$; ▽ : $\kappa_0 = 3\%$; □ : $\kappa_0 = 7\%$; △ : $\kappa_0 = 12\%$.

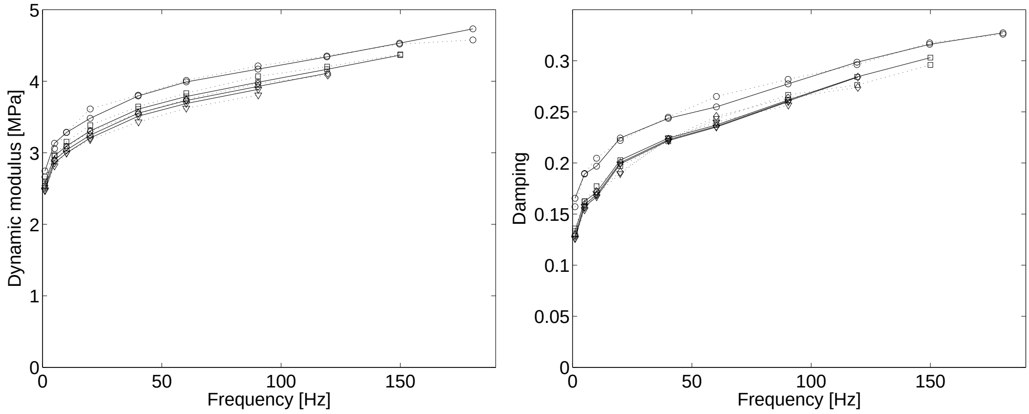

Figure 10: Dynamic shear modulus (left) and damping (right) of HGSD78. Solid line: material model. Dotted line: experimental data. ○ : $\kappa_0 = 1\%$; ▽ : $\kappa_0 = 3\%$; □ : $\kappa_0 = 7\%$; △ : $\kappa_0 = 12\%$.

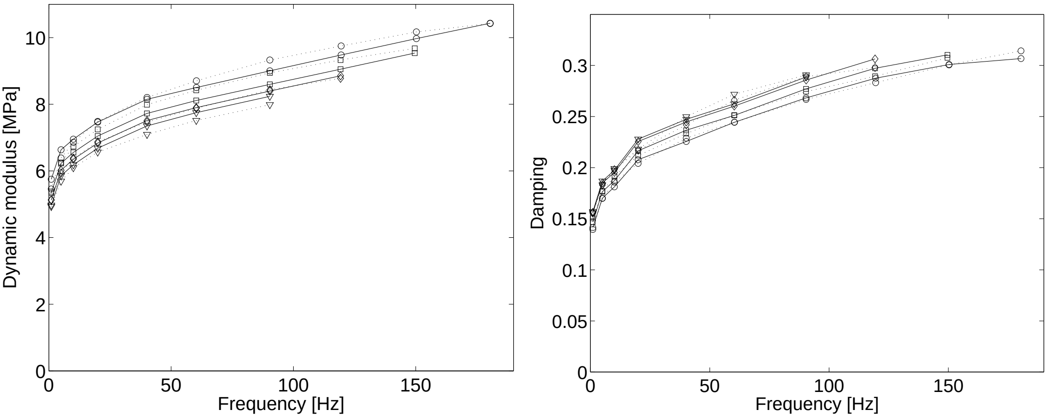

Figure 11: Dynamic shear modulus (left) and damping (right) of HGSD85. Solid line: material model. Dotted line: experimental data. $\bigcirc$ *:* $\kappa_0 = 1\%$*;* $\bigtriangledown$ *:* $\kappa_0 = 3\%$*;* $\square$ *:* $\kappa_0 = 7\%$*;* $\bigtriangleup$ *:* $\kappa_0 = 12\%$*.*

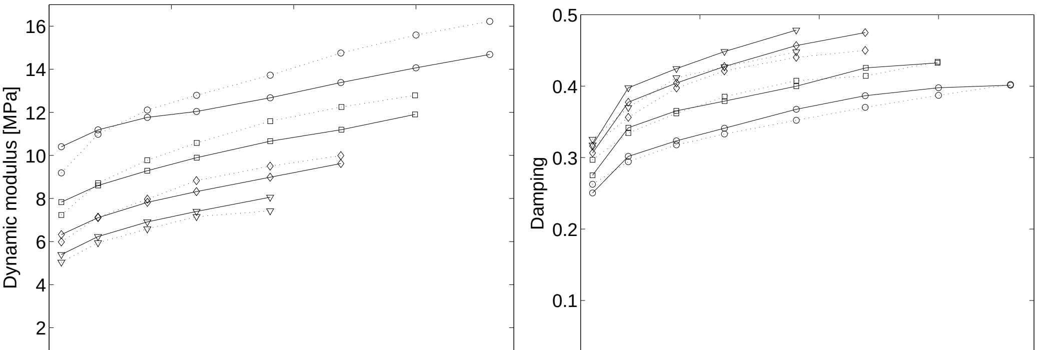

Figure 12: Dynamic shear modulus (left) and damping (right) of HNBR. Solid line: material model. Dotted line: experimental data. $\bigcirc$ *:* $\kappa_0 = 1\%$*;* $\bigtriangledown$ *:* $\kappa_0 = 3\%$*;* $\square$ *:* $\kappa_0 = 7\%$*;* $\bigtriangleup$ *:* $\kappa_0 = 12\%$*.*

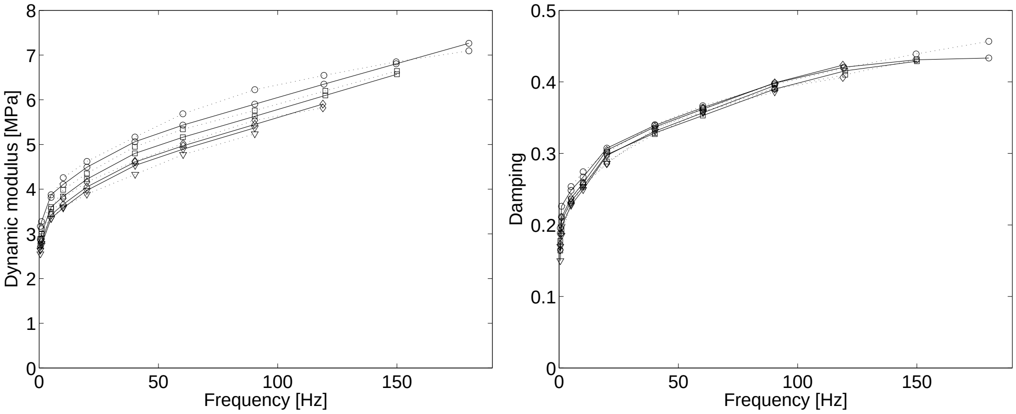

Figure 13: Dynamic shear modulus (left) and damping (right) of Hypalon72. Solid line: material model. Dotted line: experimental data. ◯ : $\kappa_0 = 1\%$; ▽ : $\kappa_0 = 3\%$; □ : $\kappa_0 = 7\%$; △ : $\kappa_0 = 12\%$.

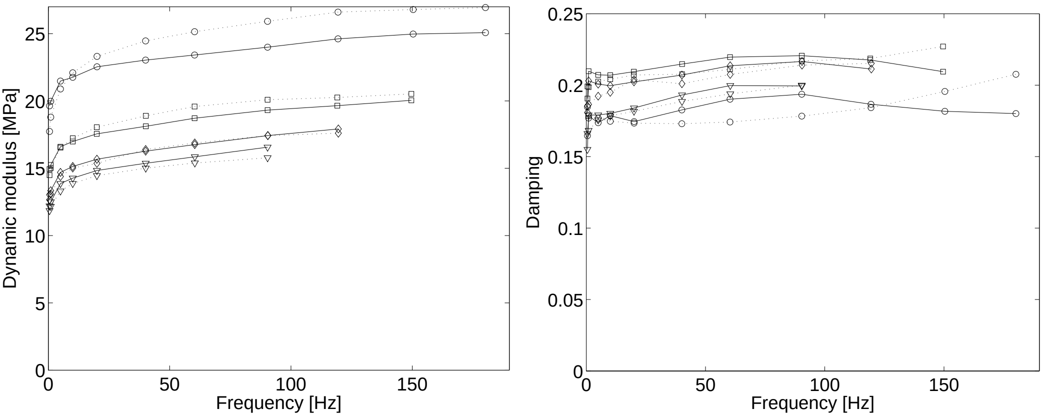

Figure 14: Dynamic shear modulus (left) and damping (right) of EPDM. Solid line: material model. Dotted line: experimental data. ◯ : $\kappa_0 = 0.667\%$; ▽ : $\kappa_0 = 2\%$; □ : $\kappa_0 = 4\%$; △ : $\kappa_0 = 6.7\%$.

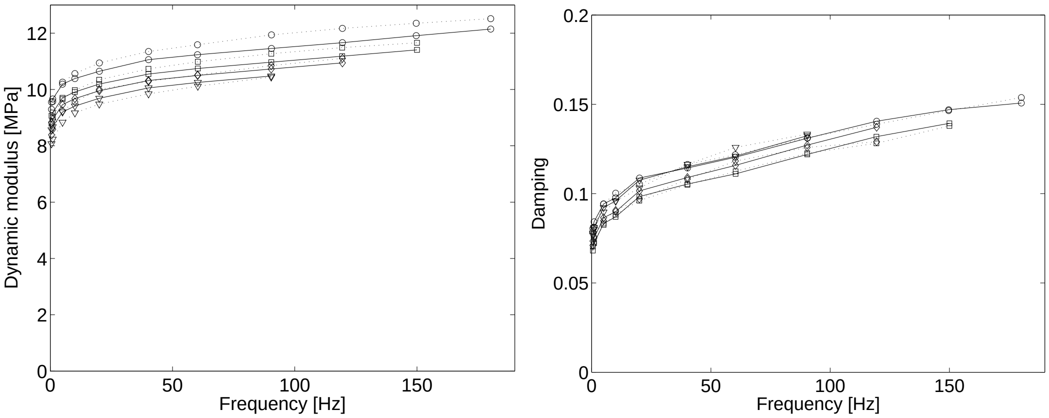

Figure 15: Dynamic shear modulus (left) and damping (right) of Pur9180. Solid line: material model. Dotted line: experimental data. ○ : $\kappa_0 = 0.667\%$; ▽ : $\kappa_0 = 2\%$; □ : $\kappa_0 = 4\%$; △ : $\kappa_0 = 6.7\%$.

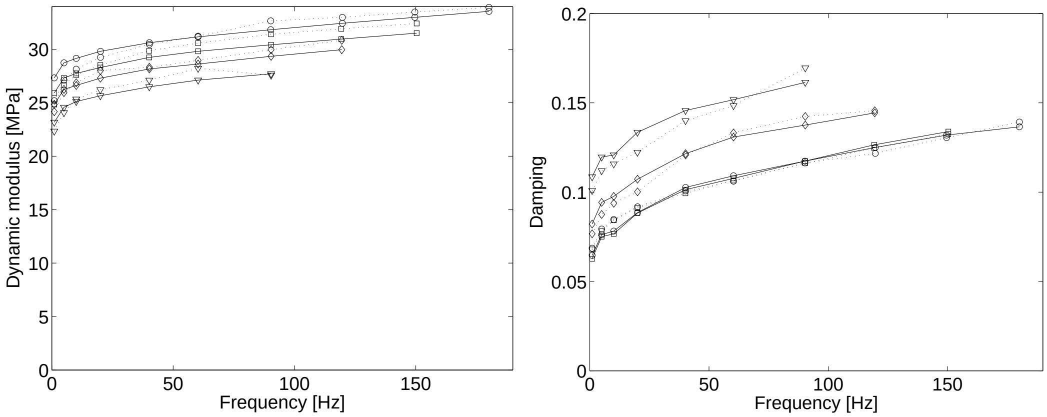

Figure 16: Dynamic shear modulus (left) and damping (right) of Pur9190. Solid line: material model. Dotted line: experimental data. ○ : $\kappa_0 = 0.667\%$; ▽ : $\kappa_0 = 2\%$; □ : $\kappa_0 = 4\%$; △ : $\kappa_0 = 6.7\%$.

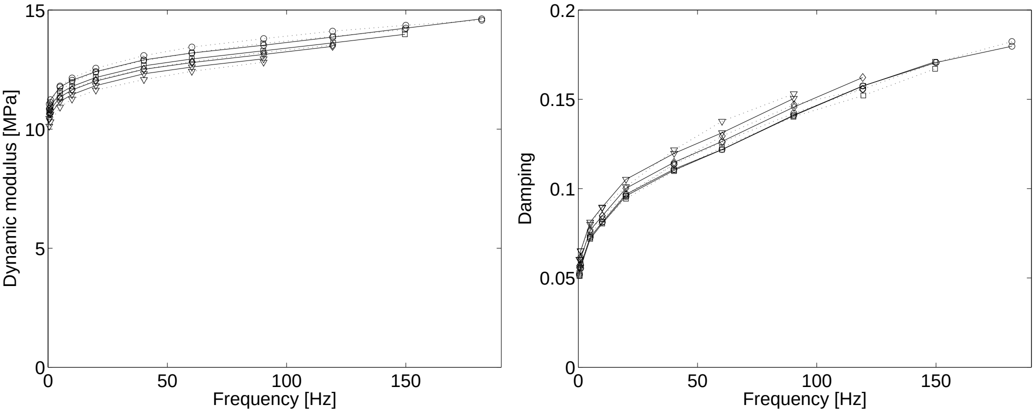

Figure 17: Dynamic shear modulus (left) and damping (right) of Pur9290. Solid line: material model. Dotted line: experimental data. ◯ : $\kappa_0 = 0.667\%$; ▽ : $\kappa_0 = 2\%$; □ : $\kappa_0 = 4\%$; △ : $\kappa_0 = 6.7\%$.

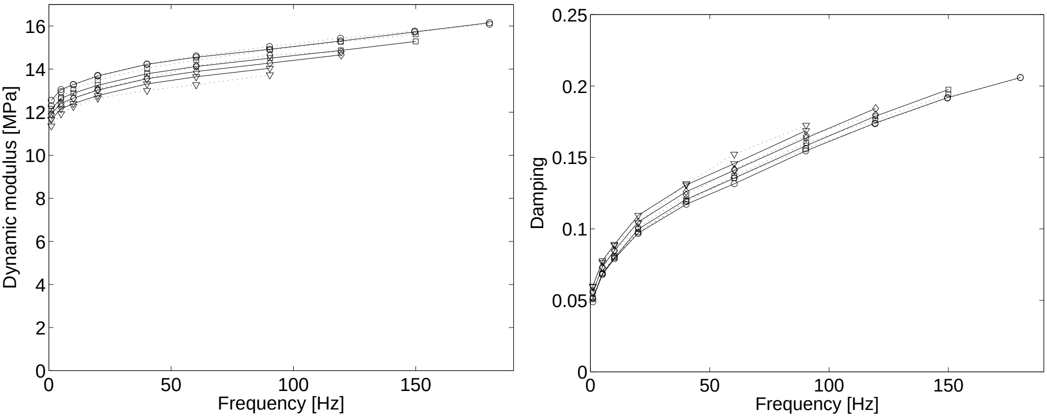

Figure 18: Dynamic shear modulus (left) and damping (right) of SamiIII. Solid line: material model. Dotted line: experimental data. ◯ : $\kappa_0 = 0.667\%$; ▽ : $\kappa_0 = 2\%$; □ : $\kappa_0 = 4\%$; △ : $\kappa_0 = 6.7\%$.

The four tested polyurethanes (figure 15-18) all exhibit a relatively low damping and low amplitude dependence. The lack of amplitude dependence is especially obvious for the dynamic modulus.

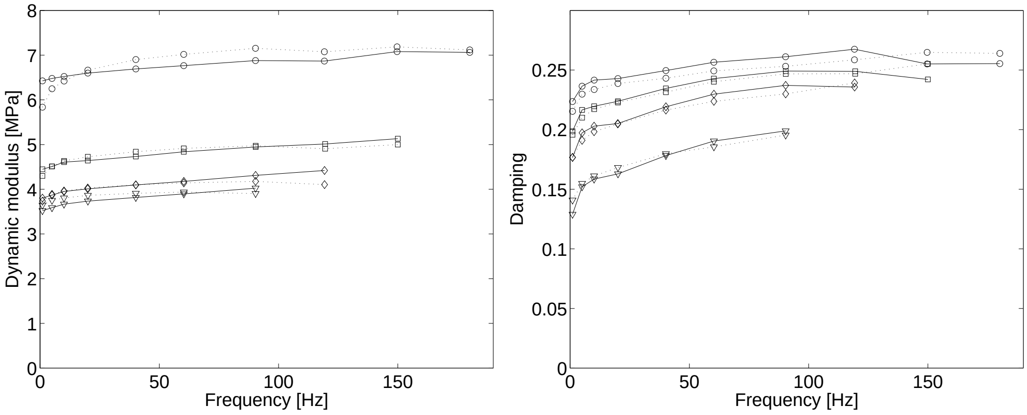

Figure 19: Dynamic shear modulus (left) and damping (right) of Silicon. Solid line: material model. Dotted line: experimental data. ○ *:* $\kappa_0 = 1\%$*;* ▽ *:* $\kappa_0 = 3\%$*;* □ *:* $\kappa_0 = 7\%$*;* △ *:* $\kappa_0 = 12\%$*.*

6 Limitations of the viscoelastic-elastoplastic model

As previously mentioned this material model has two basic limitations. Firstly, it assumes independence between frequency and amplitude. Secondly, it does not include any damage effects.

As seen in section 5, the assumption of independence between rate and amplitude behavior does not hold entirely for all materials. This is most clearly seen in the dynamic shear modulus for the two natural rubbers in figure 7a and 8a. Due to independence between viscoelastic and elastoplastic effects in the model, the modelled frequency dependence will be the same for all amplitudes.

The second limitation means that the model is best suited to model conditioned rubber or rubber with negligible damage properties. For a rubber without damage effects the hysteresis loops at constant frequency should fit inside each other for all amplitudes, as seen for the HNBR rubber. The opposite is seen for the NR60 material in figure 20.

For a material with little or no damage effects, such as the HNBR in figure 21, the viscoelastic-elastoplastic material model provides a good fit to experimental data. Although it is possible to fit the material model to a conditioned rubber with damage effects, it has to be remembered that the obtained material model will then be fitted to a specific level of damage. Thus, if used in a finite element model it will only yield valid results if the entire component has reached the same level of damage as previously obtained in the material tests. For an unconditioned rubber with pronounced damage effects it is not possible to obtain a good fit of the model to both damping and shear modulus, as seen in figure 20. The dashed line indicates a viscoelastic-elastoplastic model able to simulate the dynamic modulus of unconditioned NR. A model fitted like this would

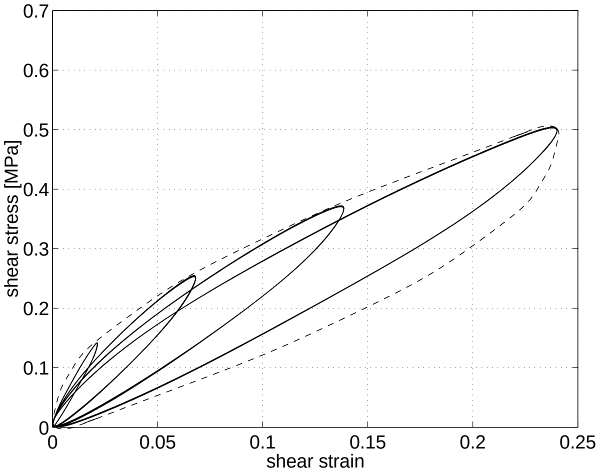

Figure 20: Hysteretic loops for an unconditioned, 60 Shore A filled natural rubber at four different amplitudes (solid line). Possible viscoelastic-elastoplastic model (dashed line).

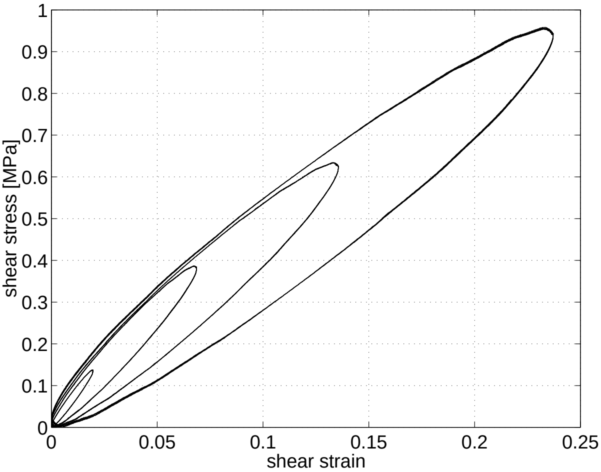

Figure 21: Hysteretic loops for an unconditioned hydrogenated nitrile rubber at four different amplitudes.

overestimate the damping severely. If the model, on the other hand, was to be fitted to obtain a correct damping property, the fit to dynamic modulus would be poor, especially when amplitude dependence is considered.

By inspecting the hysteretic loops at the lowest frequencies, it was concluded that only the two NR materials show significant damage effects.

7 Conclusion

Stationary dynamic shear tests were performed on 13 unconditioned rubbers. The tests were conducted for frequencies up to $180Hz$ and shear strain amplitudes up to 12%. These test data make up a unique material, which could be useful for other researchers.

For rubber exhibiting little or no damage effects, it was shown how the investigated viscoelastic-elastoplastic material model could be fitted to both frequency and amplitude dependence. For rubber with a more pronounced damage behavior it was shown that viscoelastic-elastoplastic material model alone was insufficient to model the dynamic modulus and damping. In order to model these effects, a damage model would have to be included.

It is thus concluded that the viscoelastic-elastoplastic material model is a suitable model for conditioned rubber or rubber with little or no damage effects.

References

Austrell P-E., Olsson A.K. 2001 *A Method to Analyze the Non-Linear Dynamic Behaviour of Carbon-Black-Filled Rubber Components Using Standard FE-codes.* Second European Conference on Constitutive Models for Rubber, Germany

Austrell P-E. 1997 *Modeling of Elasticity and Damping for Filled Elastomers.* Lund University, Division of Structural Mechanics, Report TVSM-1009, Sweden

Enelund M., Mähler L.,Runesson K., Josefsson B.L. 1996 *Unified Formulation and Integration of the Standard Viscoelastic Solid with Integer and Fractional Order Rate Laws.* 19th International Congress of Theoretical and Applied Mechanics (ICTAM), Kyoto, Japan

Harris J., Stevenson A., J.L. 1986 *On the Role of Nonlinearity in the Dynamic Behavior of Rubber Components.* Rubber chemistry and technology, Vol. 59, pp.741-762

Hibbit, Karlsson, Sorensen Inc 2003 *Abaqus 6.3,* Pawtucket, RI

Johnson A.R., Chen T., J.L. 2000 *Modeling Step-Strain Relaxation and Cyclic Deformation of Elastomers.* NASA Langley Research Center Hampton

Kaliske M., Rothert H. 1998 *Constitutive Approach to Rate Independent Properties of Filled Elastomers.* Int. J. Solids Structures Vol. 35, No. 17, pp. 2057-2071

Lindley P.B. 1974 *Engineering Design with Natural Rubber,* MRPRA

Kari L., Lindgren K. 2001 *Personal communications conserning tests* MWL, KTH, Sweden

MATLAB 2003 *"High performance numerical computation and visualization software"* Version 6.5, The Math Works Inc.

Miehe C., Keck J. 2000 *Superimposed finite elastic-viscoelastic-plastoelastic stress response with damage in filed rubbery polymers. Experiments, modelling and algorithmic implementations.* J. Mech. Phys. Solids 48, 323-365

Sjöberg M., Kari L. 2002 *Nonliear behavior of a rubber isolator system using fractional derivatives.* Vehicle System Dynamics 37(3), 217-236

Tervonen M. 1995 *From Measured Complex Modulus to Creep Compliance-Theory and Matlab Implementation.* Matlab Conference, University of Oulu, Finland

Warnaka G.E. 1962 *Effects of Dynamic Strain Amplitude on the Dynamic Mechanical Properties of Polymers.* ASME Rubber and Plastics Div., Paper 62-WA-323, New York

A. Material parameters

	NR60	NR80	Eco3575	HGSD78	HGSD85	HNBR	Hyp72
G_∞	1.65	3.84	2.31	2.32	4.52	3.94	2.48
G_1^{ve}	0.133	0.436	0.424	0.536	1.21	0.991	0.800
G_2^{ve}	0.128	1.15	2.19	0.673	1.38	0.762	1.19
G_3^{ve}	-	-	-	0.0662	0.190	8.31	6.05
G_4^{ve}	-	-	-	3.06	6.08	-	-
t_{r1}	0.0750	0.0244	0.00702	0.0629	0.0648	0.0105	0.0677
t_{r2}	0.00159	0.00148	0.000540	0.00548	0.00622	0.00399	0.00592
t_{r3}	-	-	-	0.00520	0.00496	0.000528	0.000528
t_{r4}	-	-	-	0.000447	0.000551	-	-
G_1^{ep}	4.01	14.2	5.94	0.648	0.875	7.15	4.94
G_2^{ep}	0.641	1.83	0.542	0.0834	0.401	3.21	0.380
G_3^{ep}	-	-	-	-	-	0.701	-
τ_{y1}	0.0287	0.0941	0.0321	0.00251	0.00423	0.0236	0.00254
τ_{y2}	0.0221	0.0763	0.0266	0.00420	0.0119	0.0807	0.00934
τ_{y3}	-	-	-	-	-	0.0493	-

	EPDM	Pur9180	Pur9190	Pur9290	SamiIII	Silicon
G_∞	9.08	7.70	20.6	9.94	11.2	3.14
G_1^{ve}	1.88	0.510	2.02	0.470	0.610	0.212
G_2^{ve}	1.30	0.713	0.109	0.679	0.218	0.0214
G_3^{ve}	3.55	0.904	2.22	1.16	1.25	0.786
G_4^{ve}	-	2.82	7.54	5.31	7.62	-
t_{r1}	0.0816	0.830	0.0637	0.284	0.0715	0.0215
t_{r2}	0.00975	0.0588	0.00742	0.0401	0.0197	0.00725
t_{r3}	0.00130	0.00633	0.00488	0.00601	0.00521	0.00123
t_{r4}	-	0.000583	0.000527	0.000504	0.000408	-
G_1^{ep}	10.1	1.30	3.16	0.560	0.865	4.56
G_2^{ep}	1.49	0.649	4.30	0.494	0.641	0.548
G_3^{ep}	1.89	-	-	-	-	-
τ_{y1}	0.0477	0.00499	0.0147	0.00252	0.00433	0.0266
τ_{y2}	0.0303	0.0216	0.144	0.0163	0.0209	0.0182
τ_{y3}	0.122	-	-	-	-	-

Table A1: Material parameters given in [MPa] except for t_r, given in [s].

Paper III

Finite Element Analysis of a Rubber Bushing Considering Rate and Amplitude Dependent Effects

Presented at ECCMR London 2003

Finite Element Analysis of a Rubber Bushing Considering Rate and Amplitude Dependent Effects

Anders K Olsson, Per-Erik Austrell
Division of Structural Mechanics, Lund University, Sweden

ABSTRACT: A cylindrical bushing subjected to a stationary cyclic load is analysed with emphasis on the amplitude and frequency dependent damping and modulus. The material parameters were determined from a dynamic shear test, in terms of a viscoelastic-elastoplastic model. Using an overlay of finite element meshes, the material model was implemented in a finite element model of the cylindrical bushing and subjected to a radial cyclic load. The calculated damping and stiffness for the bushing were verified with measured data from the actual bushing. Results show that the viscoelastic-elastoplastic model can be made to represent the amplitude and frequency dependence seen in the two natural rubbers investigated in this paper. It is also seen that the model, although fitted to a shear test, performs fairly well for a more general load case as well.

1 Background

The traditional way to develop new rubber components is through manufacturing prototypes, testing, modifying the prototype and more testing. The ability to model the dynamic behaviour of rubber components introduces advantages in terms of less testing and prototyping, resulting in faster development times and reduced costs. The finite element model also provides a tool to analyse local stresses and strains within the component in a more detailed way than can be done in testing. Thus, providing the engineer with useful information of how to optimise the geometry of the component in order to make better use of the rubber material and to increase the expected life-time of the component.

It is a well-known fact that the dynamic properties of rubber are dependent on both amplitude and frequency. An increase in amplitude yields a decrease in modulus. This softening effect is usually referred to as the Payne effect (Payne 1965, Warnaka 1962). The frequency dependence can be observed through an increase in modulus and damping for increasing frequency.

The frequency dependence is usually modelled with a viscoelastic model, whereas the Payne effect can be described with an elastoplastic model. Arguing that there is no connection between the amplitude and rate dependence, authors such as Sjöberg & Kari (2002), Miehe (2000) and Austrell (1997) have coupled the viscoelastic and elastoplastic models in parallel, adding the stress contributions from each branch. This simplified approach has shown good agreement with measurements.

2 Methods

Austrell et al. (2001) presented a simple finite element method, with the capability to model the amplitude and frequency dependent properties of filled rubber. A method to fit this material model to experimental data was suggested by Olsson & Austrell (2001). The purpose of this paper is to evaluate these two methods by investigating the dynamic behaviour of a rubber bushing. Two different grades of NR were investigated. For each of the two materials one double shear test specimen and one cylindrical rubber bushing were manufactured.

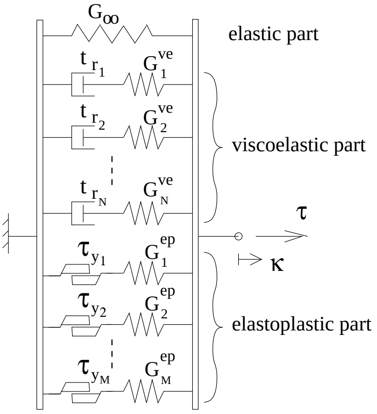

Figure 1: A one dimensional symbolic interpretation of the material model.

For simple shear, the material model can be interpreted as a one-dimensional symbolic model as shown in Figure 1. The fundamental assumption of this model lays in the ability to model the amplitude and frequency dependence as two separate behaviours. Thus, enabling the frequency dependent viscoelastic branch to be coupled in parallel with the amplitude dependent elastoplastic branch. This parallel coupling is also the foundation of the overlay method suggested by Austrell et al. (2001), which was used to create the finite element model presented in this paper.

The dynamic shear test was used to obtain the viscoelastic-elastoplastic material model according to Olsson & Austrell (2001). The non-linear elastic foundation of the model was obtained through an extra quasi-static shear test. The material model was then implemented in a finite element model using an overlay of finite element meshes as discussed by Austrell et al. (2001). Measurements of the real bushing were used in order to verify the finite element model when a harmonic radial load was applied. Hence, the material model is fitted for simple shear, but evaluated for a more general load case.

3 Mechanical testing

The cylindrical bushings and the double shear test specimens were tested in a $Schenk$ tensile machine with a 7kN load cell. Tests were carried out by Lars Janerstål at Volvo Car Corporation.

Since the mechanical properties of rubber are sensitive to temperature changes, it is important that the experiments are carried out at a constant temperature. To avoid heat build-up in the rubber only a few cycles were performed at each frequency and amplitude.

During the first load cycles most NR show a significant softening effect, the so called Mullins effect (Mullins 1969). To remove this softening effect from the measurements, the rubber components were conditioned at an amplitude 10% higher than the highest measured amplitude. Furthermore, the tests were conducted starting with the highest amplitudes and finishing with the lowest.

3.1 Materials

Two different carbon-black-filled natural rubbers were examined. Both grades had a hardness of 50 IRHD, which according to Lindley (1974) means they should have roughly the same shear modulus. One grade is a low filled rubber commonly found in automotive applications, referred to as material A in this paper. The other grade with slightly more filler and higher damping is referred to as material B in this paper. To achieve the same hardness for both materials softener was added to material B.

4 Shear test

For simple shear, the elastic part of the rubber behaviour is almost linear at moderate strains. This property is advantageous when characterizing the material, since it makes it easier to isolate the non-linear dynamic properties. For this reason the material parameters were obtained solely from the double shear test. The utilized, double shear test specimens consist of three steel cylinders connected with two circular rubber plates, as shown in Figure 1.

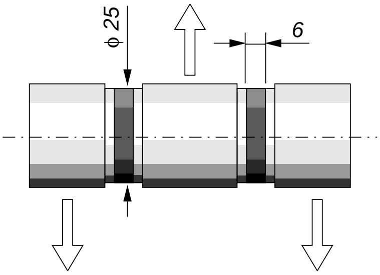

Figure 2: The double shear test specimen used in the evaluation of the material parameters.

The dynamic shear tests were performed as described in Section 3. Dynamic shear modulus G_{dyn} and damping d were measured at frequencies ranging from 0.1-50Hz and shear strain amplitudes ranging from 1-50%. The dynamic shear modulus and damping were defined according to

$$G_{dyn} = \frac{\tau_0}{\kappa_0}, \quad d = \frac{U_c}{\pi \kappa_0 \tau_0} \tag{1}$$

where τ_0 represents the stress amplitude, κ_0 the strain amplitude and U_c the hysteretic work per unit volume and load cycle.

As suggested by Olsson & Austrell (2001) a good fit to damping and dynamic shear modulus was sought through a minimization of the error function ψ given as

$$\psi = \alpha \sum_{i=1}^{m} \left(\frac{d_i - d_{exp,\,i}}{d_{exp,\,i}} \right)^2 + (1-\alpha) \sum_{i=1}^{m} \left(\frac{G_i - G_{exp,\,i}}{G_{exp,\,i}} \right)^2 \tag{2}$$

where m is the number of measurements. The error function is solely dependent on the material parameters. Hence, minimizing this function yields the sought material parameters. By choosing the weight factor α it is possible to decide whether to focus on a good fit of the dynamic modulus or damping. This is further discussed by Olsson & Austrell (2001).

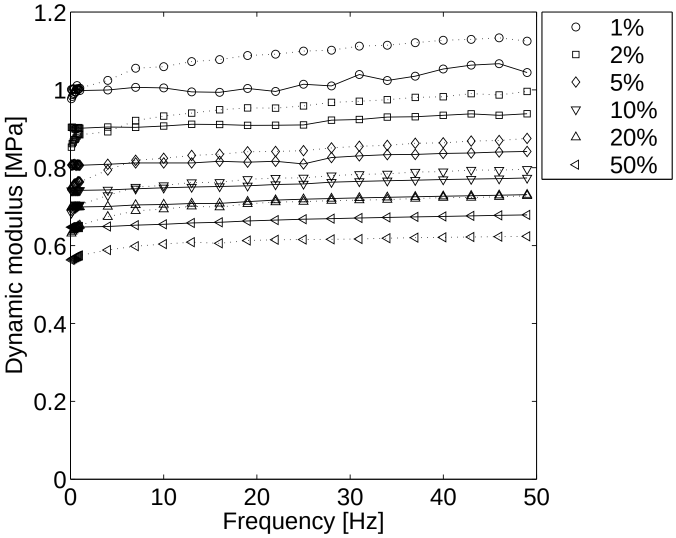

Figure 3: Dynamic shear modulus of material A at different strain amplitudes. Dashed line: Measured data. Solid line: Model.

The models slight deviation from the expected smooth curve (see Figure 3-6) is due to problems to keep a constant amplitude during the tests. Since the model is evaluated at the exact amplitudes and frequencies as recorded in the test, the lack in accuracy of the amplitude will also be reflected in the model curve. It should be noted that the test equipment experienced difficulties at the lowest amplitudes due to the very small displacements and forces. Hence, the result for the lowest amplitudes might be somewhat unreliable.

The obtained material parameters are presented in Table 1. Further increasing the number of viscoelastic and elastoplastic contributions will give a slight improvement of the model, best seen in an improved fit of the dynamic shear modulus for low frequencies. It was however decided that this slight improvement was not worth the extra computational costs involved when implemented in the finite element model.

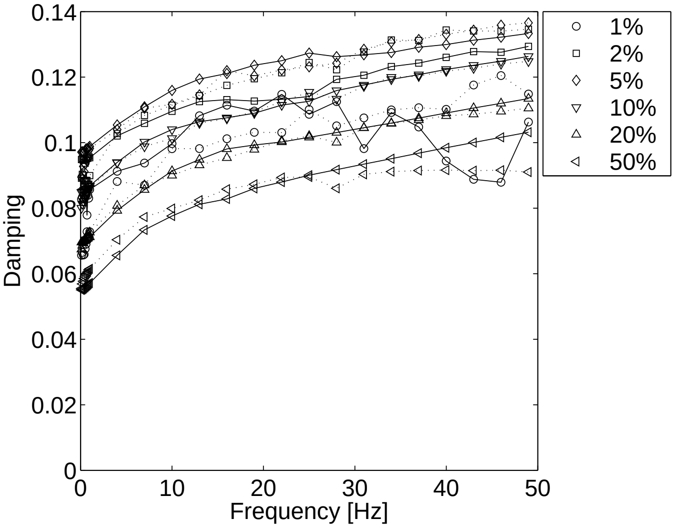

Figure 4: Damping of material A at different strain amplitudes. Dashed line: Measured data. Solid line: Model.

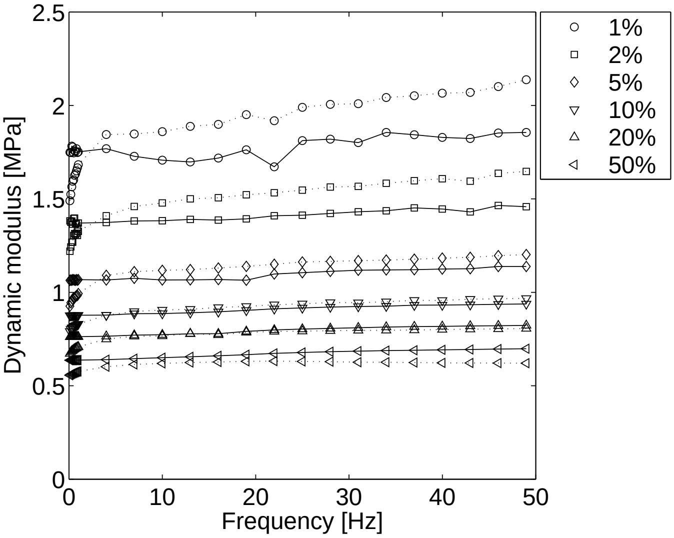

Figure 5: Dynamic shear modulus of material B at different strain amplitudes. Dashed line: Measured data. Solid line: Model.

4.1 Fit of non-linear elasticity

In order to capture the non-linear elastic characteristics with the Yeoh-model (Yeoh 1990) a quasi static shear test according to Figure 7 was performed. The three parameters were then fitted with a standard least square method (Austrell 1997).

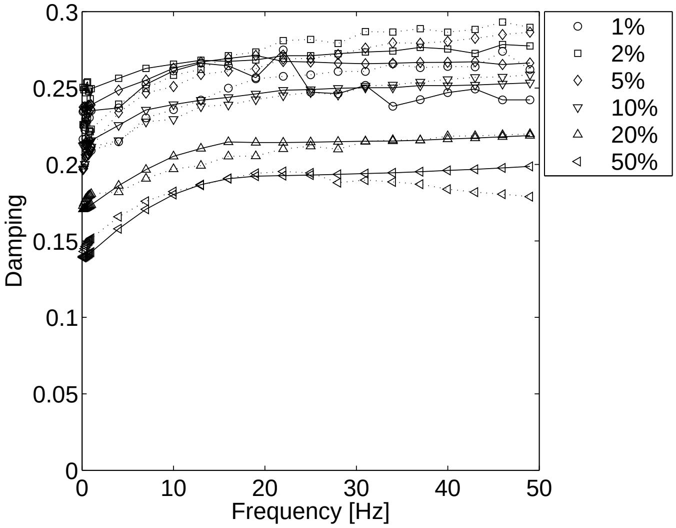

Figure 6: Damping of material B at different strain amplitudes. Dashed line: Measured data. Solid line: Model.

Table 1: Material parameters

Material	A	B
G_∞ $[MPa]$	0.613	0.495
G_1^{ve} $[MPa]$	0.0227	0.0108
G_2^{ve} $[MPa]$	0.103	0.0457
G_3^{ve} $[MPa]$	-	0.152
t_{r1} $[s]$	0.0110	0.00921
t_{r2} $[s]$	0.00105	0.00874
t_{r3} $[s]$	-	0.000798
G_1^{ep} $[MPa]$	0.291	1.31
G_2^{ep} $[MPa]$	0.128	0.316
G_3^{ep} $[MPa]$	0.0626	0.130
G_4^{ep} $[MPa]$	-	0.0620
τ_{y1} $[MPa]$	0.00247	0.00793
τ_{y2} $[MPa]$	0.00573	0.0121
τ_{y3} $[MPa]$	0.0132	0.0234
τ_{y4} $[MPa]$	-	0.0318
C_{20}/C_{10}	-0.0725	-0.124
C_{30}/C_{10}	0.0153	0.0397

For simple shear the shear stress of the Yeoh-model is given as a function of the shear strain κ according to

$$\tau = 2C_{10}\kappa + 4C_{20}\kappa^3 + 6C_{30}\kappa^5 \tag{3}$$

The C_{10} parameter governs the initial shear modulus ($C_{10} = G/2$), whereas the C_{20} and C_{30}

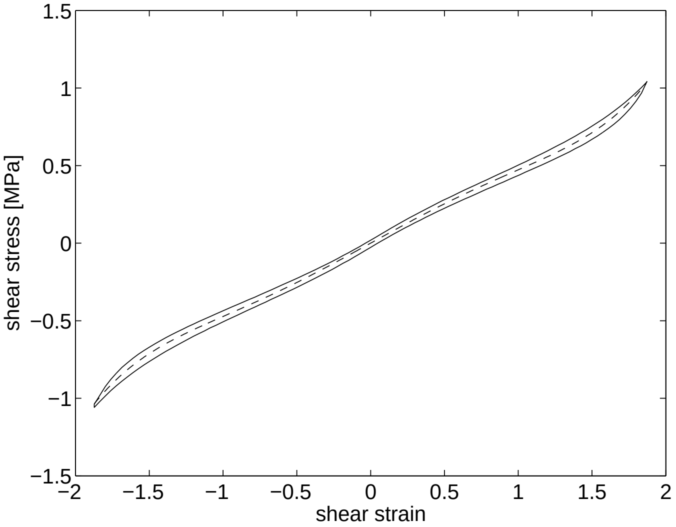

Figure 7: Quasi-static shear test of material A. Dashed line: Hyperelastic Yeoh-model. Solid line: Measured data (strain rate: 0.9%/s).

parameters govern the non-linear elastic response. Hence, the characteristic non-linear shape is determined by the ratios C_{20}/C_{10} and C_{30}/C_{10} and the overall modulus is set by the C_{10} parameter. Since the principle non-linear elastic response is thought to be independent of dynamic properties, the two ratios are kept unchanged and the C_{10} parameter is fitted to the dynamic shear test along with the amplitude and rate dependent parameters, as discussed in the next section.

5 Rubber bushing

Two bushings were examined, one of material A and one of material B. The rubber bushing consists of one outer and one inner steel tube connected with rubber. Similar bushings are found in modern automotive suspensions.

Dynamic stiffness K_{dyn} and damping d_{bush} for the rubber bushing are defined in a similar manner as for the shear test

$$K_{dyn} = \frac{F_0}{u_0}, \quad d_{bush} = \frac{W_{hyst}}{\pi F_0 u_0} \tag{4}$$

where F_0 is the amplitude of the force, u_0 the displacement amplitude and W_{hyst} the hysteretic work per load cycle.

5.1 FE-model

The FE-model was created in $Abaqus$ with 8-node hybrid elements. Due to symmetry only one fourth of the bushing had to be modelled, as seen in Figure 4. Since $Abaqus$ does not provide a viscoelastic-elastoplastic model, the FE-model was created using the overlay method. In this case

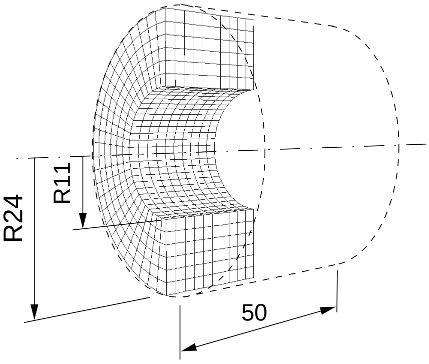

Figure 8: The cylindric bushing and FE-model.

a viscoelastic finite element model was merged with three respectively four elastoplastic finite element models, for material A and B.

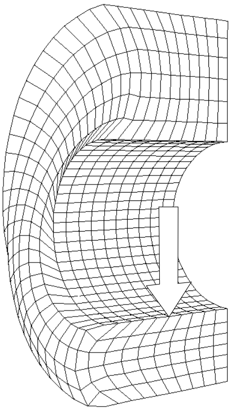

Figure 9: The FE-model subjected to a 3mm radial displacement.

The viscoelastic branch was modelled with Prony-series based on a hyperelastic Yeoh-model. It would be desirable to use the same hyperelastic Yeoh-model as a base for the elastoplastic branch. But, this type of elastoplasticity is currently unavailable in $Abaqus$. Hence, the elastoplasticity has been modelled with several ideally elastoplastic hypoelastic models coupled in parallel in accordance with the overlay method. In $Abaqus/Standard$ this elastoplastic model could also be achieved by a single model with piecewise kinematic hardening.

A radial sinusoidal displacement was analyzed for different frequencies and amplitudes. The deformed finite element model is shown in Figure 9. As can be seen in the Figure, the radial load case introduces both tension and compression, as well as shear. The calculated damping and stiffness are presented to the left in Figure 10-13.

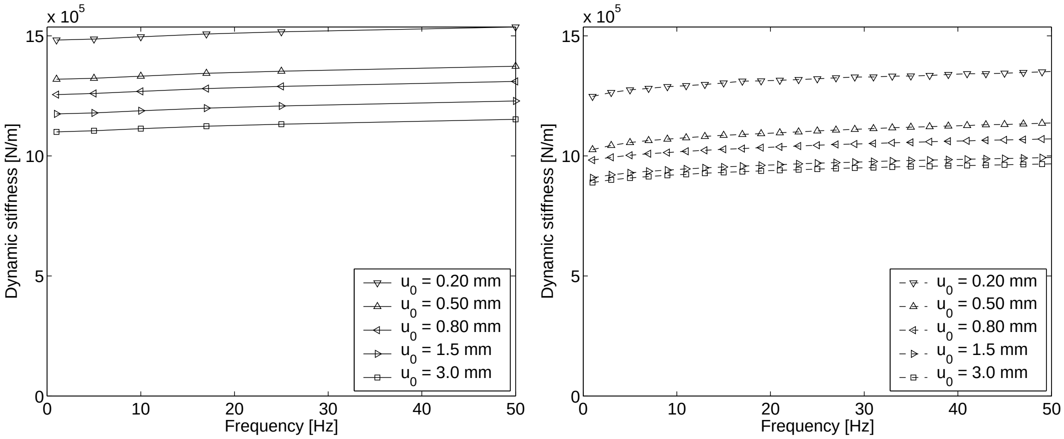

Figure 10: Dynamic stiffness for the cylindrical bushing with material A. (Left: FE-model, Right: Measurement

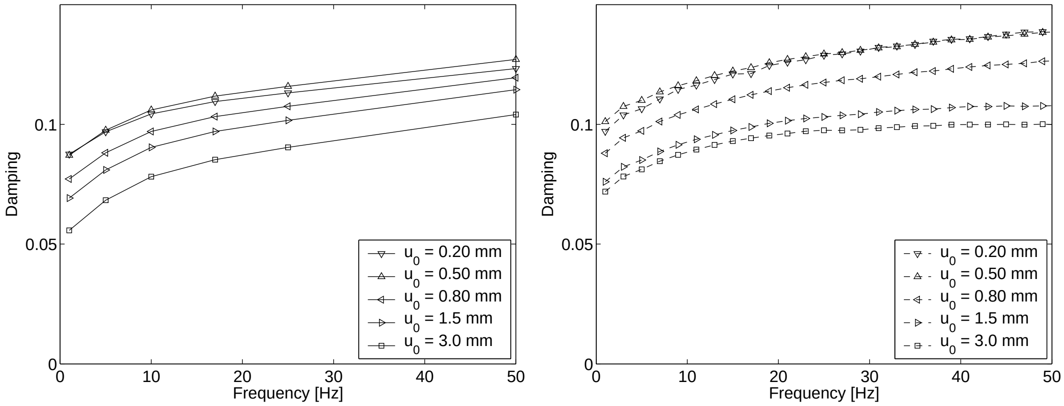

Figure 11: Damping for the cylindrical bushing with material A. (Left: FE-model, Right: Measurement

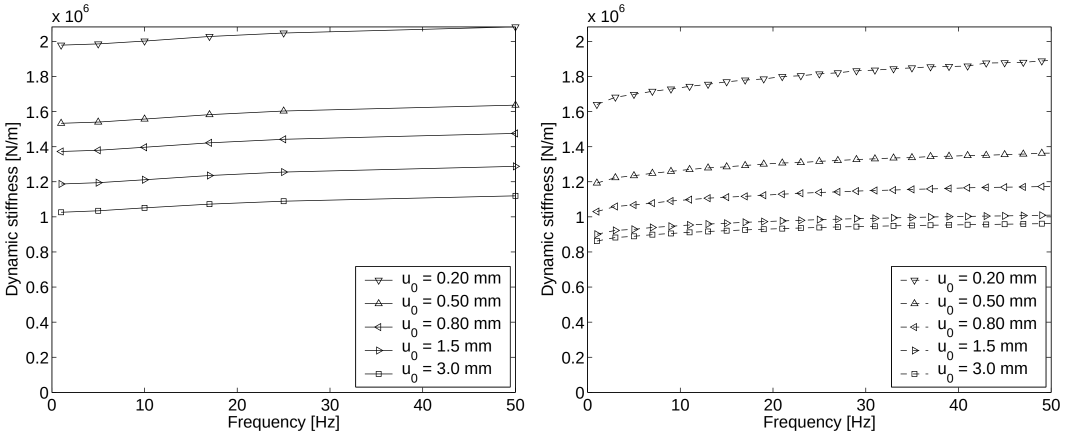

Figure 12: Dynamic stiffness for the cylindrical bushing with material B. (Left: FE-model, Right: Measurement

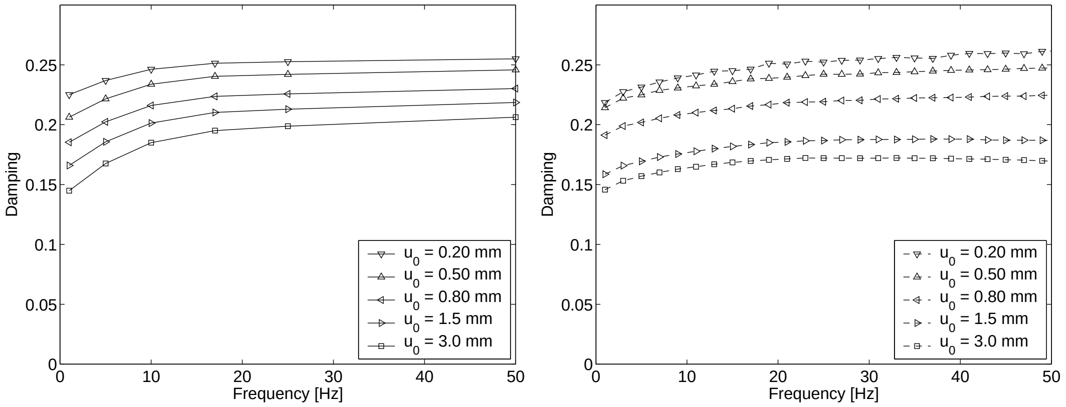

Figure 13: Damping for the cylindrical bushing with material B. (Left: FE-model, Right: Measurement)

5.2 Verification

The bushings were loaded in the radial direction as described in Section 3. Measured dynamic stiffness and damping for the rubber bushing are shown to the right in Figure 10-13. These results should be compared to the predicted results, shown to the left in Figure 10-13, obtained from the finite element model.

When the FE-model is compared to the measurements it can be seen that the dynamic stiffness of the bushing is overestimated for both materials. Damping on the other hand seems to be well predicted for material B, but underestimated for material A.

In an effort to keep the computational costs to a minimum a rather coarse finite element mesh was used for the analysis. Tests with finer meshes show that the predicted stiffness will drop approximately 3% for a fine mesh, which partly explains the deviation between measured and calculated stiffness. On the other hand, a finer mesh did not affect the predicted damping.

The slight error in the finite element model might to some extent also be explained by differences in material properties of the double shear specimen and the rubber bushing. Although the components were manufactured from the same batch, slight deviations in the manufacturing process due to different geometries, might result in different degrees of cross-linking during vulcanization.

Given the above uncertainties, and also the fact that the material model did not fit the shear test perfectly, the results are as good as could be expected.

5.3 Shape of hysteretic response

Although emphasis for the fitting procedure was on dynamic modulus and stiffness, it is also important to obtain a correct shape for the hysteresis loop during a load cycle. For a purely viscoelastic material the hysteretic response will have an elliptic shape. Whereas a purely elastoplastic model will have a more parallelogram shaped response with sharp corners.

The hysteretic response for the rubber bushing of material B is shown in Figure 14. Showing both elastoplastic and viscoelastic effects, the obtained loop is a mixture of a parallelogram and an ellipse. As expected from the dynamic stiffness presented in Figure 12, the hysteretic response of the finite element model is slightly too stiff. Apart from the deviation in stiffness, the shape of the hysteresis loop from the model seems to be in good agreement with the measured response.

5.4 Mullins effect

During the tests it was observed that Mullins effect seemed to recover faster than anticipated. However, no further measurements to verify this observation were made. Since the mechanical conditioning of the specimens were done only once, it is likely that the measurements to some extent were influenced by Mullins effect. To investigate this observation, a discontinuous damage model (Miehe 1995) given by

$$\tau = \tau(1 - d_{\infty}(1 - e^{\frac{-a_{max}}{\eta}})) \tag{5}$$

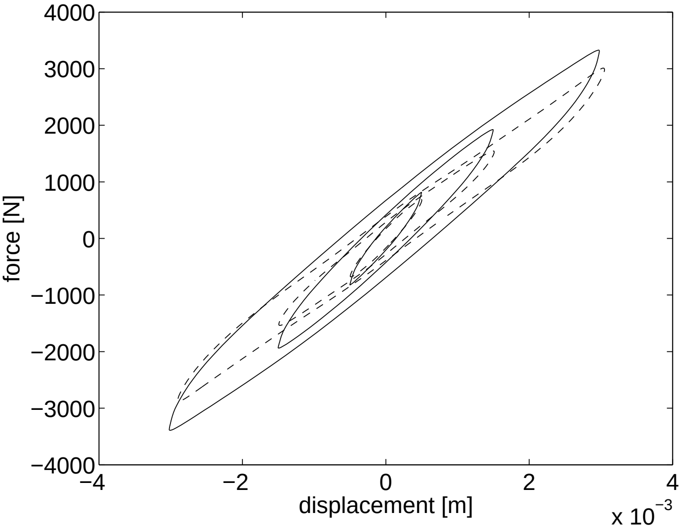

Figure 14: Hysteretic response for the rubber bushing of material B at $f = 50Hz$. Solid line: FE-model, Dashed line: Measurements

was added to the viscoelastic-elastoplastic model. The viscoelastic-elastoplastic stress is referred to as τ and η and d_∞ are material parameters. This damage model is solely dependent on the highest strain energy a_{max}, given by the hyperelastic Yeoh-model.

When fitted to the dynamic simple shear tests no significant improvements were seen. The most noticeable change was a slightly improved modelling of the amplitude dependent dynamic shear modulus. As already mentioned, similar improvements could be obtained through the addition of more viscoelastic and elastoplastic contributions. It was decided that the small improvements were not worth the added complexity introduced by the damage model. Hence no further damage modelling were performed.

6 Summary and conclusions

The non-linear dynamic properties of two grades of low-filled natural rubber were examined. Measurements show that the dynamic shear modulus vary with over 100% (see Figure 5), in this case mainly due to the amplitude dependence but frequency also plays a important role.

A viscoelastic-elastoplastic material model was fitted to a simple shear test and implemented in a finite element model. It was shown that the obtained finite element model could be used to predict the dynamic properties of a cylindrical rubber bushing subjected to a dynamic radial load. When compared to measurements of the same bushing, it was concluded that the finite element model showed a principally correct rate and amplitude dependence. Although not in absolute agreement with experimental data, the result is a great improvement if compared to results obtained with purely hyperelastic or viscoelastic models.

7 Acknowledgement

All tests presented in this paper were performed at Volvo Car Corporation. The authors would like to thank Anders Wirje and Lars Jarnerstål at Volvo Car Corporation for their work and support of the project.

References

Austrell P-E., Olsson A.K. 2001, A Method to Analyze the Non-Linear Dynamic Behaviour of Carbon-Black-Filled Rubber Components Using Standard FE-codes. *Second European Conference on Constitutive Models for Rubber*, Germany

Austrell P-E. 1997, *Modeling of Elasticity and Damping for Filled Elastomers*. Lund University, Division of Structural Mechanics, Report TVSM-1009, Sweden

Kaliske M., Rothert H. 1998, Constitutive Approach to Rate Independent Properties of Filled Elastomers. *Int. J. Solids Structures*, Vol. 35, No. 17, pp. 2057-2071

Lindley P.B. 1974, *Engineering design with natural rubber* MRPRA

Miehe C. 1995, Discontinuous and continuous damage evolution in Ogden-type large-strain elastic materials *Eur. J. Mech., A/Solids*, Vol. 14, pp. 697-720

Miehe C., Keck J. 2000, Superimposed finite elastic-viscoelastic-plastoelastic stress response with damage in filed rubbery polymers. Experiments, modelling and algorithmic implementations *J. Mech. Phys. Solids*, 48, 323-365

Mullins L. 1969, Softening of Rubber by Deformation *Rubber Chemistry and Technology*, Vol. 42, pp. 339-362

Olsson A.K., Austrell P-E. 2001, A fitting procedure for a viscoelastic-elastoplastic material model. *Second European Conference on Constitutive Models for Rubber*, Germany

Payne A.R. 1965, *Reinforcement of elastomers* G. Kraus, Ed., Interscience, Chap. 3, New York

Sjöberg M., Kari L. 2002, Non-Linear Behavior of a Rubber Isolator System Using Fractional Derivatives *Vehicle System Dynamics*, Vol. 37, No. 3, pp. 217-236

Warnaka G.E. 1962, *Effects of Dynamic Strain Amplitude on the Dynamic Mechanical Properties of Polymers*. ASME Rubber and Plastics Div., Paper 62-WA-323, New York

Yeoh O.H. 1990, Characterization of Elastic Properties of Carbon-black-filled Rubber Vulcanizates. *Rubber Chemistry and Technology*, Vol. 63,pp. 792-805

Paper IV

Considering Amplitude Dependent Effects During Cyclic Loads by an Equivalent Viscoelastic Model

Yet to be submitted

Considering Amplitude Dependent Effects During Cyclic Loads by an Equivalent Viscoelastic Model

Anders K Olsson, Per-Erik Austrell, Göran Sandberg
Division of Structural Mechanics, Lund University, Sweden

ABSTRACT: Although it is well known that the dynamic properties of rubber depend on both frequency and amplitude, there are no commercially available finite element codes that take account of these effects. This paper outlines a simplified procedure to extend the usability of the commercially available frequency dependent viscoelastic finite element models, to also take account of the amplitude dependence. By first calculating the load level at each element it is possible to obtain an equivalent viscoelastic model for a cyclic load. Using this approach two different frequency dependent models are treated; one frequency and one time domain viscoelastic model. Both models are verified against experimental data with good results.

1 Background and introduction

It has long been customary to model rubber with either hyperelastic or viscoelastic material models. However, it is well known that the dynamic properties of rubber are dependent of both amplitude and frequency. Considering a harmonic load, the dynamic modulus of the rubber material will increase if the frequency increase. Likewise, an increasing amplitude will results in a decreasing dynamic modulus. The importance and influence of these two behaviours will depend on the rubber material as well as the load ranges of the particular application.

Amplitude dependence is attributed to two different phenomena, the so called Mullins (Mullins 1969) effect and the Payne (Payne 1965) or Fletcher-Gent effect. The Mullins effect is seen as a softening effect during the first load cycles. This softening effects is believed to be caused by the breakdown of the filler structure and is usually thought of as an irreversible phenomena. However when left unloaded for a couple of hours the material in this paper was observed to regain much of its virgin properties. The Payne effect on the other hand is not dependent on the number of load cycles or previous loads and is completely reversible.

The Mullins effect will temporarily disappear if the material is initially loaded at a higher amplitude. The Payne effect on the other hand is not dependent on previous load cycles.

The aim of the suggested equivalent viscoelastic approach is to model both frequency and amplitude dependent effects. The basic idea is that, even though the rubber material is not purely viscoelastic, it is possible to create a suitable equivalent frequency dependent viscoelastic model for any given amplitude. Hence the choice of material parameters for this equivalent viscoelastic model is governed by the strain amplitude. Using this approach, the model is restricted to modelling stationary dynamic loads, for which an amplitude can be determined. By a simplified engineering approach this method works well in conjunction with commercial finite element codes, using the already available material models.

The combined frequency and amplitude dependent properties of rubber material have previously been modelled by coupling a viscoelastic material model in parallel to an elastoplastic (Miehe 2000) (Austrell & Olsson 2001) forming a viscoelastoplastic model. By coupling the two constitutive branches in parallel the frequency and amplitude dependence are assumed to be independent of each other. No such assumption is needed for the studied equivalent viscoelastic model. Unlike the viscoelastoplastic model the suggested equivalent viscoelastic model can capture a coupled dependence between amplitude and frequency. Another interesting feature of the equivalent viscoelastic model is that it makes no distinction between the Mullins or Payne effect as they are both only treated as amplitude dependence. I.e. if the material tests of which the model is based on contain Mullins effect, so will the model.

2 Measurements

Two different rubber components were used for this study: one double shear test specimen and one cylindrical rubber bushing. Both components were manufactured using the same carbon black filled natural rubber and subjected to sinusoidal loads using a hydraulic test rig. Fitting the model only to the shear test and comparing the resulting finite element model to the real bushing provides a good verification of the model. The same two components were previously used to verify the viscoelastic-elastoplastic model described in (Olsson & Austrell 2003) using an overlay method (Austrell & Olsson 2001).

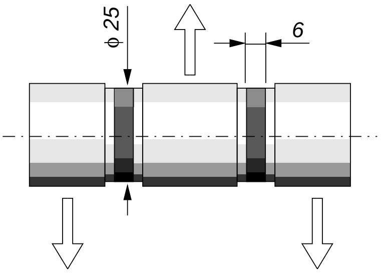

Figure 1: The double shear test specimen used in the evaluation of the material parameters.

To remove the influence of the Mullins effect in the measurements, both components were conditioned at a 10% higher displacement than the highest recorded amplitude. The tests were then conducted starting at the highest amplitude and finishing at the lowest. Both material and component tests were carried out by Lars Janerstål at Volvo Car Corporation in Gothenburg, Sweden.

2.1 Material test

The double shear test specimen as shown in figure 1, consists of three steel cylinders connected together with two thin rubber pieces. The purpose of the double shear test is to obtain a true simple shear deformation. However finite element calculations of the test specimen show that a shear modulus obtained from this test has to be increased by 6 percent to yield the same values as the ideal simple shear test, indicating that a perfect simple shear load case is not obtained. This deviation was accounted for when fitting the material models used in the finite element model.

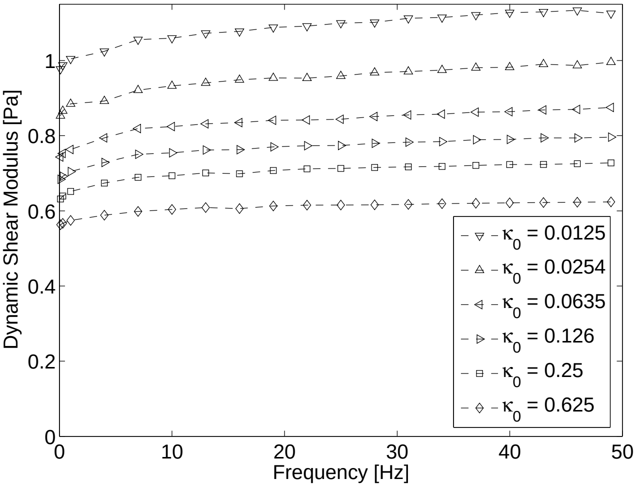

Figure 2: Measured dynamic stiffness of the rubber material.

Using a hydraulic test rig, the dynamic shear modulus G_{dyn} and damping d were measured at frequencies ranging from 0.1-50Hz and shear strain amplitudes ranging from 1-50%. The dynamic shear modulus and damping as seen in figure 2 and 3 were defined according to

$$G_{dyn} = \frac{\tau_0}{\kappa_0}, \quad d = sin(\delta) = \frac{U_c}{\pi \kappa_0 \tau_0} \tag{1}$$

where τ_0 represents the stress amplitude, κ_0 the strain amplitude, δ the phase angle and U_c the hysteretic work per unit volume and load cycle.

Both material models presented in this paper were based on the dynamic shear data presented in figure 2 and 3.

2.2 Radially loaded bushing

A cylindrical rubber bushing as seen in figure 4 was subjected to a sinusoidal load in the radial direction. The rubber bushing consists of one outer and one inner steel tube connected with rubber. Similar bushings are found in the flexible joints of most modern car suspensions.

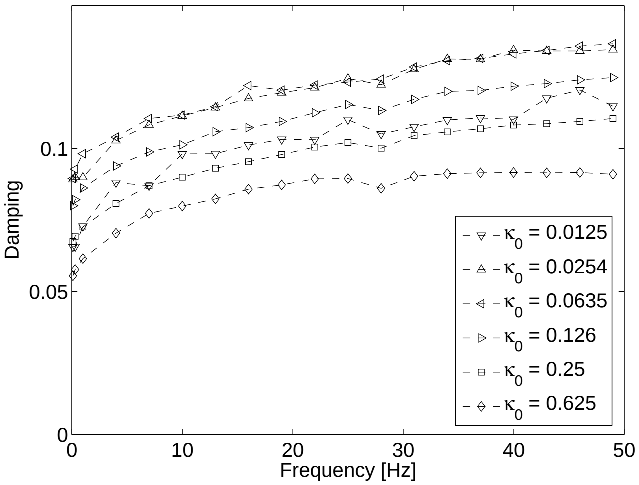

Figure 3: Measured damping of the rubber material.

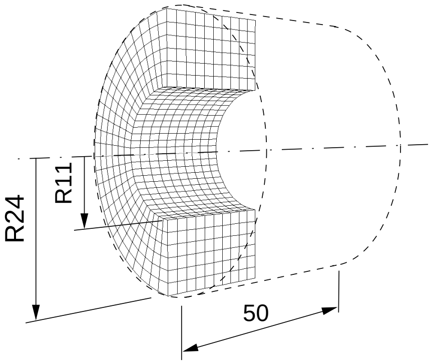

Figure 4: The cylindric bushing and FE-model. Dimensions are given in mm.

Dynamic stiffness K_{dyn} and damping d_{bush} for the rubber bushing are defined in a similar manner as for the shear test

$$K_{dyn} = \frac{F_0}{u_0}, \quad d_{bush} = \frac{W_{hyst}}{\pi F_0 u_0} \tag{2}$$

where F_0 is the amplitude of the force, u_0 the displacement amplitude and W_{hyst} the hysteretic work per load cycle. The dynamic stiffness and damping were measured at frequencies ranging from 1-50Hz and amplitudes ranging from 0.20-3.0mm. Experimental data from the bushing are presented in figure 5 and 6. This data was only used for the purpose of verifying the finite element models.

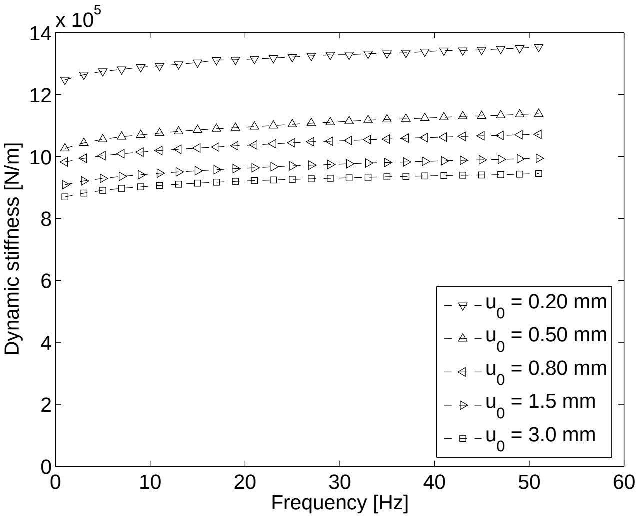

Figure 5: Measured dynamic stiffness of the rubber bushing.

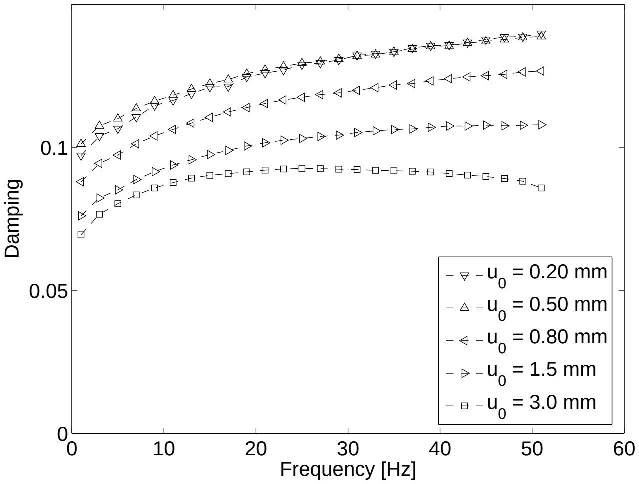

Figure 6: Measured damping of the rubber bushing.

3 Equivalent viscoelasticity

Two different equivalent viscoelastic models are presented in this paper. The first model is based on time domain viscoelasticity and the second on frequency domain viscoelasticity. The basic idea of both models is that the material can be modelled as purely viscoelastic for a given amplitude. I.e. each different amplitude will give rise to a unique viscoelastic model. Considering a finite element analysis, for every element the equivalent shear strain amplitude has to be determined so that an appropriate viscoelastic model can be assigned to each element. Therefore the finite element analysis is carried out in four steps:

- An initial displacement controlled elastic FE-analysis is performed using a hyperelastic material model.
- The output file is read and the equivalent shear strain amplitude is calculated for each element with equation 4.
- Based on the obtained amplitudes each element is assigned an appropriate viscoelastic material model.
- A new input-file is then created and executed with the new equivalent viscoelastic material models assigned to each element.

In case of a load controlled analysis the above procedure needs to be repeated to find an appropriate elastic modulus for the initial finite element model to ensure that the elastic and viscoelastic model yield the same global displacements.

In this paper the elastic analysis of the first step was performed with a Neo-Hooke hyperelastic model with the strain energy potential $W = C_{10}(I_1 - 3)$. For a simple shear load case the first strain invariant is $I_1 = \kappa^2 + 3$. For a general load case an equivalent shear strain κ_{eq} can be calculated from the strain energy amplitude W_0 according to:

$$\kappa_{eq} = \sqrt{\frac{W_0}{C_{10}}} \tag{3}$$

I.e. the simple shear load case and the general load case are compared by putting their elastic strain energy equal.

It should be clear that even though the equivalent viscoelastic models can be made to yield a correct dynamic modulus and damping, their response to a harmonic load will be slightly different considering the shape of the hysteretic loop. Whereas the measured hysteretic loop may in some cases be asymmetric with sharp corners, the equivalent viscoelastic loop will always be more ellipsoidal with rounded corners.

An attempt to further improve the accuracy of the equivalent viscoelastic procedure was made by computing the the equivalent strain amplitude using an iterative scheme for which the equivalent strain amplitude was updated each step. Although the global behavior converged within the first iteration the element stresses did not fully converge and this iterative scheme was abandoned.

4 Equivalent time domain viscoelasticity

The time domain viscoelastic model in $Abaqus$ is based on a Prony-series approach. The one-dimensional mechanical analog representation of this model is illustrated in figure 7.

For each measured strain amplitude a time-domain viscoelastic material model as seen in figure 7 was fitted. Thus, an individual set of material parameters exists for each measured amplitude. The behavior of this time-domain viscoelastic model for simple shear is shown in figure 8 and 9.

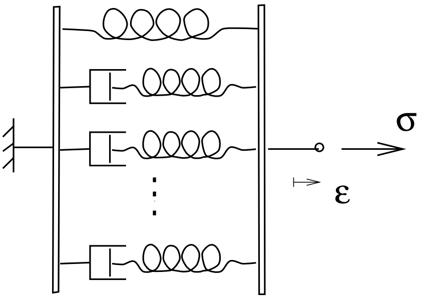

Figure 7: One-dimensional mechanical analogy for the time domain viscoelastic model.

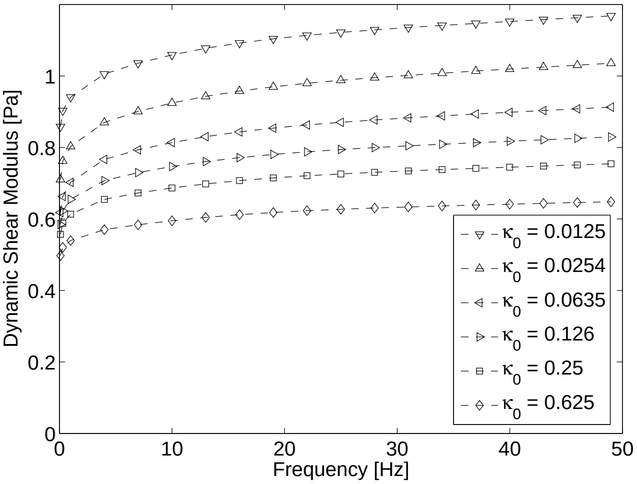

Figure 8: Simulated dynamic modulus using the equivalent time domain viscoelastic model.

Comparing the time-domain viscoelastic model with the measured data in figure 2 and 3 for simple shear it is seen that there is a good agreement between the two. The chosen viscoelastic model imposes a relation between the damping and the dynamic modulus. In short, a high derivative of the dynamic modulus with respect to frequency yields high damping. In reality damping is only partly caused by viscoelastic effects. Modelling the entire damping as purely viscoelastic leads to an overestimation of the viscoelastic part of the damping and hence also an overestimation of the derivative of the dynamic modulus with respect to frequency. This effect is clearly visible for the time-domain equivalent viscoelastic model.

4.1 Finite element model

The finite element analysis is performed in four steps as previously described. For the time domain viscoelastic model the fitted material parameters are only valid at the measured amplitudes. For all other amplitudes the material parameters are obtained by linear interpolating between the existing sets of material parameters. Choosing the relaxation times t_r the same for all sets of pa-

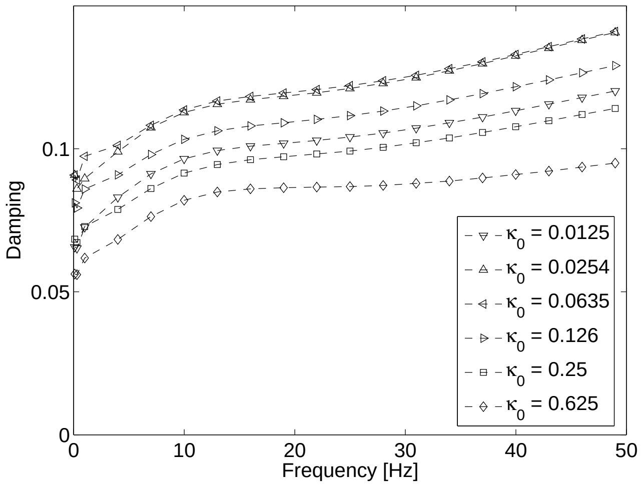

Figure 9: Simulated material damping using the equivalent time domain viscoelastic model.

rameters will simplify this interpolation. For amplitudes outside the measured amplitude range, the material parameters are set equal to those of the nearest measured amplitude. A finite element model of the cylindric bushing in figure 4 was created and loaded with a sinusoidal load in the radial direction. Calculated stiffness and damping of the bushing is shown in figure 10 and 11.

The finite element analyzes were performed in $Abaqus/Implicit$ using the hyperelastic large strain viscoelastic material model which is based on Prony-series. Eight-node hybrid formulation brick elements were used to model the rubber material and the steel was modelled as rigid.

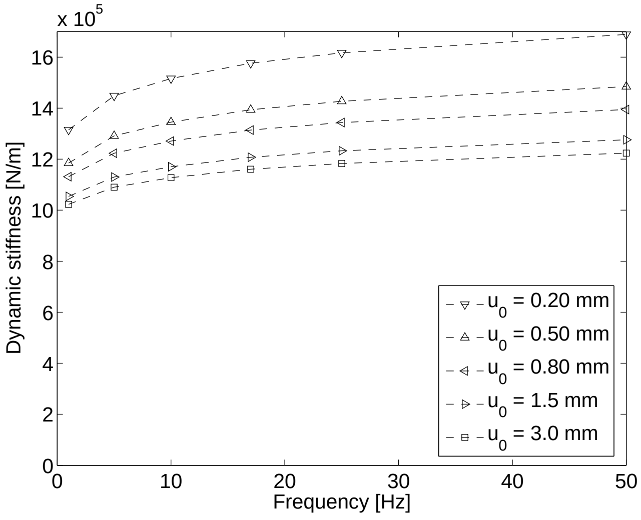

Figure 10: Simulated dynamic stiffness for the rubber bushing using the equivalent time domain viscoelastic FE-model.

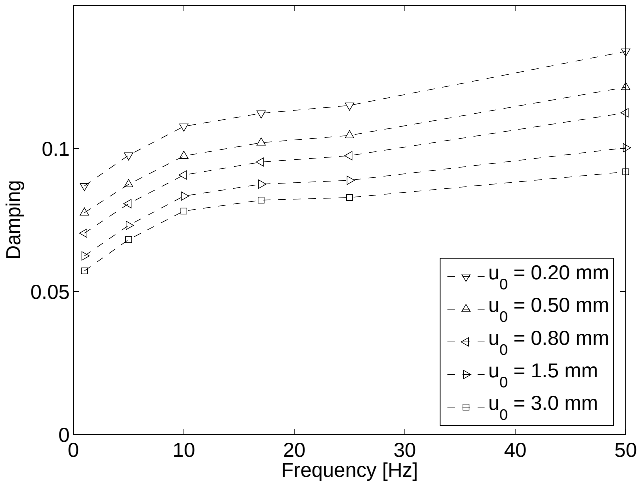

Figure 11: Simulated damping for the rubber bushing using the equivalent time domain viscoelastic FE-model.

5 Equivalent frequency domain viscoelasticity

Considering a steady state stationary dynamic analysis the dynamic modulus and damping can be described in terms of a complex modulus. In this analysis the vibration is treated as a perturbation around an elastically predeformed state. Thus the equations describing the stationary load case is reduced to a linear system of complex equations. This yields a very fast solution compared to a time domain viscoelastic model which must be solved through time-stepping. In $Abaqus$ the frequency dependent complex modulus is given in tabular form such as recorded from a frequency sweep. Thus there is no fitting of material parameters for this model.

For the equivalent frequency domain viscoelastic model the frequency dependence is determined from the amplitude obtained from the initial hyperelastic model.

5.1 Finite element model

The cylindrical bushing was analyzed using the equivalent frequency domain viscoelastic model. Since the frequency dependence was only measured at five amplitudes for the the double shear specimen, the material parameters for all other amplitudes are obtained by linear interpolation of the measured data. For amplitudes outside the measured amplitude range, the frequency dependent material data are set equal to those of the nearest measured amplitude.

Simulated stiffness and damping of the cylindric bushing are presented in figure 12 and 13, which should be compared to the corresponding measurements in figure 5 and 6. The bushing is loaded in the radial direction.

As previously, the finite element analyzes were performed in $Abaqus/Implicit$ using eight-node hybrid formulation brick elements to model the rubber material. The used material model allows for a large strain hyperelastic initial static load case from which the small strain steady state

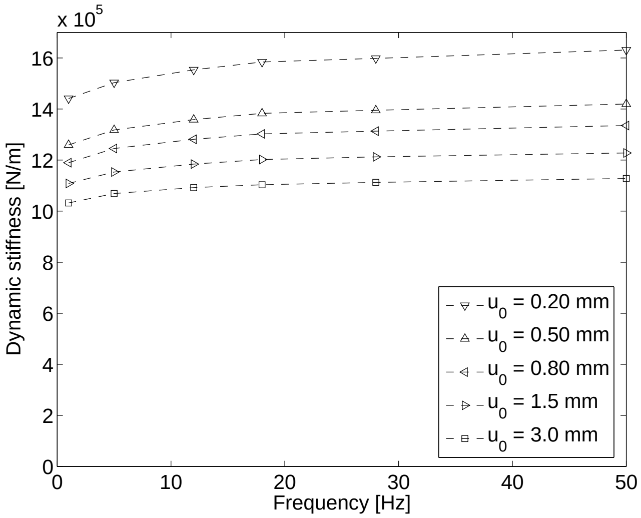

Figure 12: Simulated dynamic stiffness for the rubber bushing using the equivalent frequency domain viscoelastic FE-model.

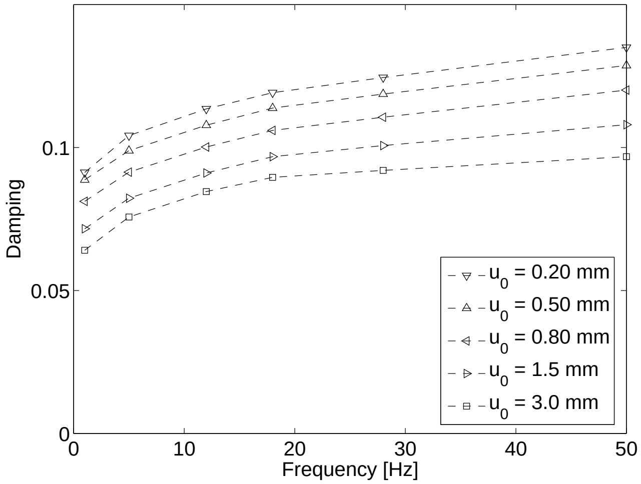

Figure 13: Simulated damping for the rubber bushing using the equivalent frequency domain viscoelastic FE-model.

analysis is performed using a frequency dependent complex modulus given in a tabular manner.

6 Result discussion

As seen in figure 10-13, both FE-models show the same behavior as the real bushing presented in figure 5 and 6. Yielding almost identical result both models overestimates the dynamic stiffness of the bushing and underestimates the damping.

The overestimation of dynamic stiffness is partly due to a fairly course finite element mesh as seen in figure 4. Calculations with finer meshes show that the stiffness can be reduced by at least 6%, whereas the damping is hardly affected at all by a finer mesh.

During manufacturing the bushing is vulcanized at an elevated temperature at which it receives its elastic properties. Thus at room temperature there will be residual stresses in the rubber material of the bushing. This pre stressed state is not included in the analysis shown in figures 10 to 13. In order to get an estimate of the influence of the residual stresses an initial temperature load was added to the equivalent frequency domain viscoelastic model. Assuming a temperature coefficient of $220 \cdot 10^{-6}/K$ a $120K$ temperature drop was modelled prior to the steady state dynamic analysis. Comparing figure 14 and 15 with figure 12 and 13, it is seen that the residual thermal stresses will lower the dynamic stiffness by roughly 20% and increase the damping with the same percentage, thus explaining much of the deviation seen in the finite element models.

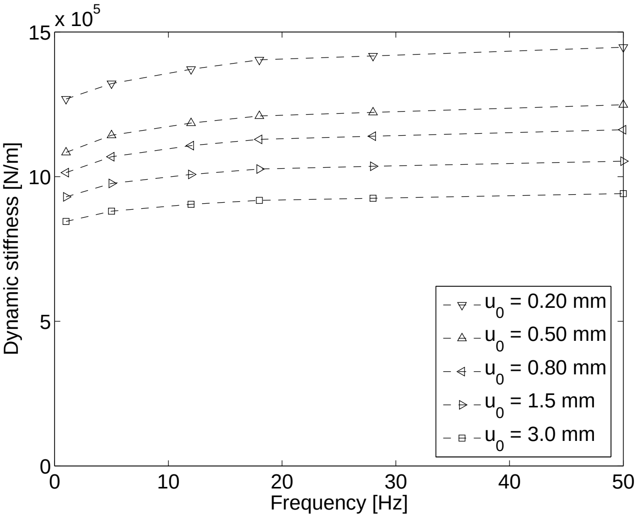

Figure 14: Simulated dynamic stiffness for the rubber bushing using the equivalent frequency domain viscoelastic FE-model, taking account for the temperature drop after vulcanization.

A parameter which was shown not to influence the result is the number of different viscoelastic material models used in the equivalent viscoelastic finite element model. A general approach would be to use one material model for each element. However by using the same viscoelastic model for several elements with approximately the same strain amplitudes the number of material models needed can be greatly reduced. For the finite element model in this paper, containing 1620 elements, using 20 material models only altered the resulting stiffness with less than 0.1% in comparison to using one material model for each element.

Comparing the results of the two equivalent finite element models with the results of the

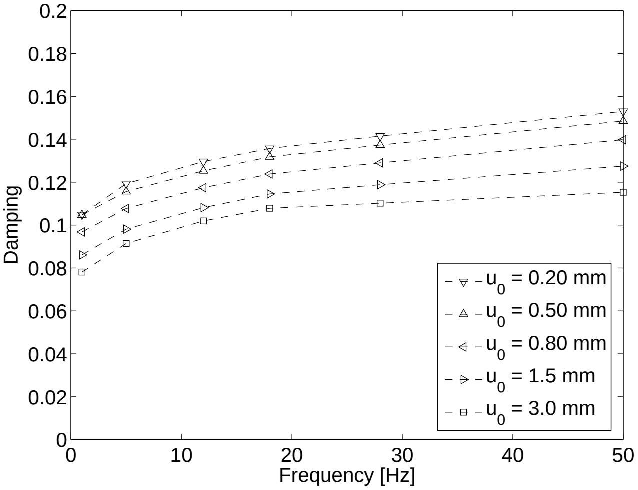

Figure 15: Simulated damping for the rubber bushing using the equivalent frequency domain viscoelastic FE-model, taking account for the temperature drop after vulcanization.

viscoelastoplastic model presented in (Austrell & Olsson 2001) it can be seen that the results are very similar. The major difference seem to be that derivative of the dynamic modulus with respect to frequency is slightly exaggerated in the time domain viscoelastic model and slightly underestimated in the viscoelastoplastic model, whereas the complex viscoelastic model is the most accurate in this respect. The reasons for this is believed to be that complex model do not use any analytical mathematic expression to describe the frequency and amplitude dependence. It simply interpolates in the measured material data.

7 Conclusions

The time domain and the frequency domain equivalent viscoelastic models yield almost identical results. It is also noted that the two models yield very similar results as the viscoelastic-elastoplastic model studied in (Olsson & Austrell 2003). All three models overestimates the stiffness and underestimates the damping. This deviation can be explained by the fact that the initial temperature loads were left out and that a rather rough finite element mesh was chosen. Identical finite element meshes were used in all three models.

The frequency domain model will fit exactly to experimental data and will be very computationally efficient since it will linearize the system of equations. In linearizing the system, the model will be restricted to smaller amplitudes and sinusoidal load cases.

The time domain model will not be as computationally efficient as the frequency domain model but more efficient than the viscoelastic-elastoplastic model studied in (Olsson & Austrell 2003). Compared to the frequency domain model the time domain viscoelastic model is better suited for larger deformations also including contact. Although it will only handle cyclic loads it is not restricted to purely sinusoidal loads.

It is thus concluded that the two equivalent viscoelastic models was shown to have different advantages and restrictions. Both models were shown to work well when modelling the harmonically loaded cylindrical bushing in this paper.

8 References

Austrell P-E., Olsson A.K. 2001, A Method to Analyze the Non-Linear Dynamic Behaviour of Carbon-Black-Filled Rubber Components Using Standard FE-codes. *Second European Conference on Constitutive Models for Rubber*, Germany

Gil-Negrete N. 2004,On The Modelling and Dynamic Stiffness Prediction of Rubber Isolators *University of Navarra*,San Sebastián, Spain

Miehe C., Keck J. 2000, Superimposed finite elastic-viscoelastic-plastoelastic stress response with damage in filed rubbery polymers. Experiments, modelling and algorithmic implementations *J. Mech. Phys. Solids*, 48, 323-365

Mullins L. 1969, Softening of Rubber by Deformation *Rubber Chemistry and Technology*, Vol. 42, pp. 339-362

Olsson A.K., Austrell P-E. 2001, A fitting procedure for a viscoelastic-elastoplastic material model. *Second European Conference on Constitutive Models for Rubber*, Germany

Olsson A.K., Austrell P-E. 2003, Finite element analysis of a bushing considering rate and amplitude dependent effects. *Third European Conference on Constitutive Models for Rubber*, London, UK

Payne A.R. 1965, *Reinforcement of elastomers* G. Kraus, Ed., Interscience, Chap. 3, New York

Rabkin M., Brüger T. 2001, A constituitive model of elastomers in the case of cyclic load with amplitude dependent internal damping. *Third European Conference on Constitutive Models for Rubber*, London, UK

Sjöberg M., Kari L. 2002, Non-Linear Behavior of a Rubber Isolator System Using Fractional Derivatives *Vehicle System Dynamics*, Vol. 37, No. 3, pp. 217-236

Warnaka G.E. 1962, *Effects of Dynamic Strain Amplitude on the Dynamic Mechanical Properties of Polymers*. ASME Rubber and Plastics Div., Paper 62-WA-323, New York

Appendix: Material Parameters

Table 1: Material parameters for the time domain viscoelastic model.

κ_0	G_∞ [MPa]	G^{ve} [MPa]	t_r [s]
0.0125	0.8239	0.0882	1.20
		0.0772	0.115
		0.0400	0.029
		0.1067	0.011
		0.3587	0.0010
0.0254	0.6688	0.1043	1.20
		0.0790	0.115
		0.0436	0.029
		0.1042	0.011
		0.3774	0.0010
0.0635	0.5826	0.0886	1.20
		0.0832	0.115
		0.0312	0.029
		0.0960	0.011
		0.3314	0.0010
0.126	0.5547	0.0755	1.20
		0.0672	0.115
		0.0261	0.029
		0.0807	0.011
		0.2750	0.0010
0.250	0.5334	0.0609	1.20
		0.0527	0.115
		0.0198	0.029
		0.0686	0.011
		0.2182	0.0010
0.625	0.4804	0.0448	1.20
		0.0400	0.115
		0.0115	0.029
		0.0603	0.011
		0.1466	0.0010

Paper V

Modelling the Dynamic Properties of Rubber in Rolling Contact

Yet to be submitted

Modelling the Dynamic Properties of Rubber in Rolling Contact

Anders K Olsson, Per-Erik Austrell
Division of Structural Mechanics, Lund University, Sweden

ABSTRACT: For rubber in rolling contact many different aspects of rubber properties come into play. The dynamic response of rubber is dependent of both amplitude and frequency. Modelling the amplitude and frequency dependent effects is an important step in understanding how load, rolling speed and geometry will affect the rolling behaviour. This paper studies two different finite element procedures to include amplitude and frequency dependent effects in conjunction with rolling contact. It is shown how the non-linear dynamic characteristics of the rubber material influences the rolling contact. Analyzed examples include rolling on a flat surface and rolling over a groove.

1 Introduction

Rubber in rolling contact is found in many different applications and is not only of interest to the tire industry, but also to the processing industry. In paper manufacturing and similar processes, understanding rubber covered rollers is vital to improve quality and production capacity. The ability to analyze the rolling contact of rubber offers a powerful tool for a better understanding of how material characteristics in combination with roller design variables influence the contact properties such as pressure gradient and contact width. Traditionally, analyzes treat the rubber cover as elastic, however most rubber materials also exhibit amplitude and frequency dependent properties that contribute to the above contact properties.

The purpose of this paper is twofold. The first is to examine two different methods of incorporating amplitude dependent effects into finite element models of rubber in rolling contact. The second purpose is to highlight some important aspects of non-linear material characteristics in general and amplitude dependence in particular when rolling contact is studied.

For a harmonic load, the amplitude dependence can be seen as a decrease in dynamic modulus for increasing amplitude. For an increasing amplitude the damping will at first increase until a maximum is reached after which further increased amplitude will result in decreased damping.

Partly depending on the application and partly on the specific rubber properties, the amplitude dependent effects are in many cases far more pronounced than the rate or frequency dependence (Olsson & Austrell 2001). This is especially obvious for applications with moderate amplitudes and low to moderate frequencies, as well as for rubber with a high proportion of filler particles. For very low or very high strain amplitudes these effects are usually of less interest.

Various finite element models for dealing with the non-elastic effects of rubber in rolling contact have previously been presented. A model introducing Mullins effect in terms of a damage formulation have been treated by (Kaliske & Domscheit 2001) and showed important influence on the shape of the contact surface after the initial revolutions. A non-linear viscoelastic approach (Akutagawa et al. 2003) was used to determine rolling resistance caused by amplitude dependent effects.

This paper studies two different methods to account for combined amplitude and frequency dependence in a rolling contact finite element analysis. The first method uses an elastoplastic-viscoelastic model previously presented in (Austrell & Olsson 2001) and the second is based on an approximate time-domain viscoelastic model presented in (Olsson et al. 2006). Both methods are based on simple engineering approaches and utilize commercially available finite element codes, keeping the added complexity to a minimum.

1.1 Material data

The material models of this paper have been fitted to measurements obtained from a double shear test specimen of a *78 ShoreA* HNBR (hydrogenated acrylonitrile butadiene) rubber from Trelleborg. For the measured amplitude and frequency range, the HNBR rubber exhibit equally pronounced amplitude and frequency dependence. The material tests have previously been presented in (Olsson & Austrell 2001). The test specimen was subjected to a sinusoidal load and dynamic shear modulus and damping were measured. The frequency ranged from 5 to 180 *Hz* and the shear strain amplitude ranged from 1 to 12%. The measured range should ideally cover the loads experienced in the roller in terms of frequencies and strain amplitudes. This is further studied in later sections.

2 Rubber covered rollers

From an industrial point of view, rubber covered rollers are of great importance in many industrial applications. From a scientific perspective the simple geometry and loading of rubber covered rollers make them ideal to study the dynamic effects of rubber material during rolling.

Depending on what industrial application or process the roller is found in, different contact parameters are important. Contact parameters such as contact width, maximum pressure, pressure gradient and surface strains are all governed by material properties and design variables such as rubber thickness, roller radius, applied load and rolling velocity, as seen in figure 1. In general the design variables are simple to control but are hard to correlate to what is happening in the the contact region. The contact parameters on the other hand are easier to correlate to the process but harder to control. Hence, a good model describing the relationship between contact parameters and design variables is the key to control the process.

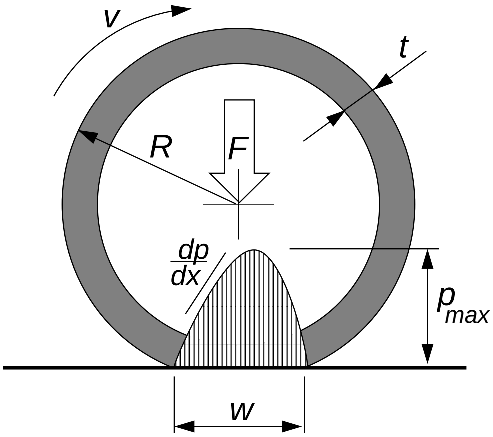

Figure 1: Rubber covered roller, design variables and contact parameters.

3 Elastoplastic-viscoelastic model

This section offers a brief introduction of the elastoplastic-viscoelastic model. A more thorough presentation is found in (Austrell & Olsson 2001). The elastoplastic-viscoelastic model is based on the assumption that the amplitude dependence and the frequency dependence can be treated as independent of each other. This approximation makes it possible to model the combined material behaviour with two parallel constitutive branches; one viscoelastic branch to account for the frequency dependence and one elastoplastic to account for the amplitude dependence. The total stress tensor is thus given as the sum of the elastoplastic and viscoelastic stress tensors:

$$\sigma_{tot} = \sigma_{plast} + \sigma_{visco} \tag{1}$$

This summation of stress tensors can be achieved by overlaying a viscoelastic finite element mesh with an elastoplastic finite element mesh.

The rubber was modelled with 4-node quad elements with reduced integration. Due to the history dependent nature of the plastic part of the model, the steady state rolling analysis was carried out by time stepping. Since the size of the time step is restricted by the contact simulation an explicit time-stepping scheme was chosen. The analysis was carried out in *Abaqus/Explicit* using a large strain viscoelastic material model in combination with a kinematic hardening elastoplastic model. Since *Abaqus/Explicit* does not contain kinematic hardening a piece wise linear hardening elastoplastic model was created by overlaying several ideally elastoplastic models.

The viscoelastic part was modelled with a large strain viscoelastic model based on Neo-Hookean hyperelasticity and a viscous behaviour defined in terms of a Prony series. The material parameters for the HNBR rubber are found in (Olsson & Austrell 2001). In figure 2 and 3 the elastoplastic-viscoelastic model is compared to measured data. The presented dynamic shear modulus G_{dyn} and damping d are defined according to:

$$G_{dyn} = \frac{\tau_0}{\kappa_0} \tag{2}$$

and

$$d = sin(\delta) = \frac{U_c}{\pi \kappa_0 \tau_0} \tag{3}$$

where τ_0 is the shear stress amplitude, κ_0 is the shear strain amplitude and U_c is the energy loss per unit volume for one load cycle.

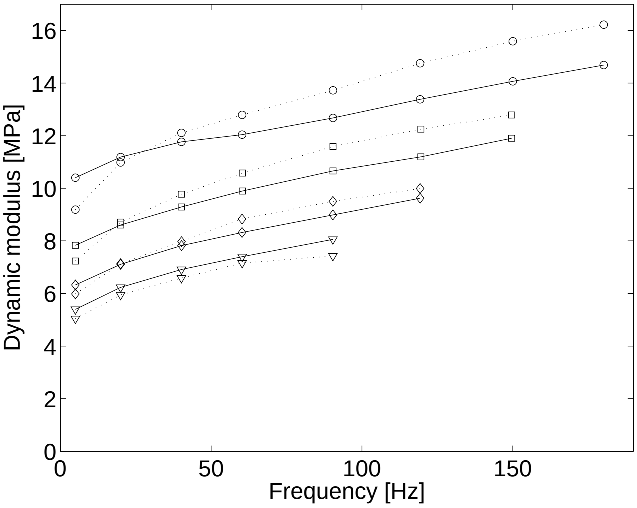

Figure 2: Dynamic shear modulus of HNBR rubber. Solid line: elastoplastic-viscoelastic model. Dotted line: experimental data. $\bigcirc : \kappa_0 = 1\%$; $\Box : \kappa_0 = 3\%$; $\Diamond : \kappa_0 = 7\%$; $\bigtriangledown : \kappa_0 = 12\%$.

4 Equivalent viscoelastic model

The equivalent viscoelastic model is limited to model periodic loads. The requirement for the load to be be periodic is due to the need to in advance estimate the maximum load level during a load cycle. The model is based on the approximation that for a known strain amplitude it is possible to model the rubber as purely viscoelastic. Although the rolling contact will not give rise to a harmonic load it will result in a periodic load when rolling over a smooth surface. Hence, when modelling rolling contact the equivalent viscoelastic model is restricted to constant speed and a smooth surface.

Considering steady state rolling, a material point will experience the same maximum strain amplitude at every revolution. I.e. for a given roller and a given compression, the strain amplitude at the material level is only related to the distance to the rubber surface of the individual material point. This means that for every amplitude a corresponding set of viscoelastic material parameters has to be created. Since the strain amplitude for the rubber coated roller is only dependent on the radial coordinate, each tangential layer of elements will have an individual viscoelastic material model. The analysis is carried out in two steps.

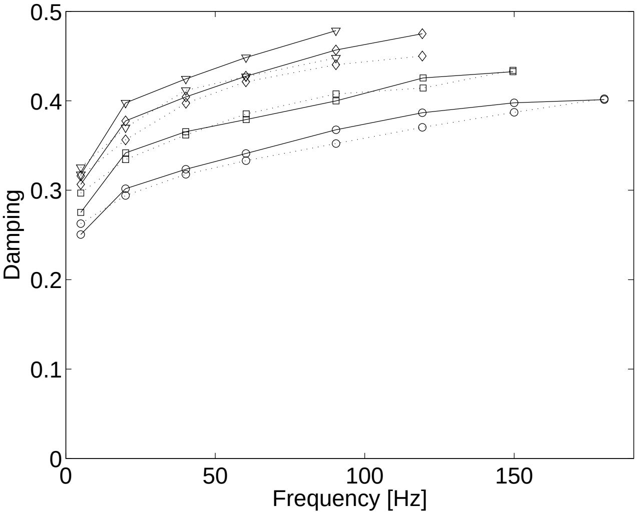

Figure 3: Damping of HNBR rubber. Solid line: elastoplastic-viscoelastic model. Dotted line: experimental data. $\bigcirc : \kappa_0 = 1\%$; $\square : \kappa_0 = 3\%$; $\lozenge : \kappa_0 = 7\%$; $\bigtriangledown : \kappa_0 = 12\%$.

- First an equivalent shear strain amplitude for each element layer is calculated from an initial elastic analysis.
- Based on the equivalent shear strain amplitude each element layer is given an individual viscoelastic model in the following analysis.

A more detailed presentation of the equivalent viscoelastic model can be found in (Olsson et. al 2006).

Since rolling contact results in a non-harmonic load, it is not possible to use a frequency domain viscoelastic model. Instead a time-domain viscoelastic model must be used. This was done with a large strain viscoelastic model based on Neo-Hookean hyperelasticity and with the viscous part given in terms of a Prony series. In $Abaqus$ the steady state rolling was modelled with a mixed Lagrangian/Eulerian formulation. In this formulation the rubber material flows through the static deformed finite element mesh. This approach makes the time-domain viscoelastic model very efficient for steady state rolling. The rubber was modelled with 4-node quad elements with a hybrid formulation suitable for incompressible or almost incompressible materials.

The behaviour of the equivalent time-domain viscoelastic model with respect to dynamic shear modulus and damping is shown in figure 4 and 5 respectively. Each curve represents one amplitude.

5 Rolling over a smooth surface

In the this section a rubber coated roller is studied when rolling over a flat surface. First the load conditions at material level is studied using an elastic finite element model. Secondly, using the

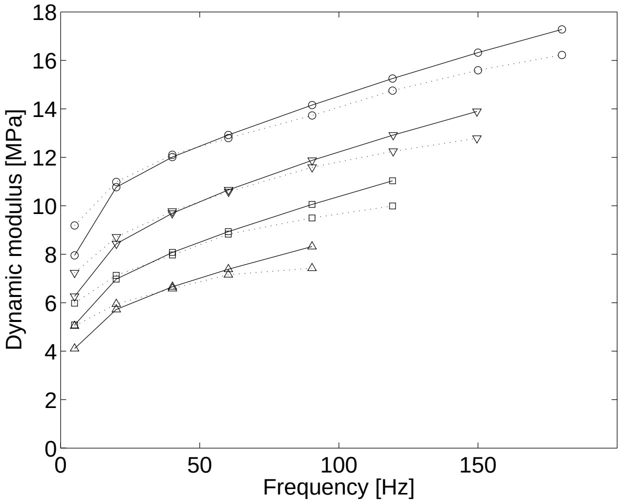

Figure 4: Dynamic shear modulus of HNBR rubber. Solid line: equivalent viscoelastic model. Dotted line: experimental data. ◯ : $\kappa_0 = 1\%$; ▽ : $\kappa_0 = 3\%$; □ : $\kappa_0 = 7\%$; △ : $\kappa_0 = 12\%$.

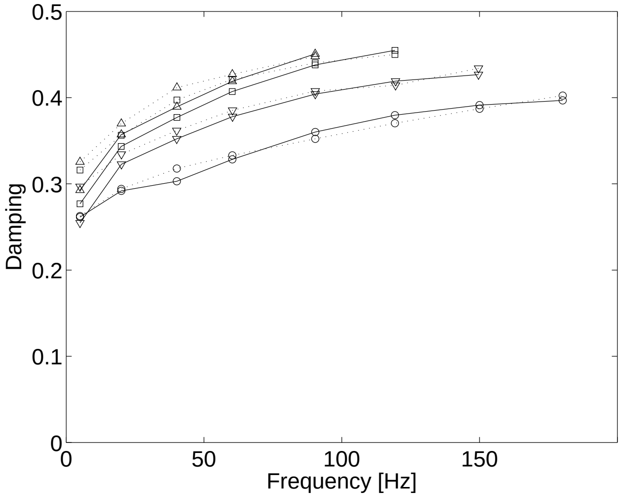

Figure 5: Damping of HNBR rubber. Solid line: Equivalent viscoelastic model. Dotted line: experimental data. ◯ : $\kappa_0 = 1\%$; ▽ : $\kappa_0 = 3\%$; □ : $\kappa_0 = 7\%$; △ : $\kappa_0 = 12\%$.

example, the two previously discussed material models are used to analyze the influence of the dynamic material properties.

The geometry of the roller is given in figure 6. The rolling velocity is $10m/s$ and the compressive displacement of the roller is $0.8mm$. The roller is modelled as a long rigid cylinder coated with a thin layer of rubber. For the initial elastic analysis the velocity can be neglected as the rubber is elastic and the speed is not high enough to result in any sizeable inertia forces.

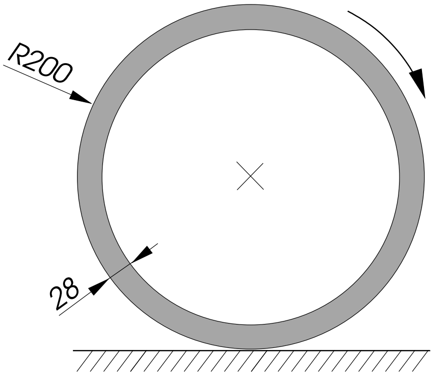

Figure 6: Analyzed rubber coated roller.

5.1 Load conditions at material level

A simple elastic static finite element model of the previously described roller was analyzed in order to study the loads experienced by the rubber material during rolling. The aim is to serve as a verification of the chosen load range for the material tests as well as to gain an initial understanding of the basic mechanics involved.

Since the roller is long in the axial direction, two-dimensional constant strain conditions are applicable. As the rubber coating is much softer than the inner steel cylinder and flat surface, both cylinder and surface is treated as rigid. Hence only the rubber is treated as a flexible body. The friction between the roller and flat surface is neglected. It is however easy to include friction if needed.

As the material parameters are derived from a harmonic material test it is important to choose frequency and strain amplitude ranges for the test that corresponds well to the load of the roller. In order to analyze the frequencies experienced by the rubber in the contact region during rolling, a purely elastic analysis was made and the equivalent shear strain according to equation 4 was derived from the strain energy amplitude W_0 and the hyperelastic Neo-Hooke parameter C_{10}.

$$\kappa_{eq} = \sqrt{\frac{W_0}{C_{10}}} \tag{4}$$

The strain pulse during one revolution for an element at the surface of the rubber coating is shown in figure 7. For the example analyzed in this paper the maximum strain amplitude experienced by the rubber is not reached at the surface as expected. Instead the maximum occurs at approximately one third of the rubber thickness measured from the surface and in. The two dips in the curve at either side of the largest pulse marks the outline of the contact surface. Outside the contact area the rubber will bulge outward due to its incompressive nature.

The corresponding fast Fourier transform of the time signal is shown in figure 8. As seen in this frequency plot there are two major frequency contributions at $10 Hz$ and $140 Hz$ respectively. These frequencies are important for deciding the frequencies for the material tests.

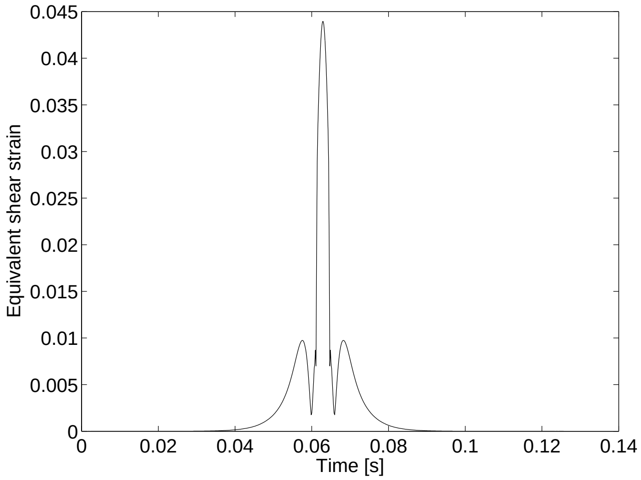

Figure 7: Equivalent shear strain pulse for one element at the surface during one revolution.

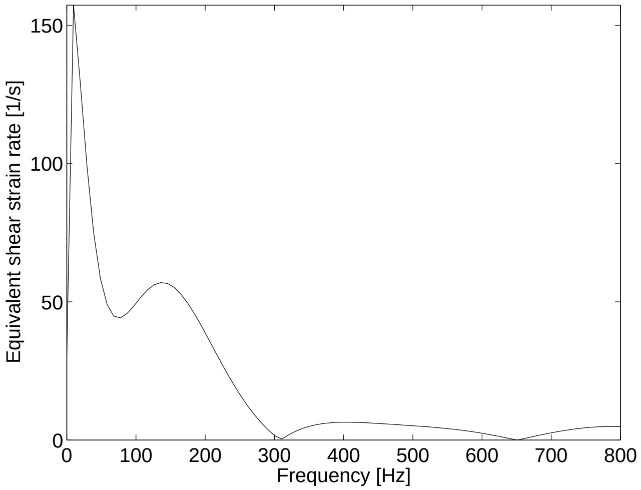

Figure 8: Frequency spectrum for an element at the rubber surface.

A simple approximation of the dominant frequency of the pulse can be made by approximating the pressure distribution with half a sine wave. Thus, for a rolling speed v and a contact width d the dominant frequency of the pulse can be obtained according to:

$$f = \frac{v}{2d} \tag{5}$$

For the roller analyzed in figure 7 and 8 the approximate dominant frequency is $167Hz$ which is in fairly good agreement with the second peak of the corresponding Fourier transform. The first peak is related to the revolution speed and can be described with:

$$f = \frac{v}{2\pi R} \tag{6}$$

which for this example yields $8Hz$, also in fairly good agreement with the Fourier transform analysis.

As mentioned earlier the material test covered a frequency range from 5 to $180Hz$ and amplitudes from 1 to 12%. From the calculated loads in figure 7 and 8, it is seen that the measured range correspond well to the loads experienced by the roller.

5.2 Comparison of material models

For comparison both the viscoelastic-elastoplastic and the equivalent viscoelastic as described earlier were used to analyze the a rubber covered roller in rolling contact with a flat smooth surface. The geometry and the load is identical to the example of section 5.1. As mentioned previously the viscoelastic-elastoplastic model was analyzed through an explicit time integration and the equivalent viscoelastic-elastoplastic model was analyzed by an implicit solver using the steady state transport formulation.

The contact pressures from both the equivalent viscoelastic and the viscoelastic-elastoplastic finite element model are shown in figure 9. Both models show good agreement with each other. Unfortunately it was not possible to obtain any experimental data to compare with, but the agreement between the two separate models suggests that the result is reliable.

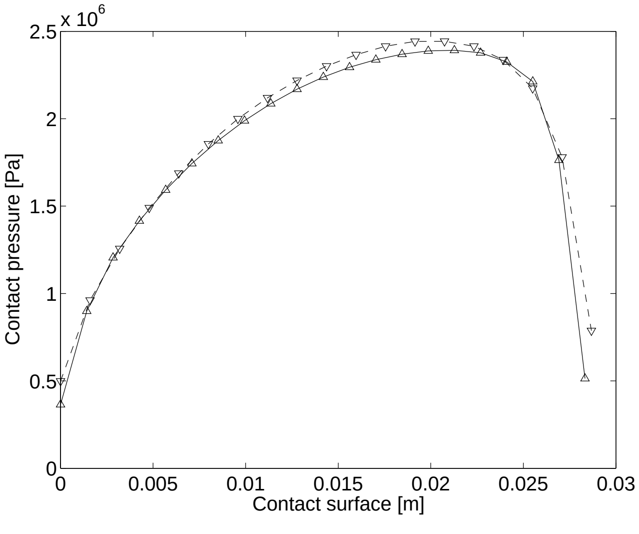

Figure 9: Contact pressure when rolling over a flat surface. Dotted line: Overlay method; Solid line: Equivalent viscoelastic method.

The asymmetric shape of the pressure distribution can be explained by the non-elastic properties of the rubber material. At the first phase of the contact surface the rubber material is loaded until it reaches the maximum contact pressure after which it is unloaded. Similar to a cyclic material test, the contact pressure response when unloading will deviate from the load curve. This behaviour is caused by damping and will result in a loss of strain energy. Thus, the asymmetric shape of the contact pressure is a result of the material damping. The asymmetric pressure results in an increased initial pressure gradient which can be beneficial for some applications where fluids need to be driven away from the contact area.

In this case the deformation is mainly controlled by the prescribed displacement. I.e. the contact width is governed by the prescribed displacement and is hardly influenced by the dynamic modulus. Hence, decreasing the rolling speed and thus also decreasing the dynamic modulus will not alter the contact width. Instead the softer response of the rubber will give a lower maximum pressure and thus a lower contact force. Decreasing the rolling speed for a load controlled roller on the other hand would result in an increased contact width and thus also a lower maximum pressure. Understanding and controlling these phenomenons is vital to many industrial applications.

6 Rolling over a non-smooth surface

In this section a rubber covered roller is studied to see how different material properties will influence the contact prpoerties. The radius of the roller is 175*mm*,the thickness of the rubber layer is 9*mm* and the compressive load is 30*kN/m*.

6.1 Fictive materials

As was seen in figure 9 both the equivalent viscoelastic and elastoplastic-viscoelastic model will give the same pressure distribution rolling over a flat surface. Trying different material models indicated that the pressure distribution was not affected by the material characteristics. The pressure distribution over the contact area was the same irrespective if the rubber were modelled as elastoplastic or viscoelastic.

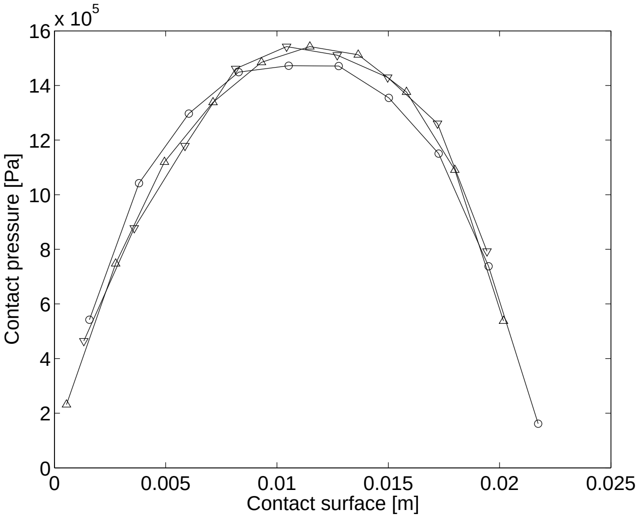

Figure 10: Contact pressure when rolling over a flat surface using fictive material models. ○*: Elastic model;* ▽*: Elastoplastic model;* △*: Viscoelastic model.*

To further prove this point two fictive materials were derived; one purely viscoelastic and one purely elastoplastic. Both material models were fitted to exhibit a constant damping of $d = 0.35$ for a frequency range of 5 to 180 *Hz* and a shear strain amplitude range of 1 to 12%. This resulted in an amplitude dependent modulus for the elastoplastic model and a frequency dependent modulus for the viscoelastic model with the same damping.

When rolled over a flat surface both models gave the same shape of the contact pressure distribution, only differing in the maximum pressure. Through some trial and error simulations the modulus of both material models were chosen so both models gave the same maximum pressure when running over a flat surface. When fitting the material parameters this way the elastoplastic and the viscoelastic model will yield the same result in terms of contact width and maximum contact pressure for the chosen roller geometry and load.

Figure 10 show the contact pressure as both models are rolling at a speed of 10*m/s* over the flat surface. A purely hyperelastic model is also shown as a reference. For a given geometry and load, the maximum contact pressure and contact width is mainly given by the dynamic modulus.

In figure 10 it can also be noted that the two models exhibit the same asymmetric pressure distribution. The asymmetric shape is caused by the material damping. The material damping can be regarded as a dimensionless measure of the difference between loading and unloading. In this case, the equal plastic and viscous damping will give the same asymmetric distortion. I.e. the asymmetry of the contact pressure is governed by the amount of damping regardless of what phenomenon is causing the damping. Both material damping and asymmetric pressure distribution is a result of the difference between the loading and unloading curve of the material. Compared to the contact pressure in figure 9 the contact pressure in figure 10 show less asymmetry. This is explained by the thinner rubber coat of the latter roller which will result in a more volumetric load.

6.2 Shallow groove

Using the previously derived fictive material the same roller was studied when rolling over a shallow groove. The groove is 5*mm* wide and 0.8*mm* deep with the same length as the roller and situated in the axial direction of the roller.

As seen from figure 11 to 13, the elastic and viscoelastic model show similar deformations whereas the elastoplastic model better adapts to the shape of the groove. Unlike the other two models the elastoplastic model incorporates amplitude dependence. Since the dynamic modulus of the amplitude dependent material will decrease for an increasing in amplitude, the highly strained areas of the roller close to the hole will behave in soft manner if modelled by the elastoplastic model. Although the viscoelastic and elastoplastic models give the same result when rolled over a flat surface, it can be concluded that including the amplitude dependence, as done in the elastoplastic model, will result in a softer and more deformable contact region. Hence, a correct model of the amplitude dependence is important when modelling the rolling contact of a rough surface. Another implication of this result is that when a smooth contact between the surface and the rubber is desirable, it may be wise to choose a rubber with pronounced amplitude dependence.

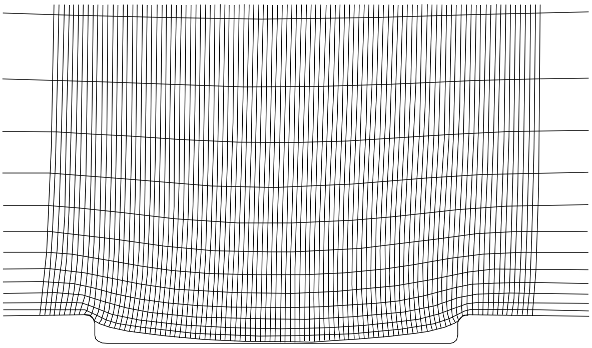

Figure 11: Element deformation when running over a small groove using an elastic finite element model.

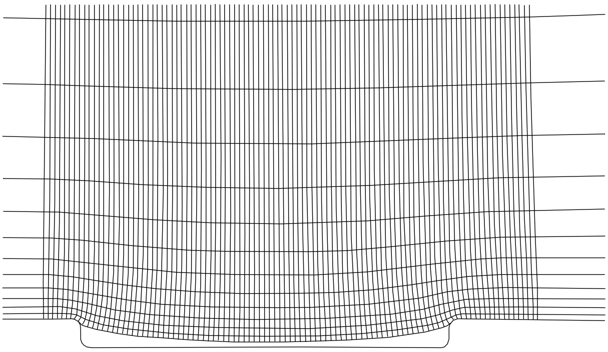

Figure 12: Element deformation when running over a small groove using an viscoelastic finite element model.

7 Summary

The topic of this paper is finite element modelling of rubber covered rollers. Two different methods to include frequency and amplitude dependence are studied, one viscoelastic-elastoplastic model and one equivalent viscoelastic model. Both models include both rate and amplitude dependent properties. It was shown that both models gave the same results, suggesting that the contact pressure when rolling over a flat surface is mainly governed by dynamic modulus and damping and is not dependent on how the damping is modelled.

For the equivalent viscoelastic model the mixed Eulerian/Lagrangian formulation as supplied by *Abaqus* in combination with the equivalent viscoelastic model eliminates the need for time

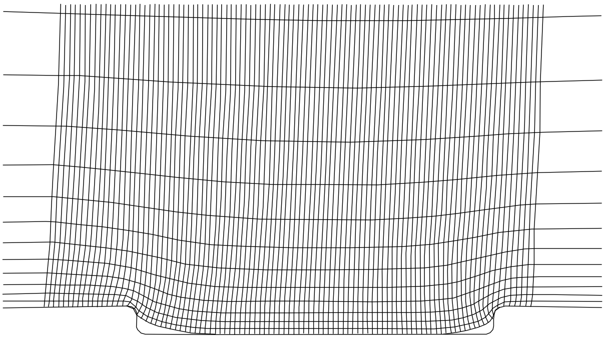

Figure 13: Element deformation when running over a small groove using an elastoplastic finite element model.

stepping during steady state rolling and is a very efficient solution. This model is however restricted to periodic loads, which for rolling contact translates to constant velocity and smooth surfaces.

The viscoelastic-elastoplastic model was used in combination with *Abaqus/Explicit* as the small time steps needed for the contact simulation, fits the small time steps needed for convergence in an explicit scheme. This model differs from the equivalent viscoelastic in the ability to model rolling over a arbitrary surface and at varying velocities.

The model was used to analyze a roller rolling over a small groove in a flat surface. For this load case the steady state rolling approach is not valid as the groove will not come into contact with the same material point at every revolution. When comparing viscous and plastic damping mechanics, it was seen that amplitude dependent rubber resulted in much softer behaviour of the high strain regions of the rubber surface. This local softening effect will make the rubber deform more easily and better adapt to the geometry of the groove.

8 References

Abaqus Inc., *Abaqus Theory Manual, Version 6.5*, Providence, RI, USA

Akutagawa K. et al. 2003, Application of non-linear FEA to tyre rolling resistance simulation *Third European Conference on Constitutive Models for Rubber*, UK

Austrell P-E., Olsson A.K. 2001, A Method to Analyze the Non-Linear Dynamic Behaviour of Carbon-Black-Filled Rubber Components Using Standard FE-codes. *Second European Conference on Constitutive Models for Rubber,* Germany

Kaliske M. & Domscheit A. 2001, Modelling of softening effects in elastomeric material and its application in tire computations. *Second European Conference on Constitutive Models for Rubber*, Germany

Olsson A.K., Austrell P-E. 2001, A fitting procedure for a viscoelastic-elastoplastic material model. *Second European Conference on Constitutive Models for Rubber*, Germany

Olsson A.K. 2006, Considering amplitude dependent effects during cyclic loads by an equivalent viscoelastic model. *PhD thesis, Modelling the dynamic properties of elastomers, Paper IV*, Lund University, Sweden

Gil-Negrete N. 2004,On The Modelling and Dynamic Stiffness Prediction of Rubber Isolators *University of Navarra*,San Sebastián, Spain

Miehe C., Keck J. 2000, Superimposed finite elastic-viscoelastic-plastoelastic stress response with damage in filed rubbery polymers. Experiments, modelling and algorithmic implementations *J. Mech. Phys. Solids*, 48, 323-365

Mullins L. 1969, Softening of Rubber by Deformation *Rubber Chemistry and Technology*, Vol. 42, pp. 339-362

Austrell P-E., Olsson A.K. 2001, A Method to Analyze the Non-Linear Dynamic Behaviour of Carbon-Black-Filled Rubber Components Using Standard FE-codes. *Second European Conference on Constitutive Models for Rubber*, Germany

Olsson A.K., Austrell P-E. 2003, Finite element analysis of a bushing considering rate and amplitude dependent effects. *Third European Conference on Constitutive Models for Rubber*, London, UK

Payne A.R. 1965, *Reinforcement of elastomers* G. Kraus, Ed., Interscience, Chap. 3, New York

Rabkin M., Brüger T. 2001, A constituitive model of elastomers in the case of cyclic load with amplitude dependent internal damping. *Third European Conference on Constitutive Models for Rubber*, London, UK

Part III

Appendix

A1 Notation

The following symbols are used in this thesis:

G = shear modulus
G_{dyn} = dynamic shear modulus
G_{exp} = measured dynamic shear modulus
G_R = relaxation shear modulus
G_∞ = long term shear modulus
G_0 = instant shear modulus
t_r = relaxation time
τ = shear stress
τ_0 = shear stress amplitude
τ_y = yielding shear stress
$\boldsymbol{\tau}$ = stress tensor
κ = shear strain
κ_0 = shear strain amplitude
κ_y = yield shear strain
d = damping
d_{exp} = measured damping
d_{bush} = component damping
δ = phase angle
U_c = dissipated energy per volume for a closed hysteresis loop
a_{max} = highest strain energy
W_{hyst} = dissipated energy for a closed hysteresis loop
η = viscosity coefficient
u = displacement
α = weight factor
ψ = error function
ω = angular frequency
H = thickness
M = number of elastoplastic components
N = number of viscoelastic components
m = number of measurements
u_0 = displacement amplitude
K_{dyn} = dynamic stiffness
F_0 = force amplitude
W_0 = elastic strain energy amplitude
κ_{eq} = equivalent strain energy amplitude
σ_{tot} = total stress tensor
σ_{plast} = elastoplastic part of stress tensor
σ_{visco} = viscoelastic part of stress tensor
f = frequency
v = rolling velocity
d = contact width
R = radius of roller

Superscripts

e = elastic
ep = elastoplastic
ve = viscoelastic